C-Grid as Shear Reinforcement in Concrete Bridge Girders

John Charlton Ward III

Thesis submitted to the Faculty of the
Virginia Polytechnic Institute and State University
in partial fulfillment of the requirements for the degree of

Master of Science
In
Civil Engineering

Carin L. Roberts-Wollmann, Chair
Thomas E. Cousins
John J. Lesko

February 26, 2016
Blacksburg, VA

Keywords: C-Grid, CFRP, Shear, Transverse Reinforcement, Concrete Bridge Girders

C-Grid as Shear Reinforcement in Concrete Bridge Girders

John Charlton Ward III

Abstract

Corrosion of reinforcing steel causes shorter life spans in bridges throughout the United States. The use of carbon fiber reinforced polymer (CFRP) materials as the flexural reinforcement in bridge girders has been extensively studied. However, CFRP transverse reinforcement has not been as rigorously investigated, and many studies have focused on CFCC stirrups. The use of C-Grid as an option for transverse reinforcing has not been previously investigated. This thesis concludes that C-Grid is a viable shear design option and presents the initial recommendations for design methods. These methods provide a basis for the design of C-Grid shear reinforcing that could be used as a starting point for future testing of full scale specimens.

This testing program first determined the mechanical properties of C-Grid and its development length. Four 18 ft long 19 in. deep beams, modeled after prestressed Bulb-T beams, were created to test the C-Grid, as well as steel and CFCC stirrups. The beams were loaded with a single point load closer to one end to create a larger shear load for a given flexural moment. Overall beam displacement was measured to determine when flexural reinforcement yielding was reached, and beams were fitted with rosettes and instrumentation to capture initiation of shear cracking. Shear capacity calculations following four methods were compared to test results.

The design method should follow the AASHTO modified compression field theory with equations for β and θ. The manufacturer's guaranteed strength should be used for design as long as that strength is the average reduced by three standard deviations. Shear crack widths are controlled to a similar size as steel stirrups when using at least two layers of grid.

C-Grid as Shear Reinforcement in Concrete Bridge Girders

John Charlton Ward III

Abstract - Public

Corrosion of reinforcing steel in concrete bridges in the United States requires costly repairs and replacements every year. The corrosion of the steel is due mainly to chlorides from deicing salts or seawater. The use of carbon fiber reinforced polymer (CFRP) materials as the reinforcing in bridges has the ability to prevent this corrosion, as carbon fiber does not corrode like steel when exposed to these chlorides. Some CFRP materials have been previously tested as the reinforcing in concrete beams, but this thesis concentrates on a material named C-Grid.

The C-Grid is a CFRP material that has strips in both directions to form a grid pattern. This material was placed in the concrete beams to act as the shear reinforcing for the beams, replacing the typical steel reinforcing bar used in these areas. Small-scale concrete bridge beams were created and tested using multiple shear reinforcing options. Other beams used standard steel shear reinforcing and a previously studied carbon fiber shear reinforcement option to compare to the C-Grid.

Results showed that C-Grid performed well compared to other shear reinforcing options. Comparing the failure to different other design methodologies showed this method provided a reasonable estimate of the strength of the beam. Using this methodology with a full size design example proved that C-Grid is a viable alternative to steel reinforcing bar as shear reinforcement. The use of C-Grid should allow a longer lifespan for bridges in the United States due to the lack of corrosion. This thesis provides the starting point for the design and future study of C-Grid reinforced concrete beams.

Acknowledgements

I would like to thank the following people:

- Dr. Carin Roberts-Wollmann for advising me throughout the project and letting me know when I was making bone-headed mistakes
- Dr. Tommy Cousins for sticking through the project with me throughout his move to Clemson University, especially when ridiculing me about coming from UVA.
- Dr. Jack Lesko for his advice and expertise into the world of FRP materials. Your help was much needed as the rest of the committee really understood concrete.
- Brett Farmer and Dennis Huffman for all their help in the laboratory. Without their guidance many graduate students would be lost out in the lab.
- Dr. David Mokarem for his help in test set-up, instrumentation, and general ridicule when the Hoos lost. He did provide me the valuable advice that "concrete is strong in tension".
- Mitch Magee and Carrie Field for their multitude of help in the lab during this project. Also, lest I not forget all my friends in the SEM department who helped me through classes and offered additional help in the lab when needed.
- Dr. Jose Gomez for his help in getting into graduate school at VT and ensuring Dr. Cousins picked me up on a project.
- VCTIR and CAIT at Rutgers for providing the funding to make this research and thesis possible.
- My sister for her love and support through graduate school.
- My mother for her constant encouragement and notes in the mail.
- My father for showing me what true strength and faith is this past year.
- My fiancée, Kristen Priamo, for her support, love, and words of encouragement throughout everything the past few years. I look forward to many more years with you.

Contents

List of Figures:

List of Tables:

1 - Introduction

Virginia is experiencing significant corrosion problems in prestressed bridge girders in the coastal areas such as Hampton Roads and Newport News. The chlorides in the sea water are leading the steel stirrups and prestressing cables in these bridges to corrode at an accelerated rate. The premature aging of this infrastructure will lead to expensive repairs and retrofits, so new alternatives must be found to extend their design life of new bridges.

Prestressed concrete bridges are used extensively in Virginia due to their long spans, ease of construction, and long lifespan with minimal maintenance. The major factor that determines lifespan of prestressed concrete beams in coastal regions is the reduction of load capacity due to corrosion of the reinforcing and prestressing. With the introduction of advanced materials and the increasing design life necessary for highway bridges, the use of materials other than steel is growing throughout the United States and Canada.

1.1 – Carbon Fiber Reinforced Polymers

Carbon fiber reinforced polymer (CFRP) is a material that has quickly gained footing as a replacement for steel reinforcing. CFRP is a material that does not corrode and has similar strength and modulus of elasticity to that of traditional steel reinforcing and prestressing. However, one of the major concerns with CFRP products is the brittle nature of the material. The use of CFRP as shear reinforcing is of great interest to Virginia Department of Transportation (VDOT), due to the increased design life and mitigation of corrosion in coastal areas.

Tokyo Rope in Japan produces a carbon fiber composite cable (CFCC) that is used in place of steel prestressing strand (Tokyo Rope, n.d.). The CFCC can be formed into stirrup shapes to use as transverse reinforcing in concrete beams. The fibers are bent into shape after the

polymer is applied, but before the polymer cures and creates a rigid bar (K. Ushi, personal communication, February 1, 2016). A typical CFCC stirrup is shown in Figure 1. While the performance of the CFCC stirrups is similar to steel, they are not a perfect solution, making VDOT interested in other CFRP transverse reinforcing alternatives.

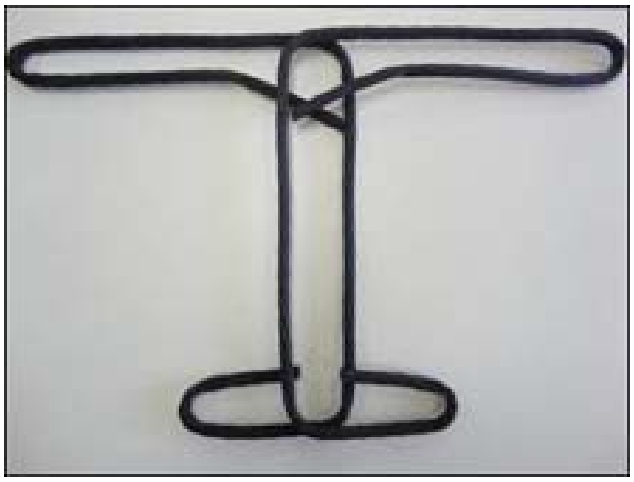

Figure 1: Typical CFCC Stirrup
(from Tokyo Rope, used with permission)

The first negative about the CFCC stirrups is the high cost. These items are custom made for every design. The stirrups are shaped immediately after application of the polymer and before the polymer fully cures. Since this is a thermoset polymer, no additional modification of the stirrup geometry can be made. Any fabrication error means these products will not fit into the formwork properly, which will lead to fabrication delays and added construction expense. Also, the stirrups must be formed by Tokyo Rope in Japan and this creates a two month lead time from order until delivery.

These disadvantages led VDOT to express interest in alternative CFRP options that do not need to be custom built for each specific bridge. Having a material on hand that could be modified or cut to size would allow the contractor to fabricate the beams faster. Also, if possible, VDOT would like a product produced in the USA, as federal highway funding is often

dependent upon this stipulation. These requirements from VDOT led to the investigation of alternate CFRP products that could be modified and placed by the contractors.

1.2 – CFRP Materials Selected

Several CFRP materials were considered for use in the project, but ultimately only a few were selected for further study. One promising option is CFRP grid products as they are easy to cut to size and place as transverse reinforcing in a concrete beam. The first grid selected for use in testing was C-Grid which is a CFRP product that is made in the United States (J. Leatham,

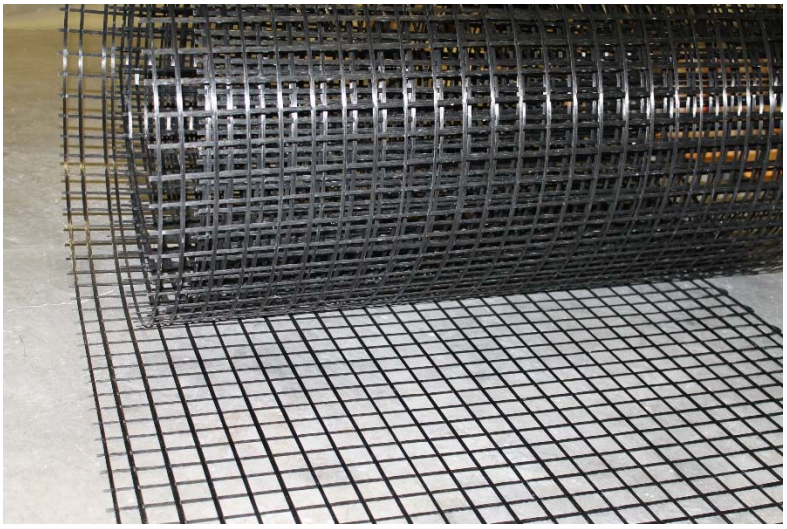

Figure 2: C-Grid Material

personal communication, August 6, 2014). C-Grid comes on large rolls, as shown in Figure 2, and can be cut easily to size. The second product chosen was NEFMAC grid, which is a heavier CFRP grid product than C-Grid (J. Crimi, personal communication, February 17, 2015). It is produced in Japan and comes in sheets of roughly 9 ft by 6 ft which can be cut to size or spliced as needed. It is shown in Figure 3. C-grid and NEFMAC grids were selected for use in the testing regime due to their ability to be field cut and adapted to use in multiple configurations. However, due to delays in manufacturing and ordering with the NEFMAC, this thesis only

contains tests using the C-grid. These items are very similar to welded wire mesh products that are used as temperature and shrinkage steel in many concrete applications.

Figure 3: NEFMAC Grid Material

1.3 – Project Objective

The original goal of the research project was to investigate C-Grid and NEFMAC grid products as transverse reinforcing in concrete beam sections. However, due to delays in the ordering and receipt of the NEFMAC, this thesis only covers the use of C-Grid material as a new shear reinforcement alternative. The first objective of the project is to determine basic material properties of the C-Grid such as tensile strength, modulus of elasticity and development length. The second objective is to investigate the behavior and strength of concrete beams containing C-Grid transverse reinforcement. To accomplish the second objective several reinforced concrete beams were tested with steel stirrups, CFCC stirrups, and C-Grid as the shear reinforcement. The tests were designed to induce a shear failure of the beams.

The third objective of the project is to determine the suitability of using shear design methodologies given by ACI (2012, 2006, & 2004) and AASHTO (2012) to determine the shear strength of a beam reinforced with C-Grid. The comparison of behavior of the beams containing C-Grid transverse reinforcement to beams containing steel and CFCC stirrups will show any

major differences in shear strength or crack propagation. The final objective is to provide recommendations for the design of beams using C-Grid transverse reinforcement for shear strength. These recommendations are presented at the end of this thesis along with a design example.

1.4 – Scope of Project

1.4.1 – Initial C-Grid Testing

C-grid was tested to examine tensile strength, modulus of elasticity, ultimate strain, and development length. First individual tows of the grid were placed in tension to test the available strength, ultimate strain, and modulus of elasticity. This was compared to the data presented by the manufacturer and used to determine if their data was conservative enough to be used for design. Development length tests were also conducted with embedment lengths of the C-Grid into concrete of 4, 5, 6, 7, and 8 in. These tests were conducted to design the flange and bulb height of the beams to ensure full development of the grid during shear testing and for recommended development length in future designs.

1.4.2 – Beam Tests

Four beams 18 in. deep and 18 ft long were built to test the steel, CFCC, and C-Grid shear reinforcing. The beams had minimum shear reinforcement ratio in one half and typical shear reinforcement ratio in the other half. One beam used steel reinforcing stirrups and acted as a control beam. For the other three beams, one used CFCC stirrups and two beams used C-Grid layers in different arrangements. All beams were designed so that the minimum and typical reinforcing sections would have similar strength as predicted by code provisions. Beams were designed to have shear failures during testing.

2 – Literature Review

2.1 – CFRP as Reinforcing/Prestressing

CFRP has a very strong case to be used as reinforcing and prestressing in concrete. One of the major benefits of CFRP is that its modulus of elasticity is nearly the same as typical steel used in prestressing and reinforcing. CFRP prestressing can also be made such that is has elastic stress-strain behavior similar to that of a typical seven wire 270 ksi strand (Tokyo Rope). However, CFRP is a very brittle material compared to steel. A CFRP prestressing rope can show about 1.7% elongation before failure (Grace, Ushijima, Baah, & Bebway, 2013). Compare this with a typical prestressing strand that yields at 1%, but then has enough ductility to continue to 4 or 5% elongation before failure (Nilson, 1987 & Tokyo Rope). In Figure 4, the stress strain behavior of prestressing strand is compared to the CFRP strand (labeled in the figure as CFCC).

2.1.1 – CFRP as Flexural Reinforcing

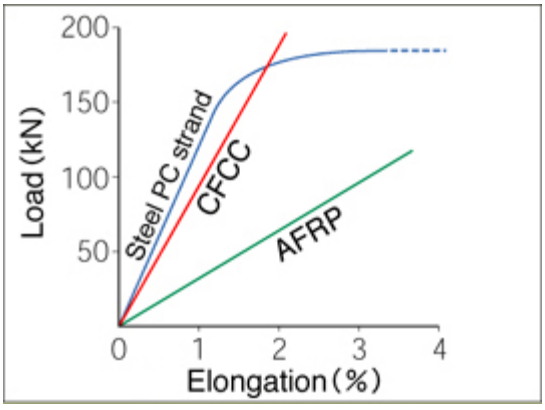

Figure 4: Elastic Modulus of Products for Concrete Reinforcement (from Tokyo Rope, used with permission)

CFRP has already been used as prestressing strand in some bridges in America (Grace, Jensen, Eamon, & Shi 2012). The CFRP prestressing currently used is very similar to seven-wire strand, and the most common manufacturer is Tokyo Rope. Figure 5 provides a picture of the typical seven-strand CFCC cable from Tokyo Rope. Grace has completed a considerable

amount of research in using CFRP prestressing strand, and provides a good starting point for considering the design of prestressed concrete using CFRP strand. One of his papers walks the reader through the design process when multiple levels of CFRP prestressing strands are used in a beam (Grace & Singh, 2003). Grace also constructed a full scale Double T beam, and tested the beam under multiple loadings (Grace, 2000), as well as box-beam (Grace, Enomoto, Sachidanandan, & Puravankara, 2006), and model bridges (Grace et al., 2013). This research in CFRP, combined with the state of disrepair of our current infrastructure s leading some DOTs to consider the use of CFRP in prestressed concrete due to the longer design life (Grace et al., 2012).

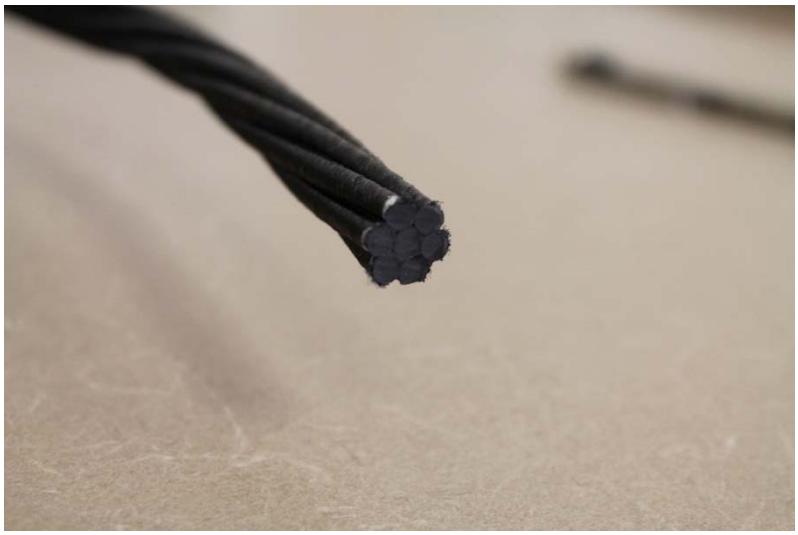

Figure 5: Seven-Strand CFCC from Tokyo Rope

Grace has a method for designing a beam with CFRP, which had previously not been developed (Grace & Singh, 2003). After determining the required moment capacity and cross-section of the beam, the balanced reinforcement ratio is calculated. This is the amount of reinforcing which results in concrete crushing occurring simultaneously with the rupture of the bottom most layer of tendons (Grace & Singh, 2003). Next, the beam's ultimate capacity is determined based upon the reinforcement ratio. The method depends on whether the beam is very under-reinforced, under reinforced, or over reinforced beams (Grace & Singh, 2003). This

method works on a stain compatibility approach with the ultimate compressive strain of concrete as 0.003 (Grace & Singh, 2003). It is also noted in this method that as the reinforcement ratio and prestressing level are increased the beams show not only more strength, but also ductility (Grace & Singh, 2003). The ductility that Grace refers to is an inelastic energy ductility, which is determined by the non-elastic area under the load-deflection plot. Over-reinforced sections show a larger area under the curve as the concrete will show some minimal inelasticity before failure. If the beam is under-reinforced, then it will fail elastically as the CFRP prestressing has no yield point and will fail when it reaches its ultimate load.

One important issue to take away from this research is the ductility of the CFRP beam is increased with a larger amount of reinforcement. This is due to the brittle failure mechanism of CFRP, as it ruptures before undergoing a large elongation like steel. This is a factor that the design engineer must understand, as it is the opposite of steel prestressing.

The designer also must ensure the strength of the CFRP used in calculations is much lower than the actual failure strength (Grace & Singh, 2003). The lack of ductility is an important aspect of bridge design, as excessive deflection can warn about impending collapses. Box beam bridges that were over reinforced were tested and again led to slightly more ductile flexural failures, but were still brittle compared to the results of a typical steel prestressed box beam (Grace et al., 2006). In 2013, Grace also tested an AASHTO I-Beam bridge, and found that his design method gave very close predictions of strength compared to actual test results. As long as the CFRP prestressing is used correctly, bridge beams can be safely designed with CFRP prestressing.

2.2 – CFRP Shear Reinforcing

While use of CFRP as flexural reinforcing has been studied and used in bridges across the US (Grace et al, 2012), the use of CFRP as additional reinforcing in reinforced concrete has not been studied extensively. One use of interest to VDOT of CFRP reinforcing products is shear reinforcing. Since shear stirrups often have the least cover, they have the most exposure to chlorides that accelerate corrosion. The uses of CFRP could help prevent spalling of the beam's outer layer caused by corrosion of the shear reinforcement, thus helping keep the bridge in better condition and mitigating the need for routine maintenance. Beam sections with CFRP transverse reinforcement have been studied, but not to the extent of longitudinal CFRP products.

Shear capacity in prestressed sections comes from the prestressing cable, concrete, and transverse reinforcement. CFRP prestressing strands add shear capacity to the beam when they are draped or harped in the section. However, CFRP is rarely harped in prestressed applications because the additional force applied laterally to the strand can cause premature failures. Reinforced sections do not have the additional benefit of additional shear resistance from the longitudinal reinforcement. Additionally, the codes specify a minimum amount of transverse reinforcement to ensure the beam does not fail in shear prematurely. Methods for shear design using CFRP are presented in section 2.3 of this thesis.

Most prestressed or reinforced concrete sections need shear reinforcement as they are not capable of carrying their maximum load otherwise. Using CFRP as transverse reinforcing helps to ensure a longer design life for beams and bridges. Transverse CFRP reinforcing research has mainly consisted of the use of CFRP stirrups. As more CFRP products continue to come to market the cost will be driven down allowing the CFRP to be more cost competitive with steel reinforcing, especially given the need for less maintenance.

2.2.1 – CFRP Stirrups

One option for CFRP shear reinforcement is solid bars similar to steel reinforcing. These "bars" can be made from the same strand material the prestressing cable is made from or more like a traditional reinforcing bar with ridges to help mechanical bond. The CFRP stirrups used in this thesis are the CFCC stirrups produced by Tokyo Rope. However, using CFRP as bent stirrups has some distinct disadvantages. First, CFRP that needs to have a bend must be produced by the manufacturer (A. Zickler, personal communication, June 23, 2014). Producing the bar offsite from the beam means that the shape must be perfect when it is shipped to the contractor as the bars need fit into the tight tolerances. Also, since the stirrups are already shaped and rigid, they must be put into place and the other reinforcing placed through or around the stirrups, which can be difficult in a congested section. Mistakes in bend radius or sizes means a long wait time when problems are found on site as most of these stirrups are made outside the US. One future solution to this problem are thermoplastic polymers that would allow the heating and shaping of CFRP materials on site. These thermoplastic polymers have not found use in concrete reinforcing products at this time.

Another issue with using CFRP bars is the fact that bending them in a tight radius decreases their strength. A radius on a bar similar to that of a No. 3 steel reinforcing bar can reduce the strength by 60% (Morphy, Shehata, and Rizkalla, 1997). The same study recommended not exceeding 50% of the parallel CFRP strength when designing CFRP stirrups to account for strength lost due to bends (Morphy et al., 1997). This creates a large cost impact as the stirrups must then be larger or spaced closer together. Since cost is such a big issue in most projects, this makes CFRP bars less cost competitive than steel bars, and hinders their use, as highway projects receive limited funding. According to Andrew Zickler at VDOT, the cost of

a CFRP stirrup is approximately nine times that of a typical steel stirrup (personal communication, June 23, 2014).

Using CFRP bars as shear reinforcing is an area that needs more research before it becomes cost effective and easy for contractors. The preforming of stirrups requires a lot of precision and lead time to get everything to fit up properly. Any problems with fit up could create huge delays and major cost overruns with the project. VDOT is hoping to find a possible solution that can be cut or bent on site by the precaster and then placed into the forms, thus eliminating the need for bars to be created by a third party.

2.2.2 – NEFMAC Grid

NEFMAC grid is a CFRP product that is a replacement for welded wire mesh. This product is produced in locations outside the US, but one company in Canada has used the material in multiple structural applications. One such application is as the reinforcing in a bridge deck in Canada (Steffen et al., 2003). Placing the NEFMAC grid was found to be faster than placing conventional steel reinforcing as it did not require a large amount of tying in place due to the large grid sheets that needed fewer connections (Steffen et al., 2003). Also, the light weight allowed the large sheets to be handled by fewer people than welded wire mesh and the sheets were easier to set in place (Steffen et al., 2003). NEFMAC grid comes in different spacing configurations and member thicknesses depending on the application. One issue noticed with the NEFMAC grid was that it floated when concrete was placed and would not stay in the proper location. Tying the grid to PVC spacers kept the grid in place and prevented it from floating to the surface (Steffen et al., 2003).

2.2.3 – C-Grid

C-Grid is a product very similar to NEFMAC grid, but it is manufactured by Chomarat North America in Anderson, SC**.** C-Grid is one of the only CFRP concrete reinforcing manufacturers in the US. C-Grid was designed for use in precast wall panels, but has also been used in the topping of precast double T's (T. Cousins, personal communication, July 2014). Its use has allowed thinner flanges in double T's due to the smaller amount of cover needed compared to steel (T. Cousins, personal communication, July 2014). C-grid has not been used as shear reinforcing in large scale members, as its tension capacity is on the order of 5 kip/ft width of material, making it much weaker than typical steel stirrups. It is possible that Chomarat could start producing a higher strength material if they see a viable market for the product in the future.

Both the C-Grid and NEFMAC fabrics show great potential for a shear reinforcing solution. These materials can be fabricated in different strengths and can easily be cut and put in place in the field. Zip ties can be used to tie the material in place when the concrete is placed, and the light weight makes handling very easy for contractors (Steffen et al., 2003). The main design hurdle to get over with these products is producing configurations that provide the needed capacity. Also, more research will be needed to learn the required development length of the grid products to ensure their safe use in bridge beams.

2.2.4 – CFRP Strip Stirrups

Another possible CFRP reinforcing method is to use fiber strips internally as reinforcing. These strips are made of the same materials that are used in exterior bridge repair and rehabilitation methods (Lee, Jeong, & Park, 2009). The stirrups are cut from sections of typical CFRP weave fabric and can be impregnated with a polymer when laid in place, or left unimpregnated. Figure 6 shows a typical layup of the fabric stirrups. The impregnation of the

polymer helps ensure composite action (Lee et al., 2009). No additional shear capacity was found in the impregnated stirrups by placing a second layer in the bend area, but unimpregnated stirrups did have an increase with more layers in the bend radius (Lee et al., 2009). The bend of the fabric stirrups is weakest area of the CFRP strips.

The impregnated fiber stirrups gave the beams a higher overall strength. This was due to the polymer causing the fibers to act as one unit instead of individual fibers that would fail independently (Lee et al., 2009). Roughening the surface of the stirrups with aluminum oxide powders increased the capacity of the beams due to the increased the mechanical bond of the concrete to the CFRP stirrups (Lee et al., 2009). Also, shear stirrups are more likely to rupture with a low strain, which is thought to occur due to the impact from shear crack propagation (Lee et al., 2009). This is due to the failure of one stirrup leading to an unzipping effect, as each stirrup that fails increases the force above ultimate on the next stirrup. The stirrups are easy to fabricate, but based on the process of laying our strips and impregnating with polymer, it is very labor intensive. Also, the polymer cure time could be of concern in projects that have a tight schedule.

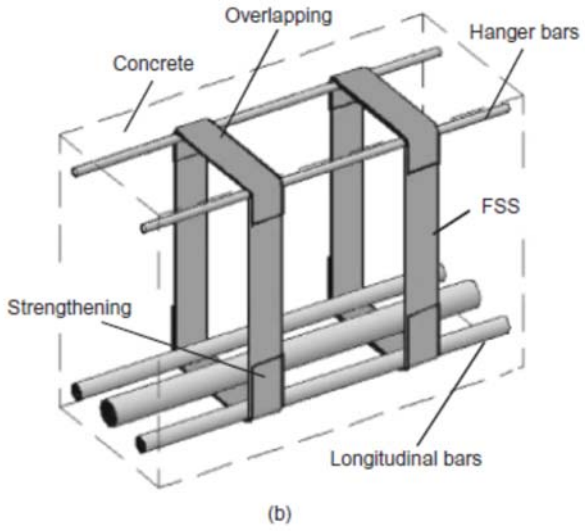

Figure 6: Fabric Stirrup Layup Example
(from Lee, Jeong, & Park, 2009, used with permission)

2.3 – Methods for Shear Design with CFRP

2.3.1 – AASHTO Shear Design Method

The American Association of State Highway and Transportation Officials (AASHTO) provides the specifications for reinforced and prestressed concrete member design for use in bridges. These stipulations are familiar to bridge engineers, but are designed for the use of steel reinforcing bars and prestressing cables. The AASHTO shear resistance is broken into three parts and presented in chapter 5 of the specifications: resistance of the concrete, resistance from transverse reinforcement, and the additional resistance from the vertical prestressing force. While the AASHTO specifications present many shear design methods, this thesis will present the general shear design method using equations.

The shear resistance of the AASHTO method is based upon the Modified Compression Field Theory, which was first developed by Vecchio & Collins (1986). This method uses a prediction for the angle of shear cracks occurring and calculates a factor, β, to account for the concrete strength. The basis of the concrete strength is the development of tensile stress in the concrete due to the capacity of the concrete pre-cracking and the aggregate interlock post-cracking. To develop appropriate aggregate interlock the cracks have to be restrained by the transverse and longitudinal reinforcement to stay small enough to allow the engagement of the aggregate. If the cracks grow too large, then the aggregate will not be able to interlock and the loss of the concrete capacity for the shear capacity can occur.

The concrete shear resistance term for concrete is given based upon the concrete compressive strength, the area of concrete resisting the shear forces (typically the thinnest portion of the web), and then a factor β that is calculated based upon the strain in the tension reinforcing. This means β is dependent upon the ratio of tension reinforcing and the load the

beam resists as it will impact the strain in the tension steel. The concrete shear resistance equation is shown below as Equation 1. β is the factor used to indicate the ability of the cracked concrete to transmit tension and shear. f'_c is the 28 day compressive strength of the concrete in ksi. b_v is the effective web width in inches, which is the minimum web width over the effective shear depth, d_v, again in inches.

$$V_c = 0.0316\beta\sqrt{f'_c}b_v d_v \quad \text{(Eq 1)}$$

The shear resistance from the transverse reinforcement is given based on the Equation 2 given below. The term s is the spacing of the transverse ties (or tows if a grid material is used) in inches. A_v is the area of transverse reinforcement between each spacing in square inches. The angle of the transverse reinforcement from the horizontal is the α term, and the units are degrees (90 degrees in most designs). The θ term is the angle of diagonal compressive stresses in the section in degrees.

$$V_s = \frac{A_v f_y d_v (cot\theta + cot\alpha) sin\alpha}{s} \quad \text{(Eq 2)}$$

If the transverse reinforcing is placed at 90 degrees to the longitudinal axis of the section then the equation simplifies to:

$$V_s = \frac{A_v f_y d_v cot\theta}{s} \quad \text{(Eq 3)}$$

This is the equation that is most common in design and θ is dependent upon the strain in the tension steel. Again, if a smaller strain in the tension steel is present, the value of θ is smaller. The strain is dependent upon the longitudinal reinforcing ratio and the loading to which the section is subjected.

Prestressed sections receive the additional benefit of additional shear resistance from the prestressing, with the term V_p. This force is the vertical component of the prestressing force due

to harped or draped tendons in kips. Using this additional capacity can help reduce the amount of shear reinforcement needed, especially in beams with a large amount of prestressing. Since the tests in this thesis use reinforced sections, there is no additional benefit from prestressing. Also, CFRP tendons are rarely harped due to the lateral force on the strands from the harping points. This force can cause premature breaking of the strands during the tensioning process.

The terms β and θ in the equations for the V_c and V_s term depend on the amount of longitudinal reinforcement in the section and the loading the section undergoes. The term ε_s is the strain in the tension reinforcement of the beam. A higher loading on the beam will result in a higher ε_s for all longitudinal reinforcement ratios. Also, if the section has a larger longitudinal reinforcement area or modulus of elasticity, then ε_s will be smaller. The equations for β and θ from the AASHTO general method in chapter 5 are presented in Equations 4 and 5 below.

$$\beta = \frac{4.8}{(1 + 750\epsilon_s)} \quad \text{(Eq 4)}$$

$$\theta = 29 + 3500\varepsilon_s \quad \text{(Eq 5)}$$

A smaller ε_s will give a larger β term, the concrete resistance to shear will increase due to increased aggregate interlock. The smaller strain also will make the angle of major shear cracking, θ, smaller, which increases the shear resistance of the transverse reinforcement as the crack will cross more stirrups. Therefore increasing the flexural reinforcement of the beam under the same loading and with the same transverse reinforcement can increase the shear capacity of the beam.

AASHTO also provides guidance on the calculations of the strain in the steel and the equation is presented below as Equation 6. The equation calculates the force in the tension steel under maximum considered loading and then divides it by the stiffness of the longitudinal reinforcing to determine the strain. M_u is the factored moment of the beam in kip-inches. N_u is

the factored axial force in the section in kips. V_u is the factored shear force in kips and it is reduced by the shear resisting component of the prestressing, V_p. E_s and A_s are the modulus of elasticity of reinforcing steel in ksi and area of tension reinforcing steel in square inches respectively. E_p is the modulus of elasticity of the tensile prestressing steel in ksi. A_{ps} is the area of the tensile prestressing steel in square inches. f_{po} is a parameter that accounts for the amount of force in the prestressing cable, which is typically taken a $0.7f_{pu}$, where f_{pu} is the ultimate stress of the prestressing steel in ksi.

$$\epsilon_s = \frac{\frac{[M_u]}{d_v} + 0.5N_u + [V_u - V_p] - A_{ps}f_{po}}{E_sA_s + E_pA_{ps}} \quad \text{(Eq 6)}$$

The AASHTO general method with equations provides a straightforward approach to the calculation of the shear resistance of prestressed and reinforced concrete sections. This method is a common method that practicing bridge engineers use to calculate the shear capacity of their sections. The increase in shear resistance from lower strain in the tension reinforcement is a direct result of studies completed using the modified compression field theory.

2.3.2 – ACI 318-14 Shear Design Method

The American Concrete Institute (ACI) 318 Building Code provides design guidelines for the shear capacity of both reinforced and prestressed beams when using steel. Since the beams in this thesis are reinforced, the method for shear capacity presented is for reinforced section. ACI provides the shear resistance through two components of the section. The first component is based on the shear resistance of the concrete. The formulas for concrete are empirically based from fitting curves to data sets previously tested. The contribution of the reinforcing is the second component of shear resistance and is based upon spacing and yield strength of the

reinforcing. The total shear resistance of the member is the sum of the concrete and reinforcing portions to provide the total shear resistance of the concrete section.

ACI 318-14 provides the general reinforced concrete provisions for designing with steel reinforcing. Equation 22.5.5.1 is show below as Equation 7 and f'_c is the 28 day design compressive strength of the concrete in psi. λ is a modification factor for the reduced tensile and shear strength of lightweight concrete (1.0 is used if normal weight concrete used). d is the depth of the section from the extreme compression fiber to center of tension reinforcement in inches and b_w is the minimum web width inches. It is the most used equation for the contribution of concrete strength in shear and flexure members from the ACI code. There are additional equations that take into account axial force, but the majority of beams do not have a significant axial force.

$$V_c = 2\lambda\sqrt{f'_c}b_w d \quad \text{(Eq 7)}$$

The contribution of steel is expressed in equation 22.5.10.5.3 which is presented below as Equation 8. s is the center-to-center spacing of the transverse reinforcement in inches. A_v is the area of transverse reinforcement in square inches within the spacing. f_{yt} is the specified yield strength of the transverse reinforcement in psi. When using CFRP f_{yt} should be the specified design strength of the tow or bar, as these products do not yield. ACI also provides a minimum amount of shear reinforcement that is required in members to ensure a sudden shear failure does not occur.

$$V_s = \frac{A_v f_{yt} d}{s} \quad \text{(Eq 8)}$$

To find the total shear strength of a reinforced member the contribution of the reinforcing and concrete contributions are summed together to find the nominal shear resistance of the section.

2.3.3 – ACI 440.4R-04 Shear Design Method

ACI 440.4R-04 proposes guidelines for the design of prestressed FRP concrete sections. It covers the complete design of prestressed concrete sections with FRP prestressing tendons as well as the additional FRP reinforcement for shear strength. The shear design method in this document mirrors the standard shear design method from ACI 318. The two equations are presented below as Equations 9 and 10, which are equations 5-2 and 5-3 respectively in the 440.4 document. One interesting note is that this document does not provide an additional shear resistance from the prestressing strands.

$$V_c = 2\sqrt{f'_c}b_w d \quad \text{(Eq 9)}$$

$$V_{frp} = \frac{A_v f_{fb} d}{s} \quad \text{(Eq 10)}$$

The concrete resistance equation uses the same factors as ACI 318-14, but removes the lightweight concrete modification factor. Many of the terms are the same as those previously described in the ACI 318 section. The reinforcing equation is the same except f_{fb} is the strength of the bent portion of the FRP bar in psi. f_{fb} is based upon the minimum design strength of the bend in the FRP stirrup, which is the weakest area of the stirrup according to past studies. It takes into account the bend radius and diameter of the bar to ensure a safe, conservative design when using FRP stirrups. Equations 11 and 12 are presented below to calculate f_{fb}. f_{fu} is the design tensile strength of the FRP in psi and E_f is the design modulus of elasticity of the FRP in

psi. ϕ_{bend} is a strength reduction factor that depends on the radius of the bend in inches, r, and also the diameter of the FRP bar in inches, d_b.

$$f_{fb} = Lesser\ of: \phi_{bend} f_{fu}\ or\ 0.002E_f \quad \text{(Eq 11)}$$

$$\phi_{bend} = \left(0.11 + 0.05\frac{r}{d_b}\right)\ and\ 0.25 \leq \phi_{bend} \leq 1.0 \quad \text{(Eq 12)}$$

This is to ensure that the bar will not rupture at the bend, and all FRP stirrups should be closed with a 90 degree bend. This bend should have a $\frac{r}{d_b}$ of 3.0 or greater and have a minimum tail length of 12 bar diameters.

2.3.4 – ACI 440.1R-06 Shear Design Method

ACI 440.1R-06 provides guidelines for the design and construction of reinforced concrete sections using FRP reinforcement. This document provides all applicable design procedures for a section where all the reinforcement is FRP and no prestressing is used. The shear capacity method still uses the concrete and transverse reinforcement shear resistance equations, but the concrete resistance equation is much different than other two methods shown previously. The 440.1R document defines the concrete contribution with Equation 13. Again all these terms except for c, which is discussed below, were defined in the ACI 318 shear design section.

$$V_c = 5\sqrt{f'_c} b_w c \quad \text{(Eq 13)}$$

This equation was developed to provide a better estimate of shear reinforcing based on the strain in place in the longitudinal steel in the section. The term c is the distance to the neutral axis from the compression face in inches, which is calculated from the cracked transformed section. The cracked transformed section takes into account the stiffness of the longitudinal tension reinforcement which is the product of the area and modulus of elasticity. If the stiffness of the longitudinal reinforcement is larger, then c will be larger to balance forces and lead to

increased shear resistance from the concrete. This is due to a larger section of concrete in compression, which will mean there is less cracking, and in turn the section will have better aggregate interlock to resist the shear forces. Also, more shear can be carried in the uncracked concrete again increasing the shear resistance of the section.

The reinforcing shear resistance is very similar to the other ACI methods that have been previously described. The FRP resistance equation is shown below as Equation 15. The terms d and s were previously defined in the ACI 318 section. A_{fv} is the area in square inches of transverse FRP reinforcement in the spacing s. f_{fv} is the design tensile strength of the FRP in psi, which is limited to the smallest of: design tensile strength of bar, design bend strength of bar as shown in Equation 14 where the terms in the equation are described in the section above, or 0.004 times the modulus of elasticity of the FRP bar.

$$f_{fb} = (0.05 \times \frac{r_b}{d_b} + 0.03) f_{fu} \leq f_{fu} \quad \text{(Eq 14)}$$

$$V_f = \frac{A_{fv} f_{fv} d}{s} \quad \text{(Eq 15)}$$

The ACI equations provide easy methods for calculating the shear resistance of concrete sections. The method presented in ACI 318 and ACI 440.4R are easy methods that are based on section geometry and previous testing to provide conservative design guidelines. The method shown in ACI 440.1R uses the same methods for reinforcing shear resistance, but moves to the method described by Tureyen and Frosch for the concrete resistance (2003). This method depends on the neutral axis depth of the section, so increasing the longitudinal reinforcing will increase the shear resistance of the concrete. This method is similar to the AASHTO method in that increasing longitudinal tension reinforcing will increased the shear capacity of the concrete.

2.4 – Prior FRP Shear Tests

2.4.1 – Shehata, Morphy, and Rizkalla - 1997

CFCC stirrups have been used as transverse reinforcement in a testing regime by Shehata, Morphy, and Rizkalla (1997). Three materials were used as stirrups in this testing: CFCC stirrups, CFRP Leadline stirrups, and GFRP C-Bar stirrups. Initial testing was done on all FRP stirrup materials to determine development length. These tests examined fully closed rectangular stirrups where each end was embedded into a block of concrete. The testing was carried out by placing a hydraulic jack between the blocks and applying a load to separate them. A total of 40 panel specimens were created for the testing. Results of the development length testing showed that the CFCC stirrups were likely to fail at the bend, especially with the larger diameter stirrups. Findings also indicated that if an embedment length before the bend of 6 in. was used, then the stirrups could develop full strength of the fibers in the parallel direction. However, if a smaller embedment length was used, then the stirrup was likely to break at the bend and have reduced strength. This premature failure could be as low as 43% of the parallel strength of the bars.

A total of six beams were created for shear testing and placed in four point bending. Three beams used CFRP Leadline stirrups, one GFRP C-Bar stirrups, one traditional steel stirrups, and the last used no transverse shear reinforcement. Testing found that the FRP materials could perform adequately as transverse reinforcement. Also, the use of CFRP Leadline stirrups resulted in a similar crack width to an equivalent ratio of steel transverse reinforcement. This is an important finding, as CFRP and steel stirrups would both provide similar performance during high loads to limit cracking of the section. Shehata additionally noted that for close spacing of the stirrups, cracks were more likely to cross the bent zone of the stirrups, which can

cause overall reduction of capacity. It was noted by the authors that CFCC stirrups should be limited to 50 percent of their parallel fiber strength when used in design.

2.4.2 – Grace, Rout, Ushijima, and Bebway - 2015

Grace, Rout, Ushijima, and Bebway (2015) completed some interesting research into the use of CFCC stirrups for shear reinforcement in bridge girders. Testing was in two parts; the first to determine bend strength of the CFCC stirrups at a small scale and the second was full scale prestressed bridge girders. This testing used full hoop stirrups with each end embedded into a block of concrete. A hydraulic jack was placed between the blocks and a load applied to separate the blocks until failure of the stirrups occurred. Findings indicated that insufficient embedment length led to slip of the CFCC stirrup before failure of the bend. If proper embedment length was provided then the stirrup would fail in the embedment region just above the bend. With proper embedment of the stirrups it was found that the strength of the stirrup was still around 50% of the parallel strength of the fibers. Additional findings also showed that the maximum strain of stirrups given in ACI 440.1R as 0.4%, 440.4R 0.2%, and AASHTO as 0.35% are conservative. Findings showed that ultimate strain at failure for a bar with and radius to bend ratio of 2.0 was 0.68%.

The second phase tests used eleven full scale prestressed beams with CFCC stirrups on one end and steel on the other end of the beam. Nine beams were 39 ft long while the remaining two beams were 40 ft long. Each beam was tested as a simple span with a point load closer to one support to ensure shear failure. Two tests were run for each beam to compare the CFCC and steel stirrups. Stirrup spacing was 4 in., 6in., and 8 in. for all the beam specimens and all were tested until flexural-shear failure.

Results indicated that failure strain at the bend of the CFCC stirrups was higher than the stirrup strain at failure in the beams, leading to the conclusion that bend failures in shear are unlikely. Also, the authors found that the failure strain of the CFCC closely matched with the 0.35% allowable by AASHTO, which was developed for any transverse reinforcement material. The CFCC stirrups also had similar performance to the steel stirrups except for the yielding that the steel exhibited. Steel and CFCC ultimate loads varied significantly, indicating that steel design guidelines are most likely satisfactory for CFCC stirrups. Also, the findings show that the ACI 440.4 method for determining shear resistance is quite conservative and tested beams had an average strength of 1.8 times the calculated capacity. However, the use of the AASHTO method had a 0.83 ratio of actual shear strength to the predicted. The authors recommend that ACI 440.4 be revised to include more accurate CFRP shear design guidelines.

2.4.3 – Fam – 1996

A study using CFRP prestressing and transverse reinforcement in five large scale I-beam was undertaken by Fam (1996). Additionally one beam using steel prestressing and transverse reinforcement was built to compare as the control for the tests. Beams were simply supported and used four point loads near the center of the span. The draping of the CFRP prestressing was varied and also the size, type, and spacing of the CFRP transverse reinforcement was varied. Transverse reinforcement included CFCC stirrups, CFRP Leadline stirrups and the steel control beam.

Findings indicated that prestressing with CFRP tendons provided similar results to using steel prestressing cable. Also, larger transverse reinforcement ratios did help limit crack width and the stress in the stirrups, as there is a larger area and more closely space stirrups to transfer the load to from the concrete. The modified compression theory also presented the best

prediction of the shear behavior of the sections tested in this study. When shear failure did occur in the beams with CFRP prestressing and transverse reinforcement, the failure was catastrophic. After the CFRP stirrups failed a large load was placed on the longitudinal CFRP which then fractured as well. This is important to note to ensure safe designs are followed to design a beam with full CFRP reinforcing and prestressing.

2.4.4 – Nabipaylashgari – 2012

Research into the shear capacity of CFRP prestressed beams was completed by Nabipaylashgari (2012). Eight T-beams were designed for the study that used CFRP prestressing, with four of the beams having no transverse reinforcement and four beams with GFRP transverse reinforcement. Six of the beams were placed under four point bending with span to depth ratios of 1.5, 2.5, and 3.5. The last two beams were placed under uniform loading.

Testing of the beams under four point bending led to shear failures, but the span to depth ratio of 1.5 carried more load due to arching action of the force. When minimum stirrups were added the shear resistance of the 2.5 and 3.5 span to depth ratio beams increased by 8%, while the 1.5 ratio beam showed no increase. Beams with distributed loading showed a 42% increase in shear cracking load and 63% increase in ultimate shear load. ACI 440.4R-04 was found to result in a conservative value for calculating the shear component of the concrete, as it ignores the increase in force due to prestressing of CFRP (Nabipaylashgari, 2012). This creates a very conservative design following the ACI 440.4R-04 criteria, which was also noted by Grace.

2.4.5 – Jeong, Lee, Kim, Ok, and Yoon – 2006

CFRP grids have had very little study as transverse reinforcement in concrete members. A study was undertaken by Jeong, Lee, Kim, Ok, and Yoon (2006) that used GFRP longitudinally reinforced concrete members with CFRP grid as the transverse reinforcing.

However, instead of laying out the grid longitudinally in the beam so it provides continuous support, this study used grid sections perpendicular to the length of the beam like stirrups. Figure 7 from the study illustrates the layout and use of the grid in the test sections. The grid sections are the vertical lines shown in the beam.

The first testing undertaken in the study was initial axial tension testing of GFRP and CFRP materials to find the ultimate strength and modulus of elasticity. The study concluded that the tested tensile strength of the materials was higher than the strength reported by the manufacturer, while the elastic modulus was the same value. From this conclusion, the authors stated that the manufacturer's reported information could be conservatively used for design.

Four beams were designed which used bundled GFRP longitudinal bars for the flexural reinforcement. All beams used CFRP grid shear reinforcement and used the following spacings: 5 in., 7 in., 10 in., and 20 in. Specimens were placed in four point bending with the two point loads being applied closer to one support to cause higher shear forces.

The study found when spacing was less the than the effective depth of the beam, flexural compression failure controlled the beams as expected. If the spacing was larger than the beam depth, then a shear failure occurred near the support. However, by design guidelines, the spacing is not allowed to be larger than the depth of the section. Shear reinforcement spacing is limited to ensure this type of failure does not occur. The design of the beams in the study was undertaking using ACI 440.1R, as it pertains to the design and construction of FRP reinforced concrete. The authors concluded that the failures matched closely with those expected when designing with the ACI 440.1R guidelines.

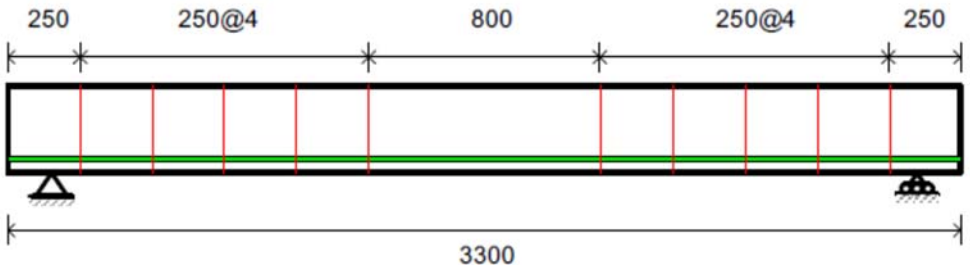

Figure 7: CFRP Stirrup Layout
(from Jeong et. al., 2006, used with permission)

2.5 – Summary

CFRP presents a promising alterative to steel reinforcing as the lack of corrosion can provide an extended service life for concrete bridge members. With this in mind VDOT is interested in the use of CFRP materials especially in the coastal areas of the state. However, the cost of the CFCC stirrups and the lack of field modification makes them less attractive to VDOT. Therefore CFRP materials are needed that can be field modified by contractors and be more cost competitive with steel stirrups.

There has been very little research into the use of CFRP grid materials as transverse reinforcement in flexural concrete members. The grids offer the flexibility of field cutting and modification which gives the contractors more control over the final beam and helps reduce lead time. Also, by laying up multiple layers of grid the can increase the shear capacity. This thesis undertakes a study of C-Grid as transverse reinforcement in reinforced concrete beams. This will provide a basis for recommendations to designers and future study into CFRP grid products.

3 – Test Methods

3.1 – C-Grid Tensile Strength Tests

Tensile testing was conducted to ensure that manufacturers' reported axial strength and modulus of elasticity were accurate (Chomarat North America, 2010). Testing included two different spacing patterns of C50 grid product cut into individual tows for a total of 20 specimens. Testing followed recommended procedures of the manufacturer, Chomarat, to ensure the most accurate results (Chomarat North America, 2011).

3.1.1 – Test Specimens

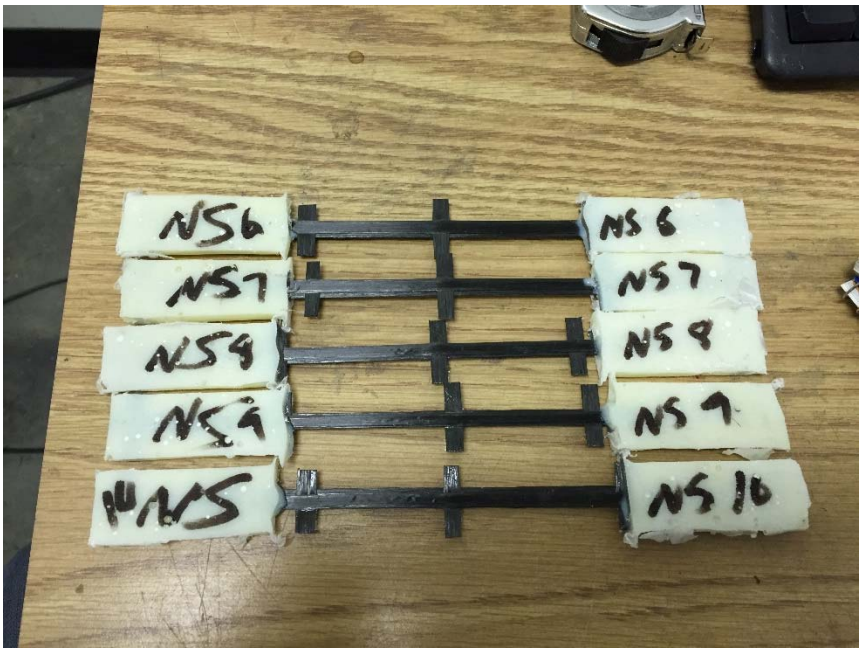

Figure 8: Tensile Strength Specimens

Testing was carried out using single tow specimens with an epoxy grip at each end. The epoxy end mitigated crushing of the fibers in the grips of the testing apparatus. Test specimens were cut from C50 1.6x1.8 grid and C50 2.36x2.36 grid. C50 refers to the amount of fibers in each tow, which determines the strength of the tow. The second two numbers refer to the spacing of the tows in each direction. Five specimens of each grid in each tow direction were used, for a total of 20 specimens. Both directions of tow were used to ensure all C50 grid was

the same strength, no matter the direction of the tows. Molds for end grips were created from plywood and lined with wax paper to allow the easily removal after the curing of the epoxy. Scotch-Weld DP 420 epoxy was used for the ends to keep the grips from crushing the CFRP tow. Epoxy was mixed in disposable cups and then poured into the forms and allowed to cure for 24

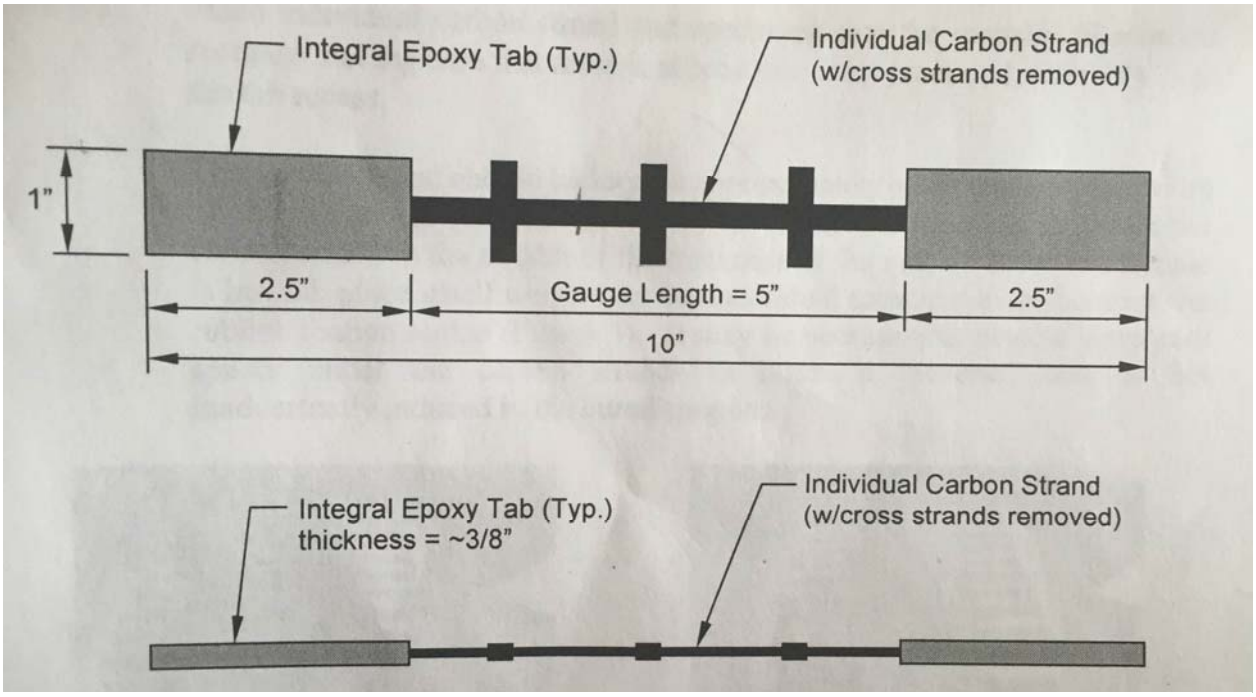

Figure 9: C-Grid Tensile Specimen Dimensions
(from Chomarat North America, 2011, used with permission)

hours before removal. Test specimens are shown in Figure 8 and the suggested dimensions, which were used during testing, of the specimens are shown in Figure 9.

3.1.2 – Test Instrumentation and Set-Up

Each specimen's width and thickness were measured using calipers to determine the cross-sectional area. Each specimen was then placed into an MTS testing machine and an extensometer was attached via orthodontic rubber bands. Elongation speed of the crossheads was set to 0.079 in/min per the supplied testing protocol from Chomarat North America (2011). Specimens were loaded in tension to failure, while continuously recording the load and

elongation data. Complete failure resulted in brittle fracture of the specimen as shown in Figure 10. This method was conducted for all 20 specimens of C-grid.

Figure 10: Typical Failure of Tensile Specimen

3.1.3 – Instrumentation

Each specimen was tested using an MTS Insight testing machine, which contained a pre-calibrated load cell to record the load on the specimen. Each specimen also used an MTS 634.25 extensometer to measure the strain of specimens under axial load. Since specimens were not flat, the extensometer would not stay attached with the built-in clips. The cross-section of the specimens was thicker in the center and thinner at the edges, which can be best described as a half dome. Orthodontic rubber bands were used to affix the extensometer to the specimen, which held the extensometer in place very well. Data acquisition was handled by a dedicated computer attached to the MTS Insight. Data was recorded continuously during testing until failure of specimen was reached.

3.2 – C-Grid Development Tests

There has been minimal research into the development length of C-Grid and it was an important factor in the overall design of the beams for shear testing. A previous test conducted by Ding, Rizkalla, Wu, and Wu (2011) served as the basis for the conducted testing. Embedment length was varied for the C50 1.6x1.8 grid with the 1.8 in. spacing in the vertical direction.

3.2.1 – Test Specimens

Previous testing of the C-Grid by Ding et al. had shown that development length for their C100 grid was 8 in., as the 4 in. test did not develop sufficient strength before slip (2011). A test specimen was designed based upon this previous testing, but specimens were designed to investigate smaller development lengths as the C50 1.6x1.8 grid had closer spacing and less strength than the previously tested grid. Tested embedment length was varied from 4 in. to 8 in. in 1 in. increments. Two specimens of each development length were built, for a total of ten specimens.

Formwork was designed to come apart easily and allow the specimens to sit on the base during testing. This was designed so that the specimens were not damaged when moving them from the concrete placement location to the testing location. The base also had a split to allow the specimen to easily separate so friction would not influence the results of the testing.

The grid tested was the same C50 1.6x1.8 grid that was used in the tensile tests, as it was one of the strongest and tightest spacing offered by Chomarat. Testing used 2 in. of clear cover on all sides of the C-grid to ensure that a proper bond was developed and that edge regions did

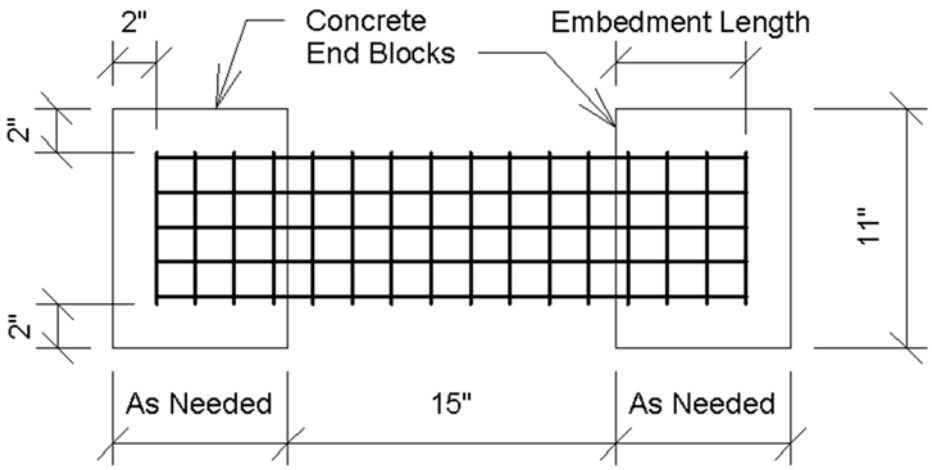

Figure 11: Diagram of Development Length Specimen

not split. Specimen naming convention followed the standard of 8-1, where the 8 represents the inches of embedment of the grid and the 1 indicates the specimen number for that embedment length. Typical specimen diagram in shown in Figure 11. All blocks were 12 in. wide and diagrams of C-Grid embedment for each length are shown in Appendix D.

3.2.2 – Test Methods

Figure 12 shows the test set-up with instrumentation and collar to catch the specimen upon fracture. Specimens were designed as rectangular prisms of different lengths to allow different embedment lengths. All ten specimens were placed from one batch of concrete to limit variability in concrete among the tests. Concrete design had a 28 day compressive strength of

Figure 12: Development Test Setup

5000 psi and used small aggregate with high range water reducer to enhance workability. Enhanced workability was necessary to ensure proper consolidation of concrete around C-Grid. This concrete was selected as it was on the low end of strength that VDOT would use in prestressed concrete and also was similar to the compressive strength of typical reinforced concrete strength.

For testing each specimen was placed on a roller table and then the formwork was removed. As shown in Figure 12, the base was split so that friction of the concrete block against the plywood had no effect on the test results. Also, difficulty was found in properly aligning the jack in both the vertical and horizontal axes, so that the load was in the middle of the blocks. A load cell was placed between one block and the jack. Extensometers were attached to each side of the specimen to measure the amount of elongation of the grid on both sides of the specimen.

The tests were conducted by increasing the load until rupture of the grid material between the two concrete blocks. In almost every test the grid ruptured on one side first. After a few tests, a collar frame was created to help control the violent fracture of the grid. A typical failure of the development specimens is shown in Figure 13.

Figure 13: Typical Development Length Failure

3.2.3 – Instrumentation

Data acquisition was handled by a System 5000 computer system produced by Vishay Instruments. Instrumentation consisted of a 50 kip load cell, and Trans-Tek 8 in. barrel LVDTs to measure elongation of each side of the specimen. The LVDT length was extended through the use of PVC pipe extenders as the LVDTs were not long enough to reach from one concrete block to the other. The LVDT data was used to determine slip in the grid on either side and also showed the amount of unequal strain in the two sides due to loading not being perfectly aligned. LVDT brackets and PVC extenders were attached to the blocks via a two part epoxy with a 60 second cure time available at any local hardware store. LVDTs were slid through the bracket and then tightened into place via a hose clamp. Figure 14 shows the typical instrumentation used in the test. The load cell is against the left concrete block in the figure.

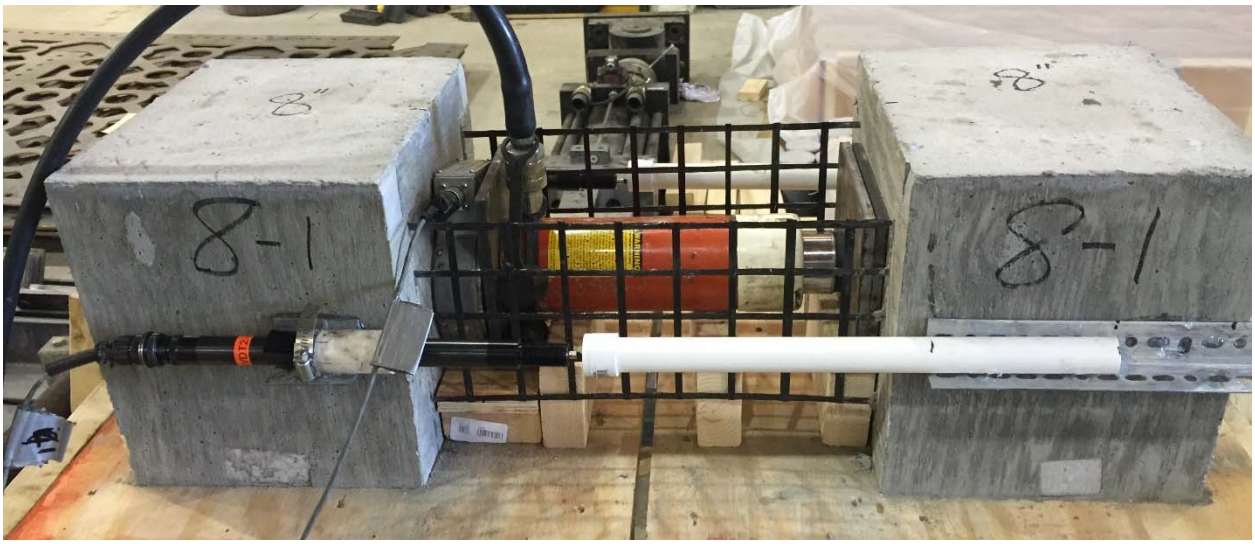

Figure 14: Development Length Instrumentation

3.3 – Beam Tests

Four beam specimens were fabricated for testing and concrete was placed for two beams at a time. One beam was a control with steel stirrups throughout, one beam used CFCC stirrups throughout, and two beams used various amounts of C-Grid as the shear reinforcing. Beams

were 19 in. deep and the cross-sectional shape was based upon a scaled down version of a typical Bulb-T beam used in highway bridges. Two tests were planned for each beam to allow for a total of eight tests.

3.3.1 – Beam Specimens

Beam specimens were small scale versions of Bulb-T beams typically used in highway bridge construction. A spreadsheet was created to calculate the gross section properties and was used to iterate the design to find the final dimensions. The top and bottom flange areas were made deep enough to ensure development of the C-Grid and the web thin enough that failure of the beam was controlled by shear. Figure 15 shows the cross-section of the beam with major dimensions.

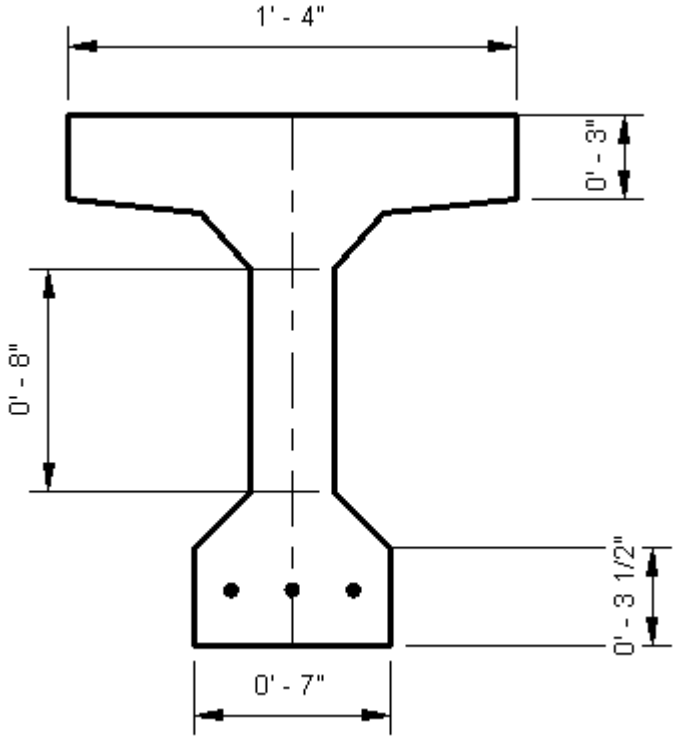

Figure 15: Beam End Elevations

The total length of the beams was 18 ft long, which allowed for two tests at a span of 12 ft each. Beams were simply supported. Loading was applied as a single point load 4 ft from one support to help ensure failure was controlled by shear. Each beam was initially designed so that one end of the beam would represent the minimum transverse reinforcing ratio used in the section and the other end would represent a typical transverse reinforcement ratio. Due to the delays in getting the NEFMAC material the fourth beam in the testing was designed as an additional C-Grid beam. A spreadsheet that calculated the moment capacity following the ACI 318 code and shear capacity following AASHTO and ACI 318 was created to determine the needed load for shear failure and the amount of longitudinal reinforcing. Each beam used a top bar in the beam for an anchor point when tying in the transverse reinforcing. Figure 16 shows the test set-up schematic for one beam, with the first test on the top and the second test for each beam on the bottom.

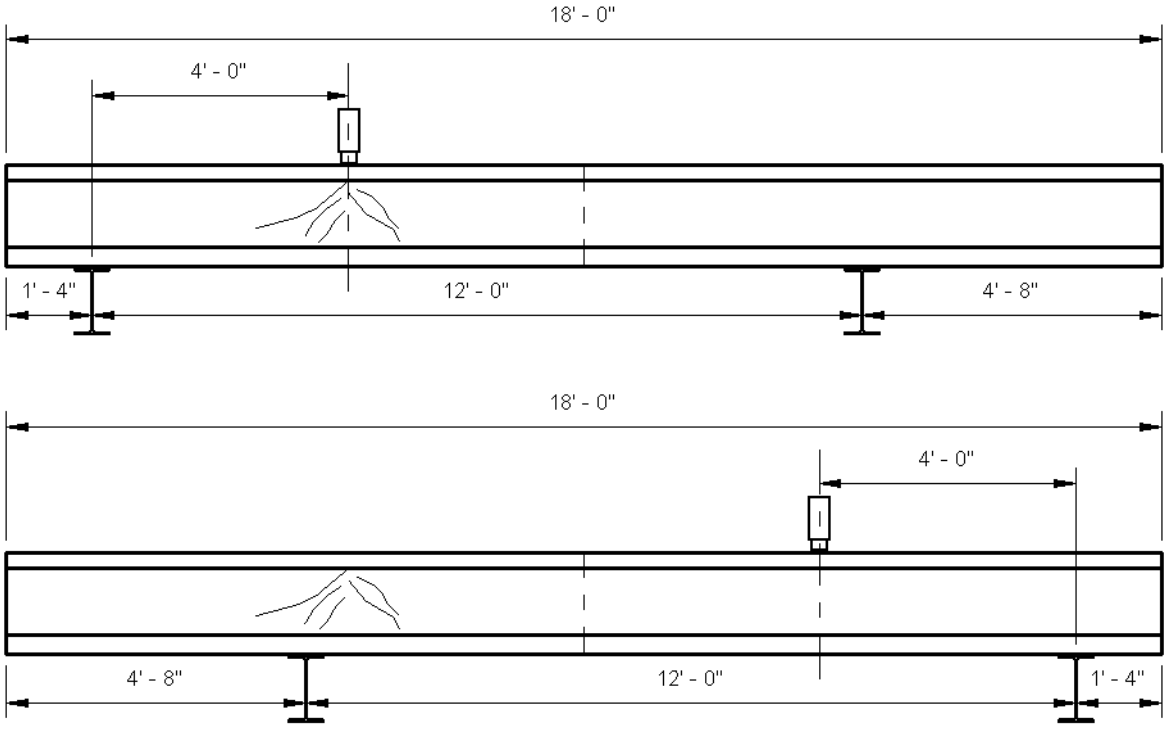

Figure 16: Test Set-up Schematic

Specimens are shown in Table 1 along with their anticipated shear strength for each of the transverse reinforcing options in the specimen. Typical transverse reinforcement ratio was determined from the typical ratio used in NCHRP report 733 (Cousins, Roberts-Wollmann, Brown, 2013). Minimum specimens were designed based on the AASHTO minimum transverse reinforcement given in Equation 16.

$$A_{v,min} = 3\sqrt{f'_c}\, b_v d_v \qquad \text{(Eq 16)}$$

Due to the delays in the NEFMAC, a second beam using C-Grid was tested because there was additional C-Grid on hand and this would allow further testing of this material. This final beam instead of using a typical and minimum transverse reinforcement ratio was designed using two layers of grid throughout the beam. However, one end used two layers with a separation to allow concrete to consolidate between the layers. The other side of the beam had the two C-Grid layers zip tied together approximately every 12 in. This testing was used to determine if placing two layers directly together would influence shear capacity of the beam.

Table 1: Beam Specimens

Specimen	Shear Reinforcing	Bar/Tow Area (in^2)	Max Stress (ksi)	Bar/Tow Strength (kips)	Spacing (in)	# of Layers	V_n MCFT (kips)	V_n ACI (kips)	Load Point (ft)	Expected Failure Load (kips)
1	Typ Steel	0.11	60	6.60	6.0	1	28.4	27.2	2.5	36
	Min Steel	0.11	60	6.60	12.0	1	17.0	17.9	4.0	32
2	Typ C-Grid	0.0029	-	0.83**	1.6	3	31.0	35.0	4.0	46
	Min C-Grid	0.0029	-	0.83**	1.6	1	18.3	17.4	3.5	26
3	Typ CFCC	0.09	45*	4.05	4.0	1	29.2	25.5	4.0	44
	Min CFCC	0.09	45*	4.05	9.0	1	19.7	16.0	4.0	30
4	C-Grid Zip Tied	0.0029	-	0.83**	1.6	2	29.5	25.9	4.0	45
	C-Grid Spaced	0.0029	-	0.83**	1.6	2	29.5	25.9	4.0	45

*** According to ACI 440.4R – Max Stress is 0.002E**
**** According to Manufacturer's Reported Data**

Due to a calculation error, Specimens 1 and 2 used three No. 5 bars for the bottom tension reinforcement, which was not enough tension reinforcement to cause a shear failure with the point load at 4 ft. Therefore the load points of Specimens 1-Typical Steel and 2-Min C-Grid

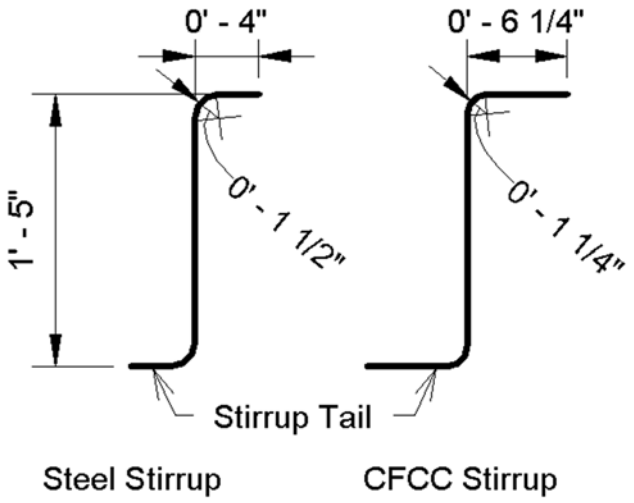

Figure 17: Stirrup Design for Beams

were modified to ensure a shear failure before flexural failure. After the error was found, Specimens 3 and 4 were designed with three No. 7 bars as the bottom tension steel reinforcement to help ensure a shear failure of the beams, prior to a flexural failure. Figure 17 shows the typical dimensions for the steel and CFCC stirrups. Provided tail length on steel stirrups is based on ACI 318 recommendations. CFCC stirrup tail lengths are based on recommendations from ACI 440.1, which is 12 bar diameters as shown in figure 9-1 in the 440 document.

Figure 18: Completed Beam Formwork with C-Grid

Formwork was built for two beams at a time, with bases built first and then one side of the form was attached to the base. Next, longitudinal reinforcing was tied in using 1-¾ in. chairs to place the center of the longitudinal reinforcing at 2 in. from the bottom of the beam. The transverse reinforcing was tied to the bottom longitudinal reinforcing and then the second side of the formwork was attached to the base. The transverse reinforcement was tied to the top bar which was held in place by pencil rod anchored through the top of the form. Figure 18 shows the end of the completed formwork with one layer of C-Grid transverse reinforcement tied in place.

Concrete was ordered from Conrock in Blacksburg, Virginia and was designed to have a 6-½ in. slump with a 28 day compressive strength of 7000 psi. The concrete was also specified with a maximum aggregate size of ½ in. to allow the concrete to easily flow through the C-Grid material. Table 2 shows the mix design for the beam concrete. The concrete was placed into the forms and a pencil vibrator was used to consolidate the concrete. After consolidation, magnesium floats were used to provide a smooth float finish the tops of the beams. The concrete was cured with wet burlap and plastic for 7 days. The forms were removed at this point to ensure drying shrinkage of the concrete did not bind the concrete and the forms. After form removal the beams were allowed to air cure for an additional 21 days before testing.

Table 2: Concrete Mix Design

Constituent	Amount
#8 Stone	1576 lbs
Natural Sand	1530 lbs
Type I/II Cement	652 lbs
Water	159 lbs
Microsilica	53 lbs
Air Entraining Admixture	1.4 oz
Retarder	24.7 oz
Water Reducing Admixture	28.2 oz
W/C Ratio	0.37

During the first concrete placement, a lack of consolidation occurred in the bottom flange of the C-grid beam on the end with three layers of grid. Upon closer inspection, it was determined that this was due to one layer of the C-Grid buckling into the middle layer, which blocked the flow of the concrete. This led to a weak area that was directly in the area of the shear testing. Due to this lack of consolidation this side of the beam was not tested. This meant only seven shear tests were carried out on the four beams instead of the proposed eight. Figure 19 shows the extent of the honeycombing that occurred in the sample. Due to this, the spacing between layers of C-Grid in the next specimen was increased to ensure adequate space for consolidation of the concrete.

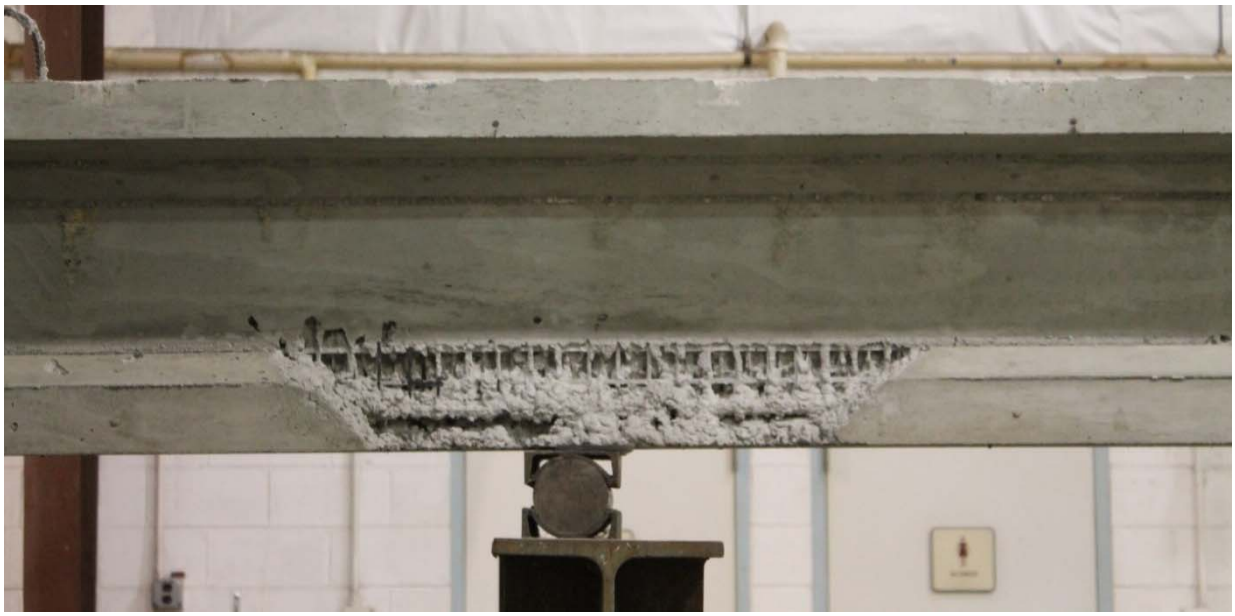

Figure 19: Honeycombing in Three Layers of C-Grid

3.3.2 – Test Set-Up

Testing was conducted in the Thomas M. Murray Structures and Materials Laboratory on the large beams that act as an additional testing area when the primary strong floor in the lab is busy. Two W 21x73 beams were clamped to the raised beams in the lab 12 ft apart. The point of load application was originally placed at 4 ft from one of the support beams. However, due to the calculation error, this was later moved to 2.5 ft for the steel stirrups 6 in. O.C. test and to 3.5 ft for the one layer of C-Grid test. For the remainder of the tests the load was applied 4 ft from a support. The loading apparatus was a single Enerpac 150 ton hydraulic ram held in place by

Figure 20: Overview of Test Set-up

columns and channels as shown in the figure. The ram was used with an SPX Power Team hydraulic pump. The complete testing frame set-up is shown in Figure 20.

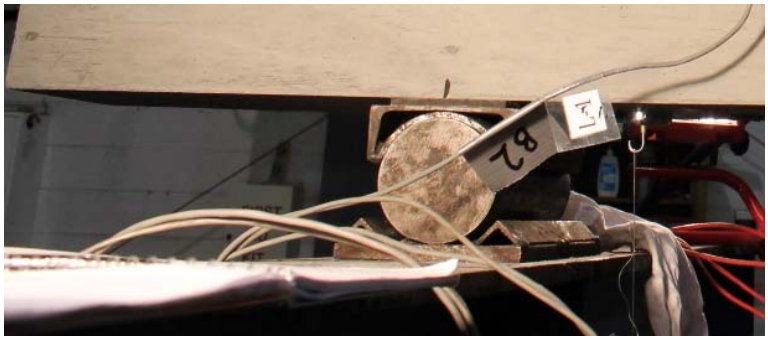

Figure 21: Roller Support for Beam End

The supports for the beam were a pin and roller at the ends to create a simply supported beam. To reduce friction, the pin and roller were greased before testing. Before the beam was set on the rollers a rubber pad was used to help distribute the load along any imperfections in the concrete. Also, the load from the hydraulic ram was transferred to the beam via a set of steel plates with a neoprene bearing pad. This was used to increase the area of applied load on the concrete and to increase the amount of travel the ram could undergo when in contact with the beam. The supports and loading plates used during testing are shown in Figure 21 through Figure 23.

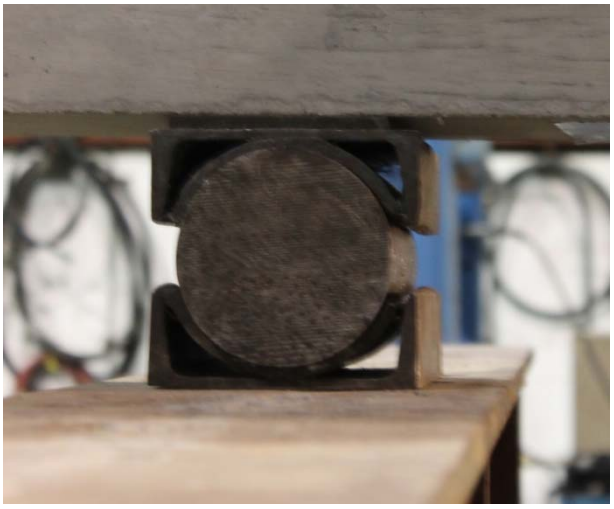

Figure 22: Pin Support for Beam End

Figure 23: Loading Plates under Hydraulic Ram

3.3.3 – Instrumentation on Beams

Data from the tests were gathered via a System 5000 computer system made by Vishay Instruments. All instrumentation was connected to the System 5000 and calibrated before testing. The load cell was made by Brett Farmer, a technician in the VT structures lab. The load cell was calibrated and checked for accuracy on a Forney concrete compression testing machine.

Each test also used three wire potentiometers produced by Measurement Specialties to measure the deflection of the beam. One was placed near the support at each end of the beam and the third was placed under the load application point. This allowed true deflection of the concrete beam to be measured by accounting for any deflection at the steel support beams. Wire potentiometers were placed on the floor with concrete blocks to keep them from moving during testing. Metal shim plates were glued to the beam using Loctite 410 instant adhesive and Loctite

7452 accelerant. Magnetic hooks were then applied to these plates and the string from the wire potentiometer was attached to the hook as shown in Figure 24.

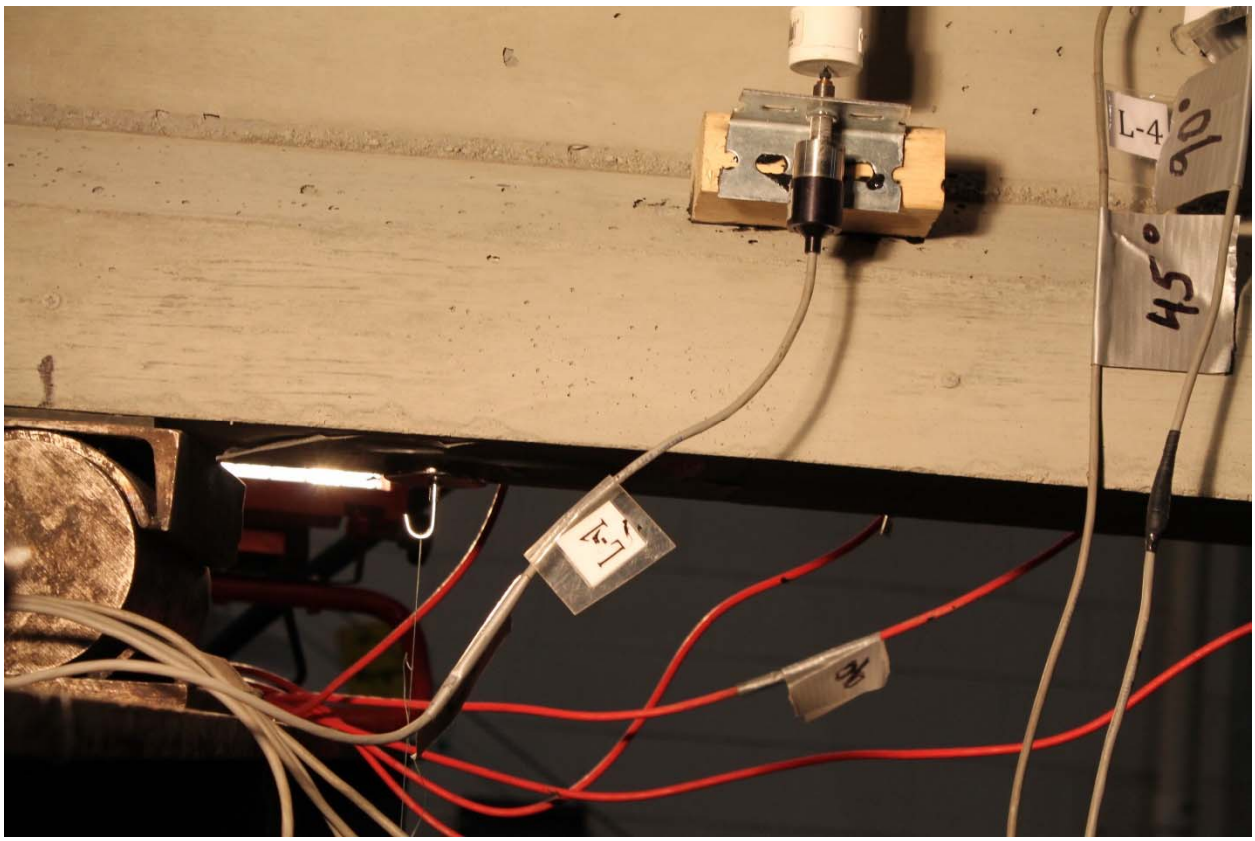

Figure 24: Hook to Attach Wire Potentiometer

Each beam was also fitted with a rosette on each side, at the midpoint of the shear span (typically 2 ft from the support). The first test used a 0, 45, 90 degree approach, but following tests used a 90, +45, -45 degree rosette. The rosette was made up of Trans-Tek 0350-0000 LVDTS and used a wooden block as the measurement point. The LVDTS were held onto the beam with steel channel brackets adhered to the beam with the same Loctite 410 adhesive. Also, there were two additional LVDTs that measured the web of the beam to capture shear cracking. These were attached to the tapered portion of the beam via a wood bracket with metal channel and again used the Loctite adhesive. The typical LVDT rosette and crack gages for each test session are shown in Figure 25.

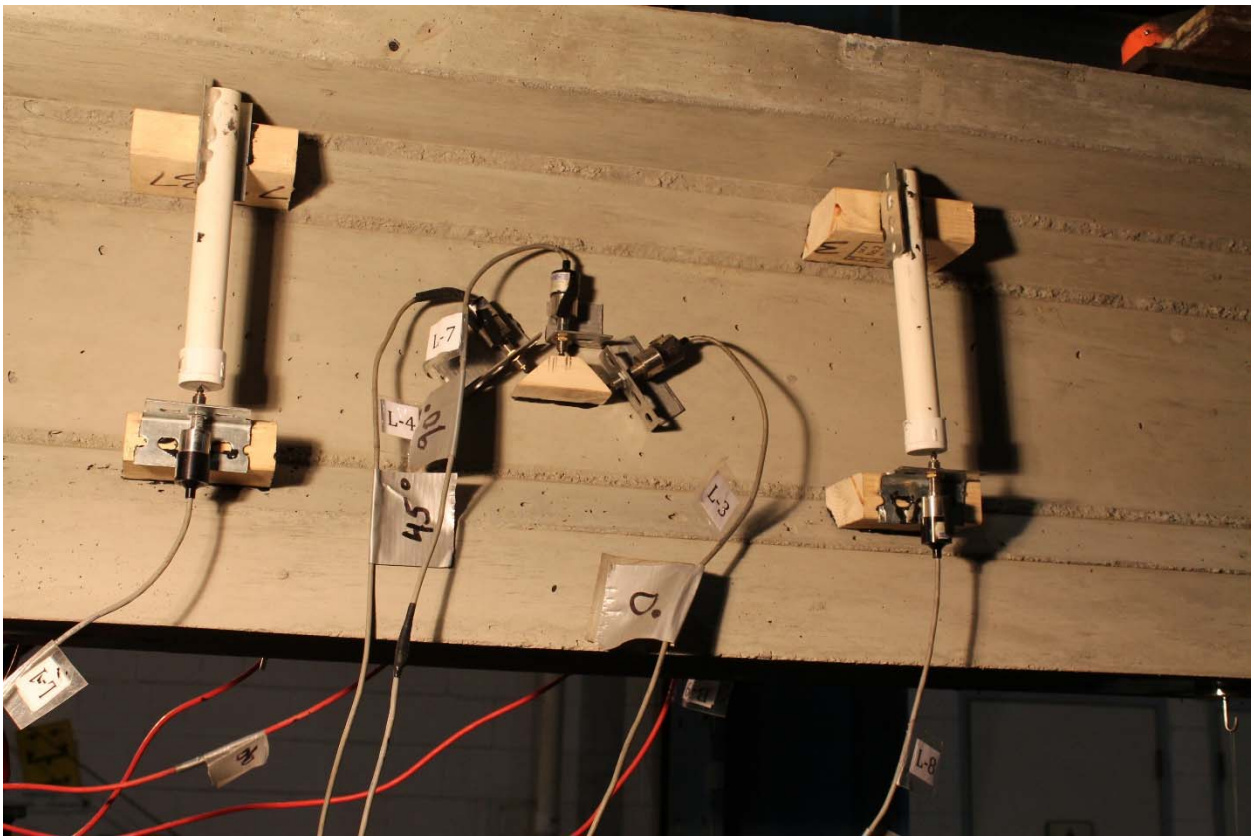

Figure 25: Typical LVDT Rosette and Bar Strain Set-up for Testing

The other side of the beam used different gages arranged in the same locations and angles. This side of the beam used Bridge Diagnostic Inc. strain transducers (BDIs) for the rosette and crack measurements. The angles for each test were mirrored from the side with LVDTs to compare values between the two gage types. The BDIs attached to the beam via metal feet that are glued to the beam using the same Loctite adhesive. Also, two additional gages were placed to try and capture the main shear crack with one placed near the load high on the web and the other placed closer to the support towards the bottom of the web. These were named B1 and B2 as they were to be aligned over the stirrup bars in the beams using CFCC and steel stirrups. B1 was always closer to the applied load and B2 was closer to the support. The BDI rosette and crack gages for each test are shown in Figure 26. The full instrumentation plan for the beam is shown in Figure 27.

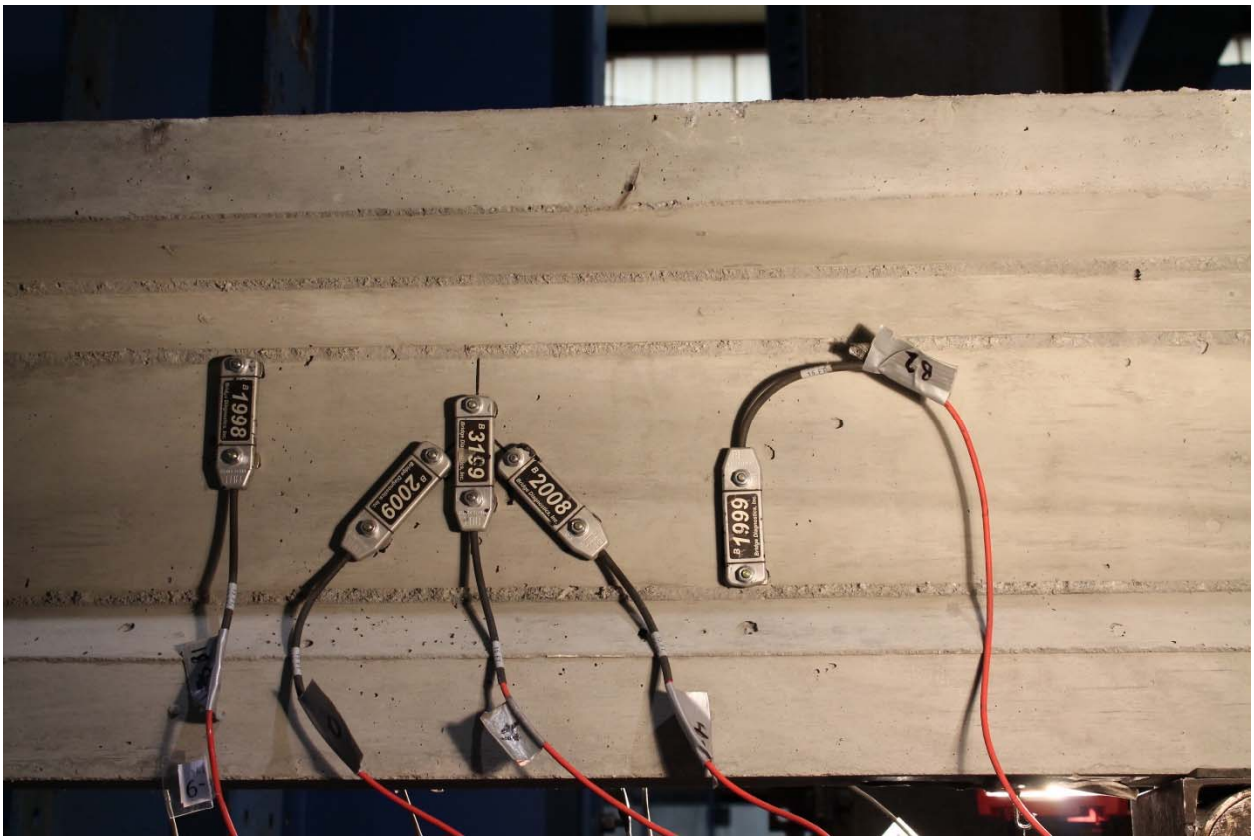

Figure 26: Typical BDI Rosette and Bar Strain Set-up for Testing

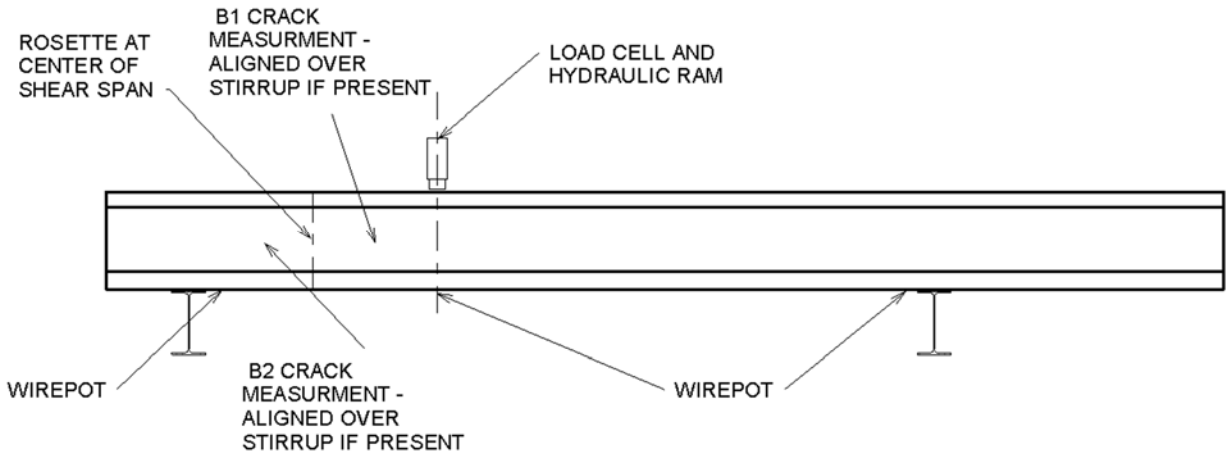

Figure 27: Full Instrumentation for Shear Testing

4 – Test Results

4.1 – C-Grid Tensile Strength Results and Discussion

Tensile tests were conducted as a preliminary assurance of values of tow strength and modulus of elasticity reported by the manufacturer. Each specimen's width and thickness were measured and then tested until failure. Results of specimen testing are shown in Table 3 below.

Table 3: C-Grid Tensile Test Results

Sample	Max Load (lbs)	Elongation (in)	Strain (in/in)	Thickness (in)	Width (in)	Area (in^2)	Max Stress (psi)	E (psi)
NS1	1210	0.027	0.014	0.048	0.215	0.010	1.17E+05	8.69E+06
NS2	1391	0.033	0.017	0.056	0.238	0.013	1.04E+05	6.33E+06
NS3	1434	0.029	0.015	0.045	0.262	0.012	1.22E+05	8.39E+06
NS4	1323	0.031	0.016	0.044	0.253	0.011	1.19E+05	7.67E+06
NS5	1384	0.030	0.015	0.052	0.200	0.010	1.33E+05	8.87E+06
EW1	1299	0.029	0.015	0.038	0.290	0.011	1.18E+05	8.13E+06
EW2	1600	0.034	0.017	0.037	0.275	0.010	1.57E+05	9.25E+06
EW3	1499	0.032	0.016	0.040	0.254	0.010	1.48E+05	9.22E+06
EW4	1453	0.031	0.016	0.044	0.227	0.010	1.45E+05	9.39E+06
EW5	1171	0.025	0.013	0.035	0.301	0.011	1.11E+05	8.89E+06
NS6	1319	0.026	0.013	0.029	0.321	0.009	1.42E+05	1.09E+07
NS7	1407	0.028	0.014	0.029	0.294	0.009	1.65E+05	1.18E+07
NS8	1379	0.027	0.014	0.037	0.253	0.009	1.47E+05	1.09E+07
NS9	1324	0.026	0.013	0.035	0.243	0.009	1.56E+05	1.20E+07
NS10	1360	0.028	0.014	0.034	0.293	0.010	1.37E+05	9.75E+06
EW6	1151	0.023	0.012	0.053	0.247	0.013	8.79E+04	7.65E+06
EW7	1042	0.034	0.017	0.049	0.247	0.012	8.61E+04	5.06E+06
EW8	1280	0.028	0.014	0.050	0.253	0.013	1.01E+05	7.23E+06
EW9	1351	0.028	0.014	0.054	0.210	0.011	1.19E+05	8.51E+06
EW10	1371	0.028	0.014	0.055	0.221	0.012	1.13E+05	8.06E+06
Average	1337	0.029	0.014	0.043	0.255	0.011	1.26E+05	8.83E+06
Std Dev	123.0	0.003	0.001	0.008	0.032	0.001	2.22E+04	1.67E+06
Avg - 3*Std Dev	968.4	0.020	0.010	0.018	0.159	0.007	5.98E+04	3.82E+06

The mean tensile strength for each tow was found as 1337 lbs. To conform to ACI requirements for design strength, the mean must be reduced by three standard deviations. This gives a value of 968 lbs, which is about 17% more than the manufacturer reported strength of 830 lbs per tow. This is probably due to the manufacturer testing a larger number of specimens and also ensuring that they provide a conservative value for design.

However, the elastic modulus found in testing is 8,830,000 psi, which is much smaller than the manufacturer reported value of 34,000,000 psi. When investigating this large discrepancy, the area of the individual tows was found to be much larger than reported by the manufacturer. The area of the tow was found by measuring the width and thickness with a set of calipers and then multiplying to find the cross-sectional area. However, the tows are not perfectly flat but instead are thicker in the center and very thin at the edges. The cross-sectional shape of a tow could be best described as a half dome. This means that the thickness taken in the middle of the tow is much thicker than the edges, which can lead to inaccurate cross-sectional area.

Recorded area values are an average of 0.011 in^2, which is much larger than the reported 0.00286 in^2 by Chomarat. This change of almost four times the area is very significant difference when calculating the elastic modulus. Using the manufacturer's reported area, the elastic modulus was recalculated and the average was found to be 32,600,000 psi, which is much closer to the value given for the C50 materials.

ACI determines the strength of FRP products as the mean strength minus three standard deviations, which is based upon a normal distribution of tow strengths. However, FRP products often exhibit a tighter distribution of strength where a Weibull distribution is a better fit for actual results. Due to this fact, a Weibull analysis was performed on the value to determine the A-allowable and B-allowable for the strength of the tows. The A-allowable value corresponds to a 95% confidence that 99% of the samples will be above the reported value, while the B-allowable corresponds to a 95% confidence that 90% of the samples are above the specified value. From the data collected through 20 tests, the A-allowable value was found to be 947 lbs and the B-allowable was found to be 1154 lbs.

The A-allowable value of 947 lbs and the mean minus three standard deviation value of 968 lbs are in a good agreement about the design strength of the fibers. While FRP products do fit the Weibull distribution well, it shows that the ACI method of three standard deviations also provides a similar level of performance. Regardless of which analysis method is used to determine the design strength of the C-Grid, a conservative value should be used to ensure safe designs. The manufacturer, Chomarat, reports a much more conservative value of 830 lbs per tow.

4.2 – C-Grid Development Length Results and Discussion

4.2.1 – C-Grid Development Length Specimen Results

Development tests were conducted on ten specimens with a slight issue on the first test. The first specimen tested was 8-1 and the jack was placed too close to the bottom of the blocks, which resulted in a bending force being put into the blocks instead of pure axial force. The bending was apparent through the lifting of the end of the blocks and only the failure of the bottom grids as shown in Figure 28. Failure of only the bottom tows meant that the jack was

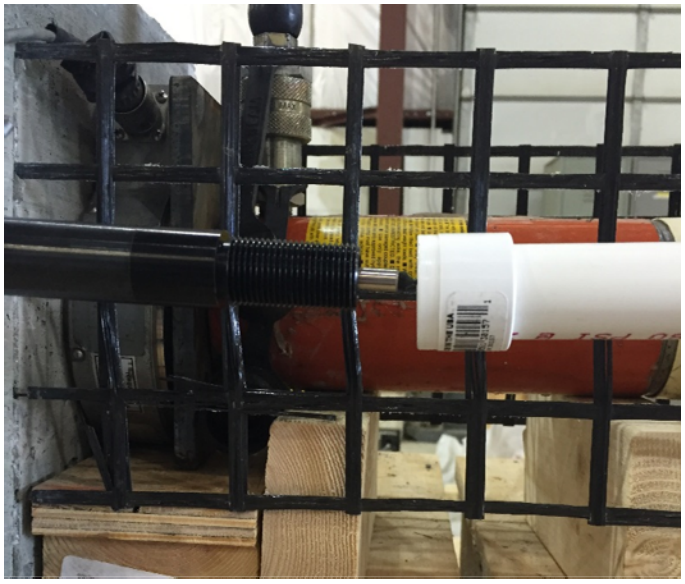

Figure 28: Failure of Specimen 8-1

placed too low in the test set-up. Specimen 8-1 was discounted from the analysis of the rest of the specimens due to this error.

For the remainder of the specimens, the jack misalignment was corrected. One interesting finding from the testing was that only one side of the grid would rupture, thus indicating that there was some unintended eccentricity in the force application. This was attributed to the difficulty in exactly centering the jack between the two grids and the fact that the concrete face and grids are not perfectly square.

Data was analyzed using the load and the two displacements from either side of the specimens. Graphs were produced showing the load versus displacement for the two sides of the grid. Slip of the grids is indicated by a change in slope of one or both of the lines before failure of the grid was reached. A representative graph from a development specimen is shown in Figure 29.

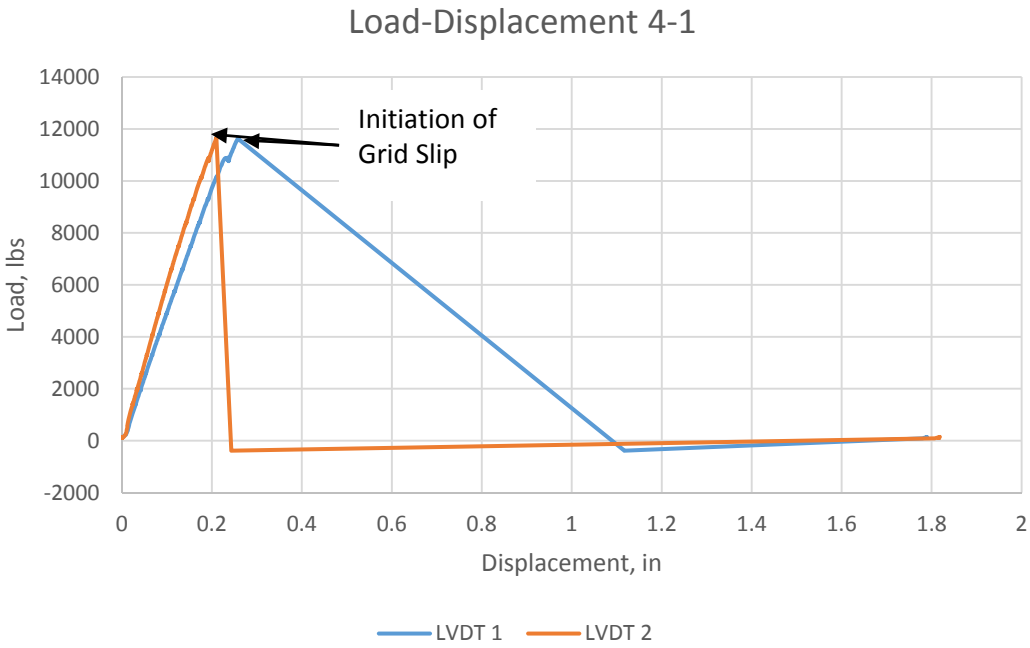

Figure 29: Typical Development Length Plot

The average load at rupture of one side of the grid in the specimens was found to be 11,400 lbs. Based on manufacturer's reported load strength of 830 lbs per tow, and the ten tows present in testing, the specimen design failure load per manufacturer's published data is 8,300 lbs. The manufacturer reported data includes the reduction of three standard deviations from the average. Using the average strength reduced by three standard deviations from tensile testing, the design failure load is 9,700 lbs, which is 970 lbs per tow times the ten tows present in testing. If the average strength is taken from the tensile tests performed, then the failure load of the specimens is 13,400 lbs.

While 13,400 lbs is more than the failure load, the specimens do not reach this ultimate load as the loading on two grids was not equal. As shown in Figure 29, at failure one of the grids has more displacement than the other due to alignment and square-ness of the testing specimens. The average difference in the LVDT readings at 10,000 lbs was 20%, so at an average failure load of 11,382 lbs one side carries 6,320 lbs while the other carries 4,900 lbs. Based on this result, the grid is taking 94% of its tested strength before rupture. This shows that the C-Grid is being stressed at a load close to its maximum loading before failure. The 6% difference accounts

Table 4: Development Length Testing Results

			LVDT 1		LVDT 2		Ratio		% Diff	
Test	Max Load (lbs)	Slip	1000 lbs	10000 lbs	1000 lbs	10000 lbs	1000 lbs	10000 lbs	1000 lbs	10000 lbs
4-1	11676	No	0.0231	0.207	0.0174	0.1737	1.33	1.19	32.8	19.2
4-2	12783	No	0.0176	0.1691	0.021	0.2086	0.84	0.81	16.2	18.9
5-1	11208	No	0.0226	0.1898	0.026	0.2095	0.87	0.91	13.1	9.4
5-2	10186	No	0.0129	0.1726	0.0238	0.2208	0.54	0.78	45.8	21.8
6-1	11883	No	0.0243	0.2278	0.0213	0.169	1.14	1.35	14.1	34.8
6-2	10692	No	0.0163	0.2433	0.0199	0.2231	0.82	1.09	18.1	9.1
7-1	11117	No	0.0353	0.2127	0.013	0.1949	2.72	1.09	171.5	9.1
7-2	12676	No	0.0155	0.2009	0.0167	0.1834	0.93	1.10	7.2	9.5
8-1*	6110	No	0.0146	0.1022	0.0233	0.1293	0.63	0.79	37.3	21.0
8-2	10213	No	0.0185	0.2258	0.0117	0.1533	1.58	1.47	58.1	47.3
Average	11382	No	0.0201	0.1951	0.0194	0.1866	1.14	1.06	41.4	20.0

*** indicates specimen was not included in average**

for a small amount of bending that is likely occurring in the grid due to the unequal loading. The results of the development length tests are shown in Table 4, and from the above analysis the development length of C50 1.6x1.8 is 4 in.

4.2.2 – Concrete Material Test Results

The concrete used for the development length tests was specified as a 5,000 psi concrete, using 1/2 in. aggregate, and having a slump of 6 to 8 in. for high workability. The concrete was purchased from the local ready-mix concrete plant and delivered to the lab. Prior to placement the slump was taken and found to be 6 in. During placement 4 in. by 8 in. cylinders were cast to be used for concrete material testing. Compression and splitting tensile tests were complete on a Forney concrete compression testing machine. Compressive tests were run following ASTM C39 protocol and splitting tensile followed ASTM C496 protocol. From testing, the 28 day compressive strength was found to be 5,540 psi, and the splitting tensile strength was 500 psi.

4.2.3 – Behavior of C-Grid in Beam Tests

Three beam tests using the C-Grid were failed in shear during testing with a development length of 4-1/2 in. as shown in Figure 30. These beams developed large shear cracks and failed upon rupture of the C-Grid reinforcing. Based on these tests specimens, the development length

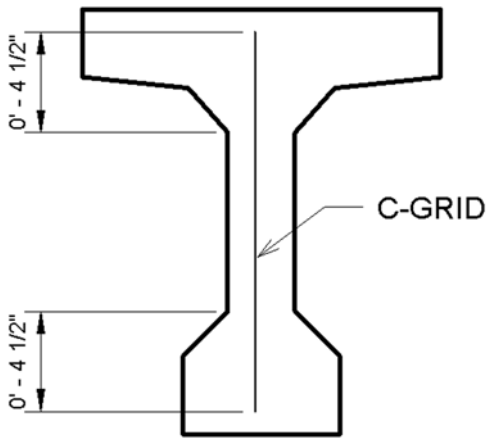

Figure 30: Development Length of C-Grid in Beam Specimens

of the C-Grid was satisfactory. The C-Grid reached full strength at rupture and signs of slipping were not evident in the specimens. This reinforces the findings of the testing that 4 in. development length is satisfactory for the C50 1.6x1.8 grid.

4.4 – Beam Test Results

4.4.1 – Specimen 1 Minimum Steel Reinforcement

Specimen 1 used a minimum reinforcement ratio according to AASHTO as previously described in section 3.3.1 of this thesis. For this beam the minimum reinforcement was provided by No. 3 steel stirrups at 12 in. on center. The beam was set-up as a clear span of 12 ft with the point load at 4 ft from the support. The cross-section of Specimen 1 is shown in Figure 31.

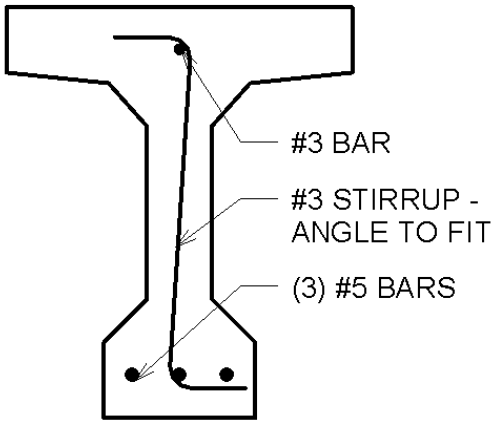

Figure 31: Cross-section of Specimen 1 Steel Reinforcement

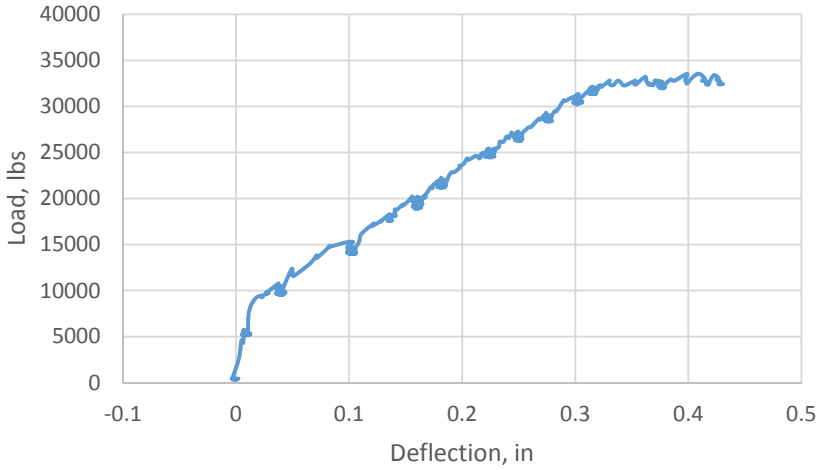

Figure 32: Load-Deflection Specimen 1 Minimum Steel

Loading was applied with the hydraulic ram in 5-kip increments up to 20 kips, and then was increased by 2-kip increments until completion of testing at 32 kips. At 10 kips, flexural cracking occurred and the first shear crack formed at 15 kips. The initial shear crack was 0.004 in. wide, at the initial measurement.

Testing was completed at 32 kips as the beam reached inelasticity in flexure even though shear failure was predicted at 27 kips of loading. The flexural inelasticity was due to a formula error in the beam design spreadsheet. Due to this error, less flexural reinforcement was used in Specimens 1 and 2 than needed to ensure shear failures prior to flexural yielding. Specimens 3 and 4 were modified to increase flexural strength beyond their expected shear failure loads. The load displacement plot for this specimen is shown in Figure 32. The beam at yielding is shown in Figure 33.

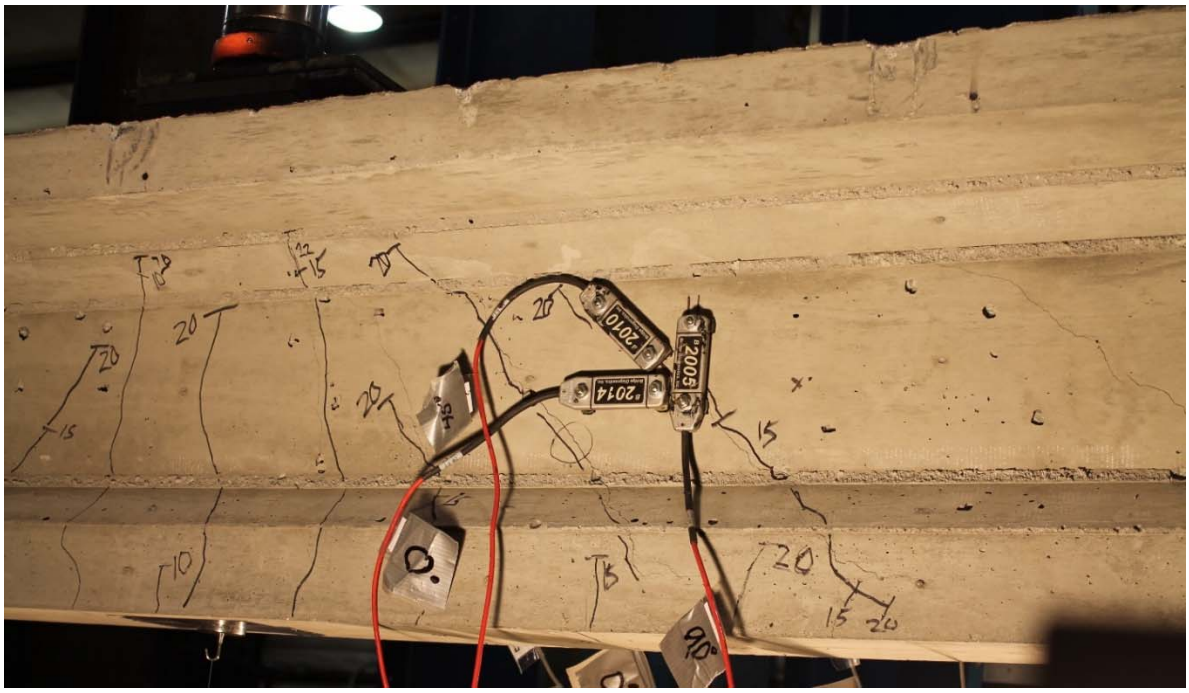

Figure 33: Flexural Yielding of Specimen 1 Minimum Steel Reinforcing

Cracking of the beam was only measured on one crack for this test. A crack microscope was used at first, but it was determined that using a crack card would be a simpler and safer

method of measuring the cracks. Crack width measurements were stopped at 15 kips for safety due to the unknown nature of specimen failure. Results of the crack width measurements are shown in Figure 34, along with the best fit linear equation for crack propagation.

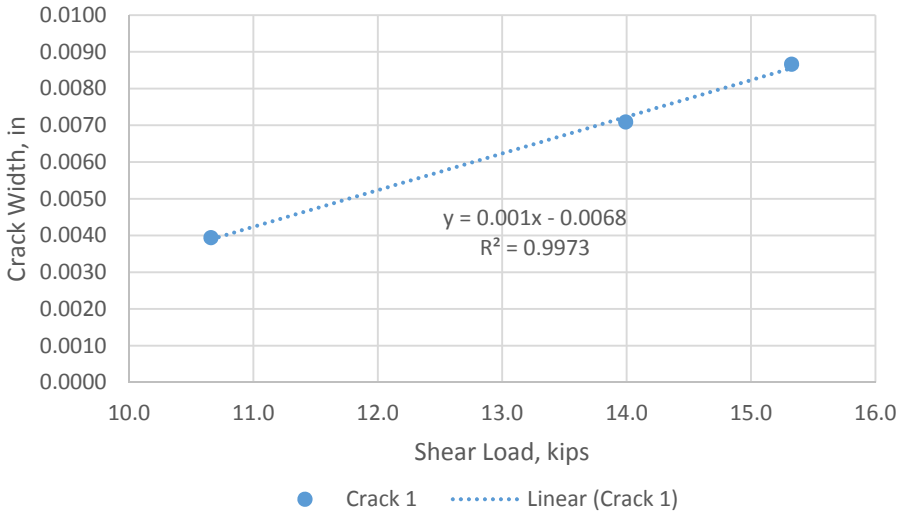

Figure 34: Crack Propagation Specimen 1 Minimum Steel Reinforcement

Also presented is the displacement of the vertical LVDTs during testing. Since the LVDTs provide a larger range of displacement than the BDI gages, they capture movement post cracking. Figure 35 below shows the movement of both B1, B2, and the vertical LVDT in the

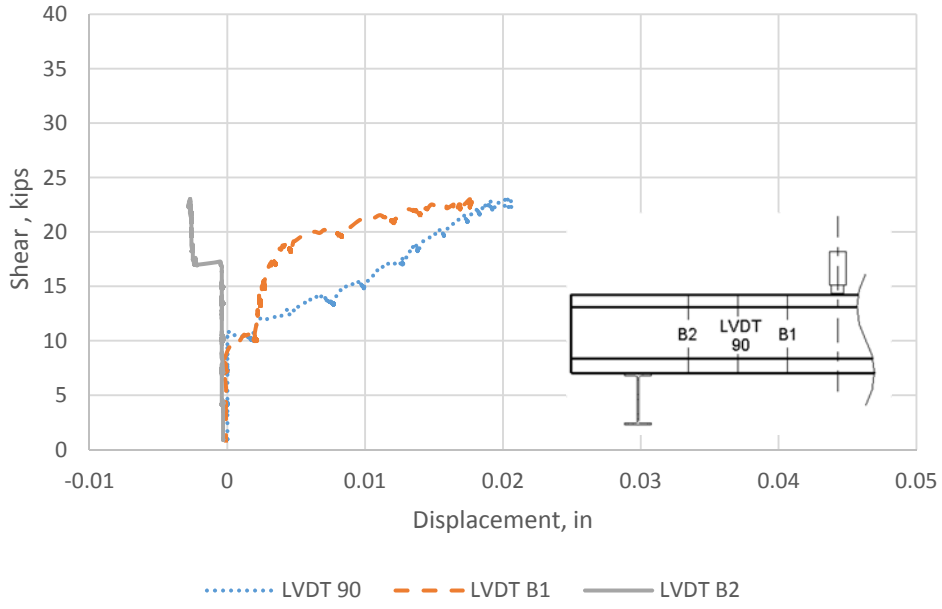

Figure 35: Vertical LVDT Displacement of Specimen 1 Minimum Steel Reinforcement

rosette set-up. From Figure 35, cracking looks to be about 10 kips of shear load, which corresponds to the first visible crack appearing at 10.5 kips of shear load. Also, the displacement of LVDT 90 and B1 match very well with the displacement of the crack data at 15 kips.

4.4.2 – Specimen 1 Typical Steel Reinforcement

The end of the specimen with typical steel reinforcement, which is defined by NCHRP 733 (Cousins, Roberts-Wollman, & Brown, 2013), had No. 3 stirrups at 6 in. on center, which increased the shear capacity of the beam. The cross-section is the same as shown in Figure 31. Due to the flexural yielding of the reinforcement in the first test, the loading point had to be modified to have a shear failure occur before flexural yielding of the reinforcing. The clear span was left at 12 ft, but the load point was moved to 2.5 ft from the support to result in a higher shear load for a given moment.

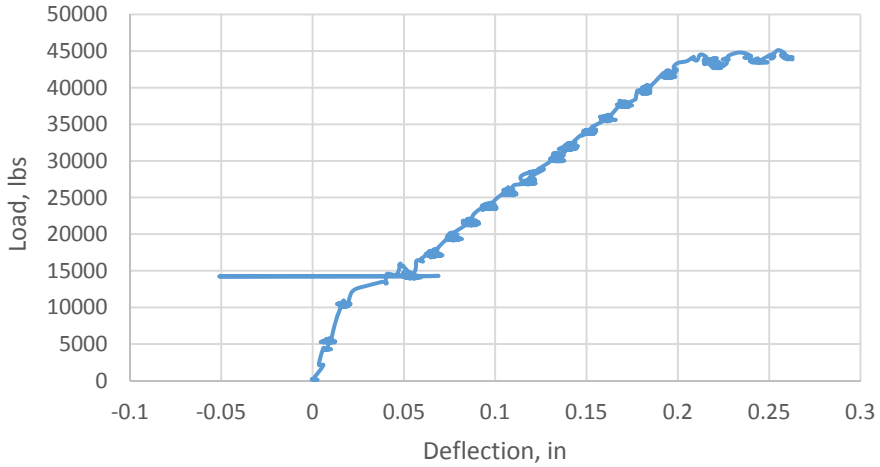

Figure 36: Load-Deflection Specimen 1 Typical Steel Reinforcement

Loading was applied in 5-kip increments up to 20 kips and then by 2-kip increments until completion of testing at 44 kips. Testing with instrumentation was concluded at 44 kips due to the beam becoming inelastic in flexure as shown in Figure 36. The blip in the deflection is due to the wire potentiometer being hit by a person marking cracks on the beam. Instrumentation was then removed from the beam to ensure it was not broken during failure, the beam was

pushed to ultimate load. The beam was loaded up to 54 kips before a flexural compression failure occurred in the beam, which is shown in Figure 37. Shear failure was predicted as 36 kips.

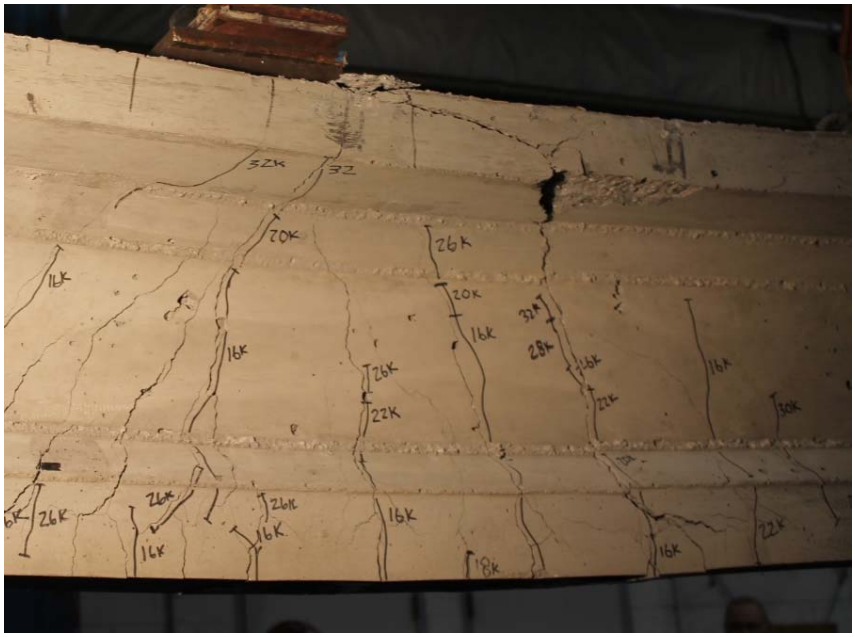

Figure 37: Compression Failure of Specimen 1 Typical Steel Reinforcement

Crack widths were measured on two shear cracks, the first one that opened on the beam and the second is the crack that took a direct path from the support to the load point. First crack appeared at approximately 13.5 kips. The cracks followed a very linear propagation rate

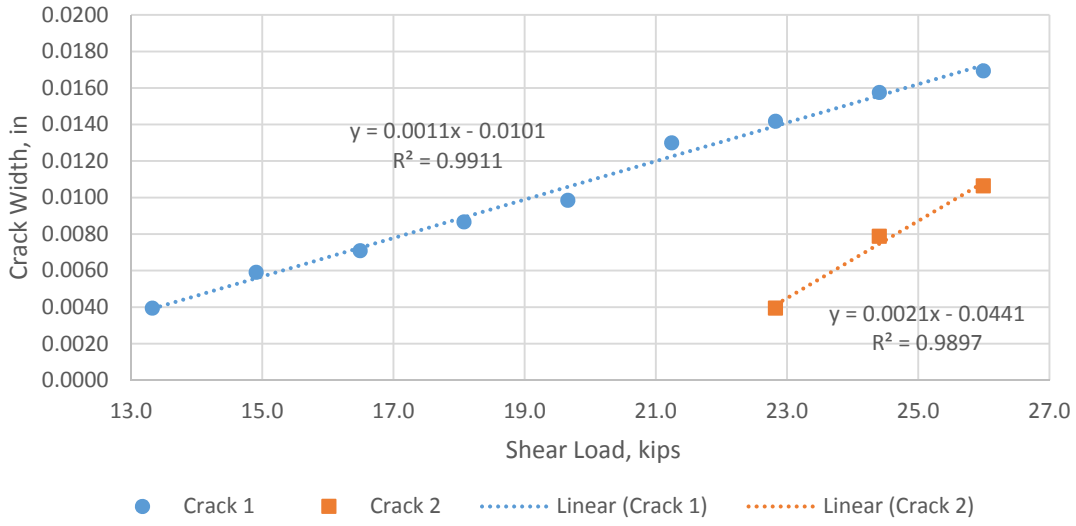

Figure 38: Crack Propagation Specimen 1 Typical Steel Reinforcement

throughout testing of this specimen. Figure 38 shows the propagation of the cracks with a best fit line for propagation of each crack.

The vertical LVDT displacements are also shown in Figure 39 for this specimen. Cracking is best shown in the movement of LVDT B1 at 13 kips of shear load. This corresponds almost exactly with the appearance of the first shear crack at 13.5 kips. Also, the overall movement of all LVDTs at 25 kips is about 0.01 in., which corresponds to a similar level of crack width at 25 kips from Figure 38.

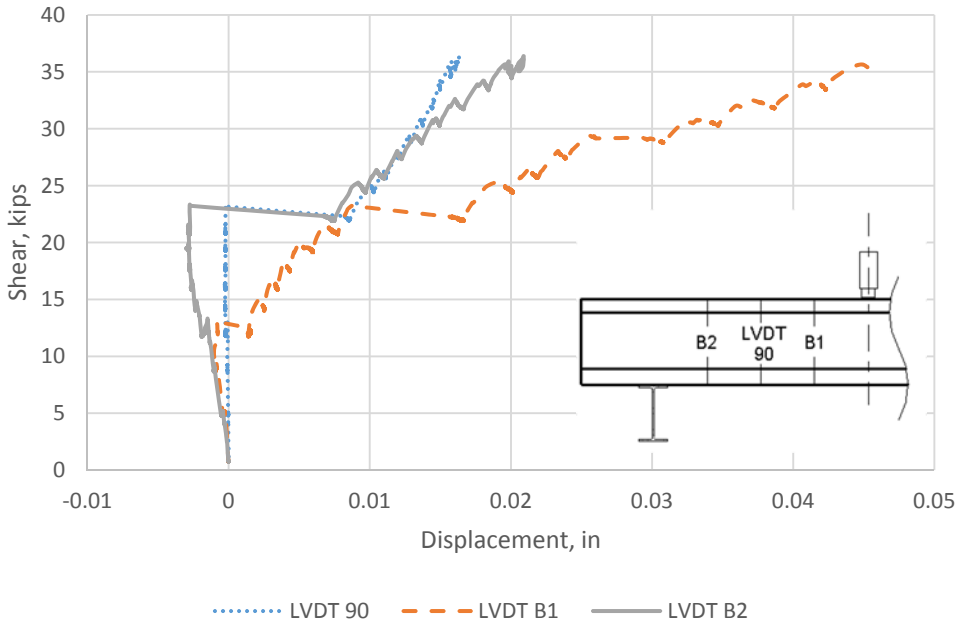

Figure 39: Vertical LVDT Displacements of Specimen 1 Typical Steel Reinforcement

4.4.3 – Specimen 2 Minimum C-Grid Reinforcement

The minimum C-Grid reinforcement in Specimen 2 was composed of one layer of C50 1.6x1.8 grid that was placed the entire length of the beam. The 1.6 in. spacing was the spacing

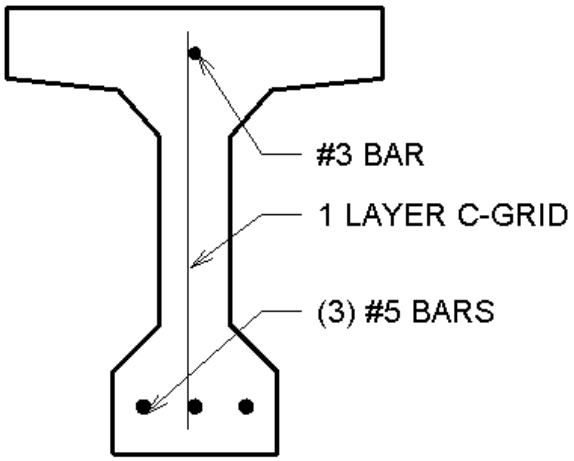

Figure 40: Cross-Section of Specimen 2 Minimum C-Grid Reinforcement

of the vertical legs of the grid that acted as stirrups. The cross-section of the specimen is shown in Figure 40. The load was applied at 3.5 ft from the support on a 12 ft span. This loading scenario should have resulted in a shear failure at approximately 26 kips.

Loading was applied in 5-kip increments to 15 kips and then 3-kip increments after. Load was applied to the beam until flexural yielding occurred at 35 kips, which was after the

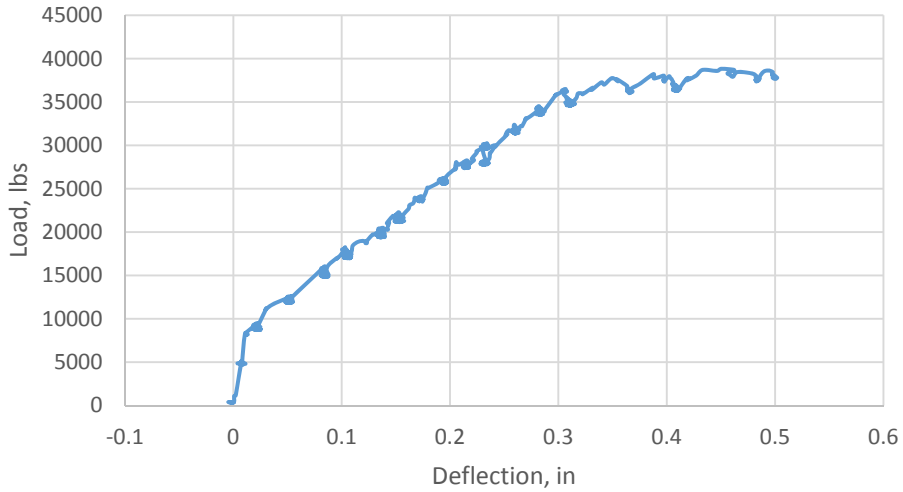

Figure 41: Load-Deflection Specimen 2 Minimum C-Grid Reinforcement

expected shear failure. Figure 41 clearly shows the yield plateau of the section and yielding was evident during testing.

After yielding, instrumentation was removed and beam was tested to ultimate failure load. Load was increased up to yielding point and then increased by 2-kip increments. Shear failure of the beam occurred at 40 kips, approximately 50% more load than predicted. At the 40 kip failure, a cracking was heard and the beam lost load and settled at 35 kips. Since the beam seemed stable the load was increased back to 38 kips and then the beam lost all load carrying ability. The beam was then unloaded and the failure crack is shown in Figure 42. Upon closer inspection of the shear crack, visible rupture of the many of the tows crossing the crack in both the vertical and horizontal direction occurred. The thought was that at 40 kips a few of the tows ruptured, but then at ultimate the vast majority crossing the crack ruptured.

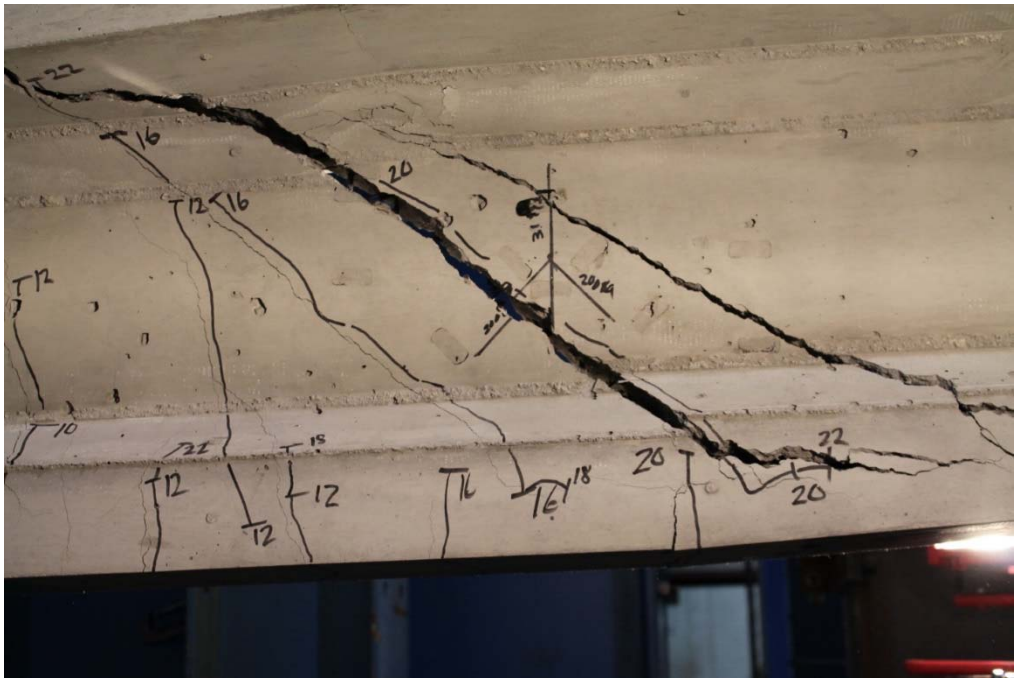

Figure 42: Shear Failure of Specimen 2 Minimum C-Grid Reinforcement

Crack widths were measured for two cracks on this beam; the first shear crack that opened and the second is the crack from the support to the loading point. Cracks were only measured up until 22 kips due to the unknown failure loadings of the C-Grid. The crack propagation along with best fit lines are show in Figure 43.

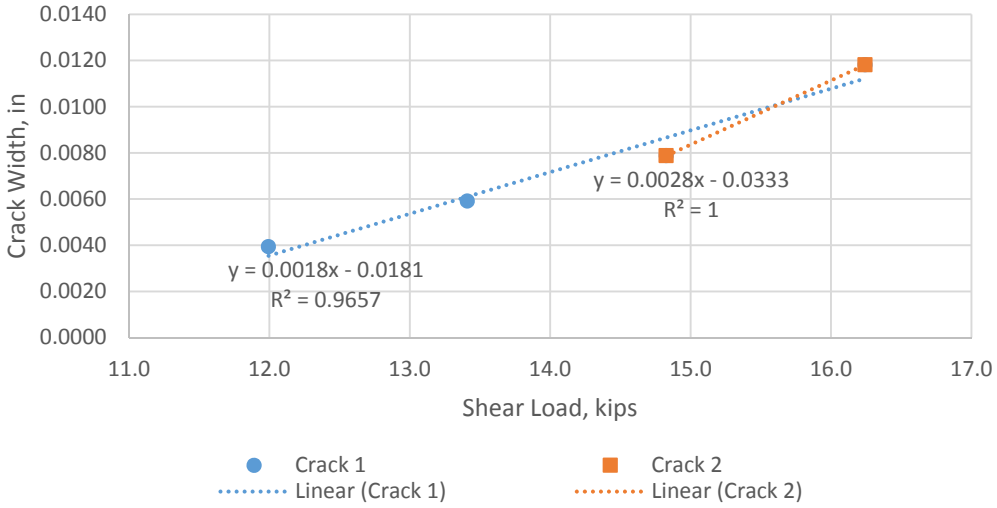

Figure 43: Crack Propagation Specimen 2 Minimum C-Grid Reinforcement

Vertical LVDT displacements are presented in Figure 44. Cracking occurred around 10 kips based on the jump in LVDT B1. This corresponds within 20% of the crack appearance shown in Figure 43. Since the crack widths are measured visually, their appearance is based on

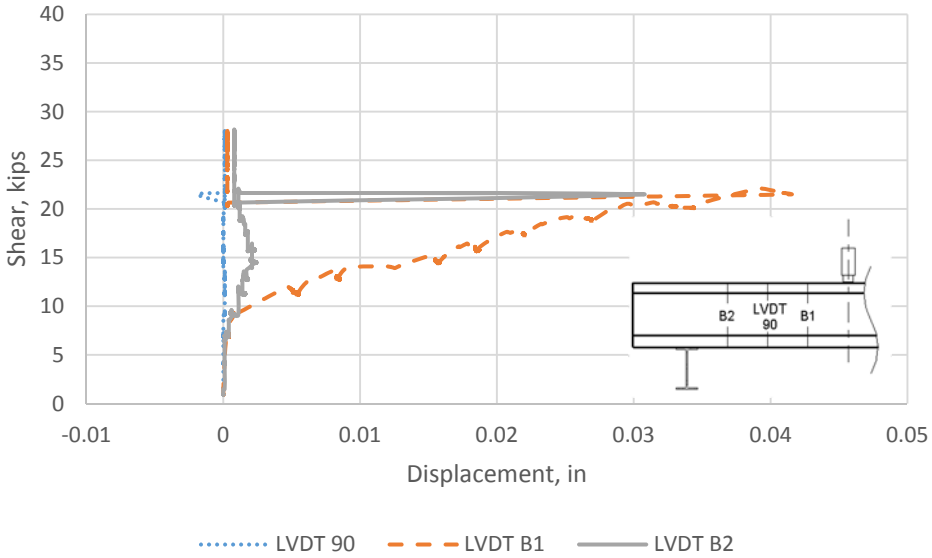

Figure 44: Vertical LVDT Displacements of Specimen 2 Minimum C-Grid Reinforcement

the increments in loading. This means they will not be as exact as those values measured by the LVDTs. However, this specimen's LVDT displacement at 15 kips is about 0.02 in., which is much higher than the crack widths of about 0.008 in. at the same shear. This probably occurred due to multiple cracks opening that were not measured during testing, so the overall movement of the web is more than at any single crack.

4.4.4 – Specimen 2 Typical C-Grid Reinforcement

The typical C-Grid reinforcement specimen was reinforced with three layers of C-Grid C50 1.6x1.8 placed in the beam. The grid was tied to the bottom and top reinforcement or top pencil rod to hold it in place during the pour. The cross-section of the beam is shown in Figure 45.

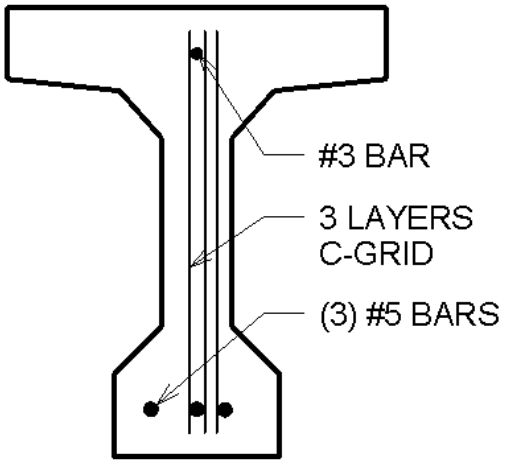

Figure 45: Cross-Section of Specimen 2 Typical C-Grid Reinforcement

Due to the tight spacing of the C-Grid in the web, the concrete did not consolidate properly in the bottom flange of the beam. The concrete pushing down on the C-Grid caused the outer grid on the right in Figure 45 to buckle in towards the next grid to the left Since the grids buckled together, the concrete was trapped between the layers and would not flow properly even though the pencil vibrator was pushed down to the bottom of the beam forms. The area where the lack of consolidation occurred was in same location as the expected shear cracking.

Since this would negatively influence the shear strength of the beam it was determined this test would not be performed. Yet, the knowledge gleaned from this problem is helpful in understanding that C-Grid needs to have support, especially when multiple layers are used close together. Proper lateral support would have prevented the honeycombing from occurring, which was previously shown in Figure 19.

4.4.5 – Specimen 3 Minimum CFCC Reinforcement

The CFCC stirrups were placed in the section in the same manner as the steel stirrups, but due to their longer tail lengths as shown in Figure 17 had to be turned approximately 60 degrees to fit into the bottom flange of the formwork. The typical cross-section of Specimen 3 is shown in Figure 46 and the stirrups were placed 9 in. on center. Due to the large size of the No. 7 bars, two of them were bundled on one side of the beam to allow spacing for the stirrup.

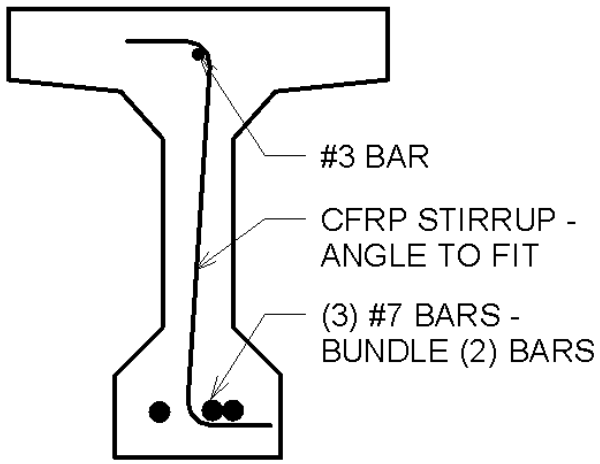

Figure 46: Cross-Section of Specimen 3 CFCC Reinforcement

Loading on the specimen was applied in 5-kip increments up to 15 kips and then in 3-kip increments until completion of testing. The expected shear failure of the specimen was 30 kips of loading. The load-deflection plot for this specimen is shown in Figure 47. Flexural yielding of the beam never occurred, but testing was stopped at 48 kips to ensure a second test could be run on the specimen.

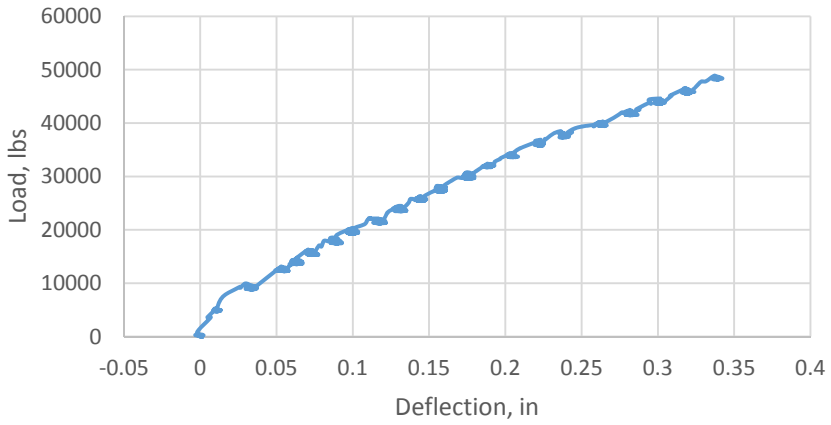

Figure 47: Load-Deflection Specimen 3 Minimum CFCC Reinforcement

Cracks were measured at two locations on the beam. Crack one was the first shear/flexure crack that opened in the web of the beam at 20 kips. Crack two was a major shear crack that opened along the web of the section at 22 kips. These cracks, along with best fit lines for propagation are shown in Figure 48.

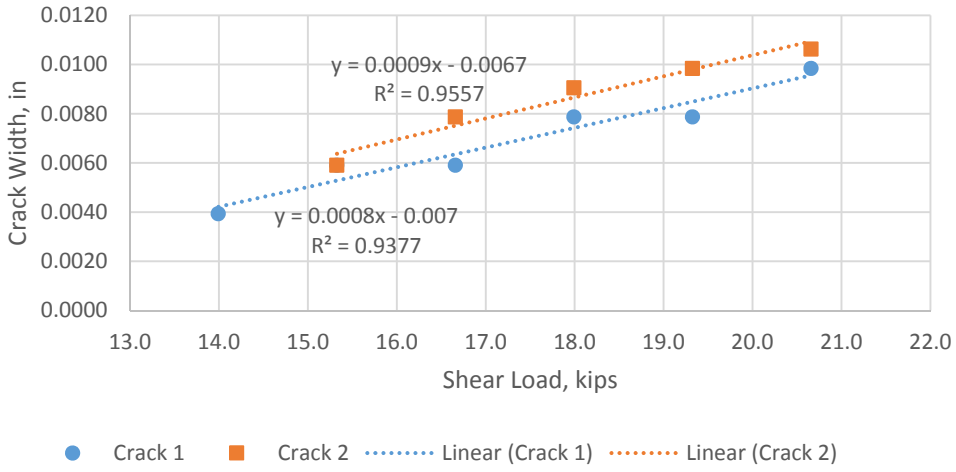

Figure 48: Crack Propagation Specimen 3 Minimum CFCC Reinforcement

Vertical LVDT displacements are shown in Figure 49 to compare to crack width measurements. The large jump in displacement at 13 kips of LVDT 90 indicates the initial shear cracking. The other LVDTs show a more gradual displacement, which does not occur in the other tests. The cracking from LVDT 90 corresponds well with the initial crack measurement occurring at 14 kips. The displacements also indicate about 0.01 in. of movement at 20 kips, which matches closely with the crack widths being about 0.009 in. at 20 kips.

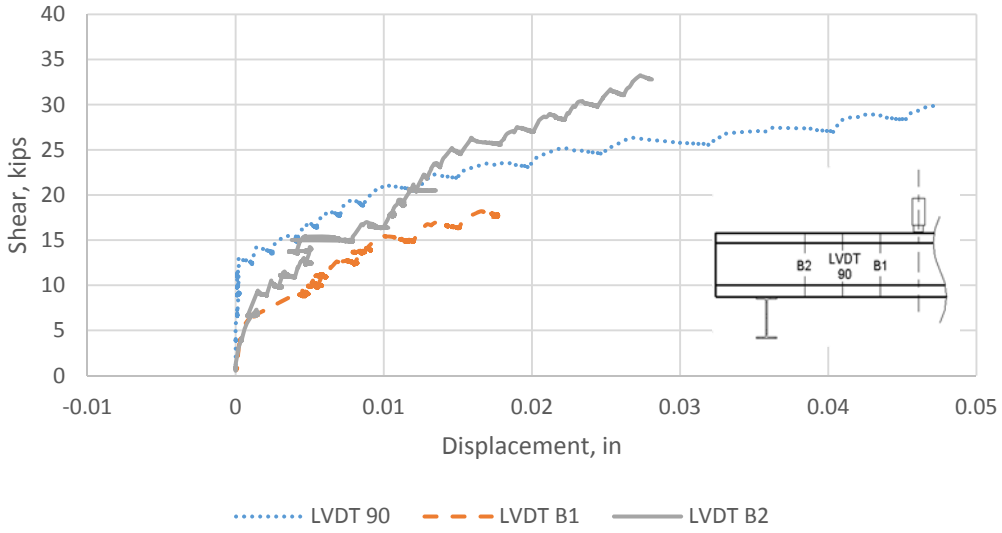

Figure 49: Vertical LVDT Displacements of Specimen 3 Minimum CFCC Reinforcement

4.4.6 – Specimen 3 Typical CFCC Reinforcement

The typical reinforcement side of Specimen 3 was the same as shown in Figure 46 with the stirrups spaced at 4 in. on center. This specimen was loaded to 15 kips in 5-kip increments and then after that by 3-kip increments up to 51 kips. Also, one of the LVDT gages in the rosette popped off the beam at 42 kips due to large cracking directly under the gage. The testing was stopped at 51 kips due to some popping noises coming from the beam. This allowed

instrumentation to be removed before ultimate failure. The load deflection plot is shown in Figure 50.

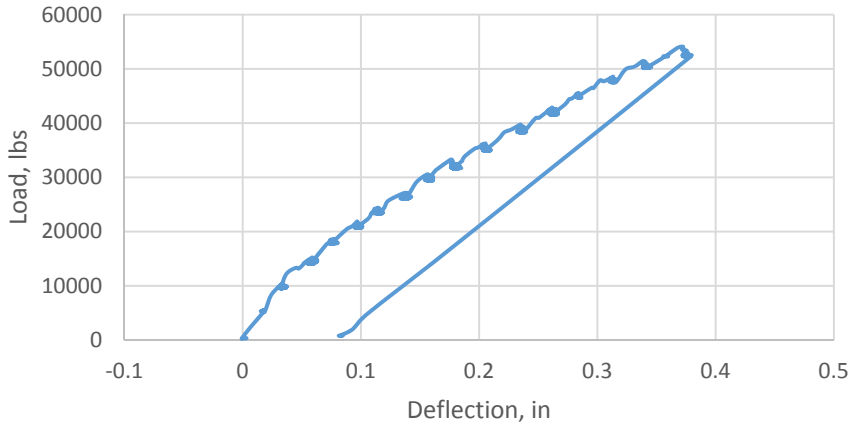

Figure 50: Load-Deflection Specimen 3 Typical CFCC Reinforcement

After the load of 51 kips was reached, all instrumentation was removed from the beam except the wire potentiometers. These were left in place on this test as the two previous ultimate tests had not fallen to the floor, presenting no crushing hazard to the instrumentation. The ultimate test was run by taking the load up to the previous final load and then slowly increasing the load by 2-kip increments. The beam took a maximum load of 63 kips before failure. At failure one of the magnetic holders for the wire potentiometers was knocked off the beam. The

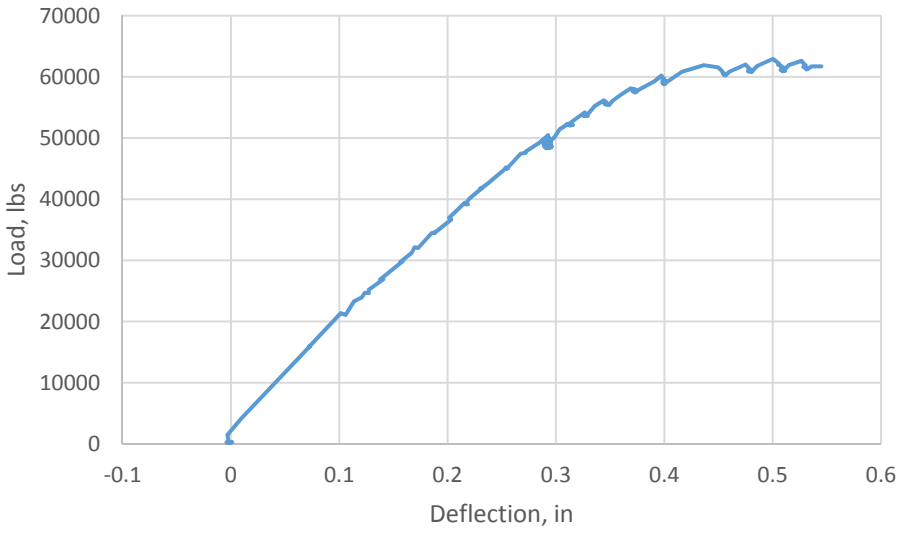

Figure 51: Ultimate Load-Deflection Specimen 3 Typical CFCCC Reinforcement

longitudinal reinforcement reached yield as shown by the plateau of the load-deflection curve in Figure 51 and was evident during testing.

The failure of this specimen appeared to be a combination of shear failure and bond failure at ultimate load due to the large splitting of the concrete at the bottom of the beam as shown in Figure 52. Also, the shear crack formed between two CFCC stirrups, and concrete was removed to check whether CFCC stirrups ruptured, and they had not. The large splitting failure along the longitudinal bars is thought to be caused by the tails of the CFCC stirrups. Due to the required length of the tail, the stirrups were angled to fit in the beam with all tails in one direction. It is possible that as the tails (see Figure 17) tried to flex under increasing axial load, they added additional stress on the concrete in the bottom bulb that resulted in the failure along the tension bars.

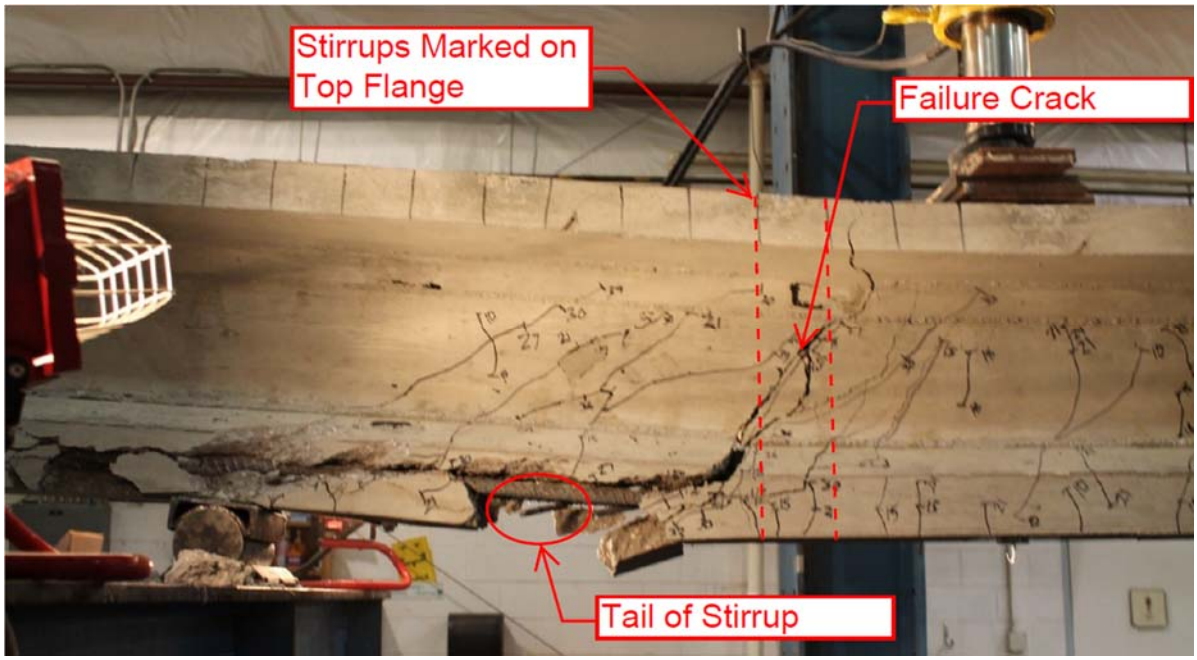

Figure 52: Failure of Specimen 3 Typical CFCC Reinforcement

Crack widths were measured at three locations on the beam during testing and they are presented in Figure 53. Cracks are numbered in order of their appearance in the web. The cracks are again presented with a linear fit for propagation.

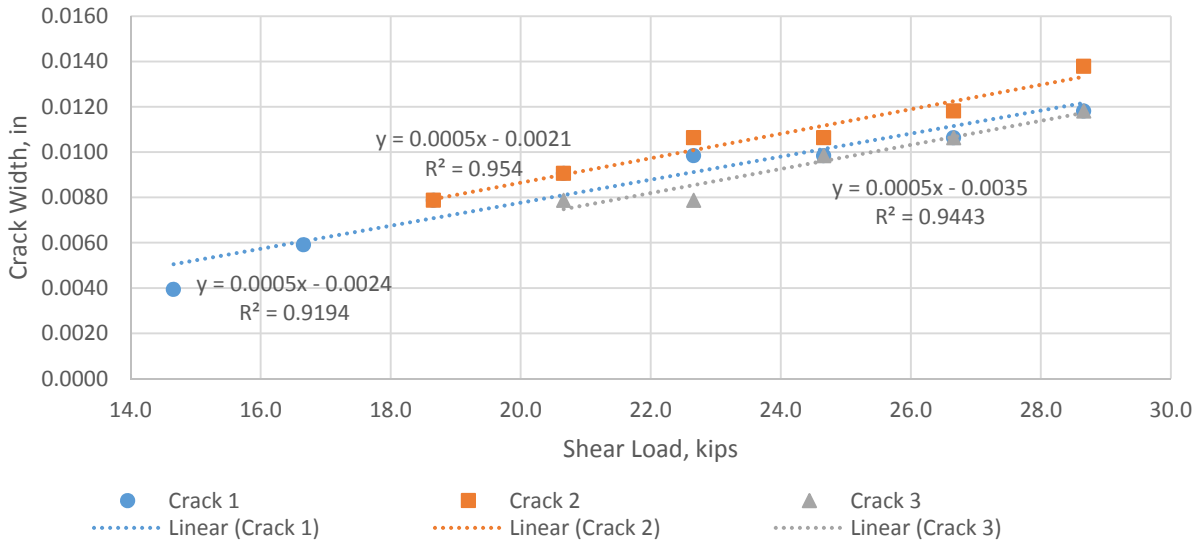

Figure 53: Crack Propagation Specimen 3 Typical CFCC Reinforcement

Vertical LVDT displacements as shown in Figure 54 again provide a good correlation to the cracking width measurements taken of the Typical CFCC specimen. According to the LVDTs, the crack occurs at about an average of 15 kips, which aligns with the initial crack as measured in Figure 53. At 20 kips, the LVDT displacements average about 0.01 in., while the cracks average 0.085 in. This shows a strong correlation between the instrumentation and the manual crack measurements and increases the certainty of accuracy of the crack width measurements.

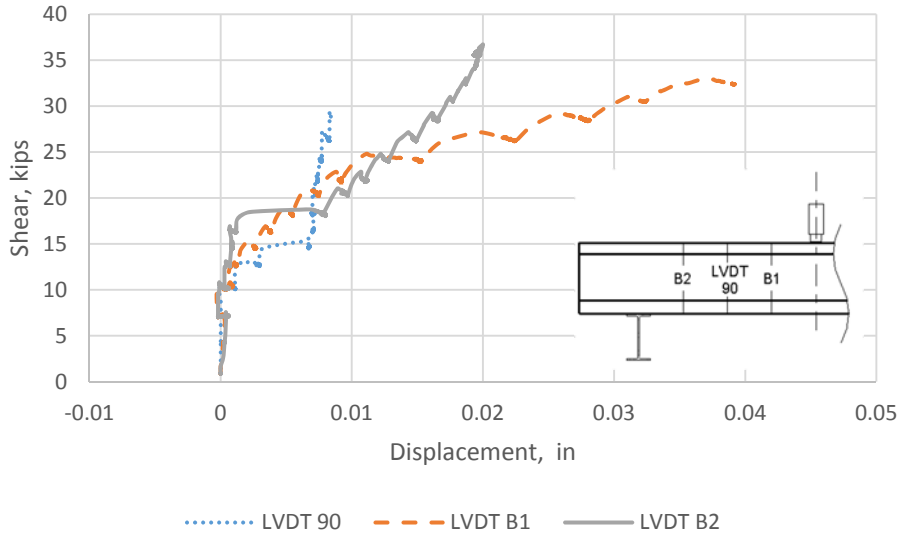

Figure 54: Vertical LVDT Displacements of Specimen 3 Typical CFCC Reinforcement

4.4.7 – Specimen 4 C-Grid Two Layers Zip Tied

The final beam specimen was a C-Grid reinforced beam to investigate whether putting layers together without room for concrete would change the strength and performance of the beam. This specimen had two layers of the C50 1.6x1.8 grid which were zip tied together at 12 in. on center with small zip ties available at a local hardware store. The layers were then placed into the beam as shown in Figure 55, and tied in place. One thing noticed about the zip tied layers was the increased stiffness made the grid easier to move and tie in place.

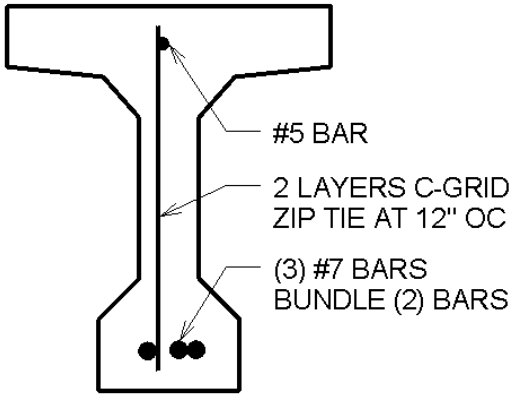

Figure 55: Cross-Section of Specimen 4 Two Layers of C-Grid Zip Tied

Loading was applied to the beam in 5-kip increments until 15 kips and then in 3-kip increments for the remainder of testing. The beam was loaded to the calculated shear failure load of 45 kips and then was increased. The testing was going to be stopped if the longitudinal steel reach inelasticity, but the shear failure occurred before inelasticity. The beam failed in

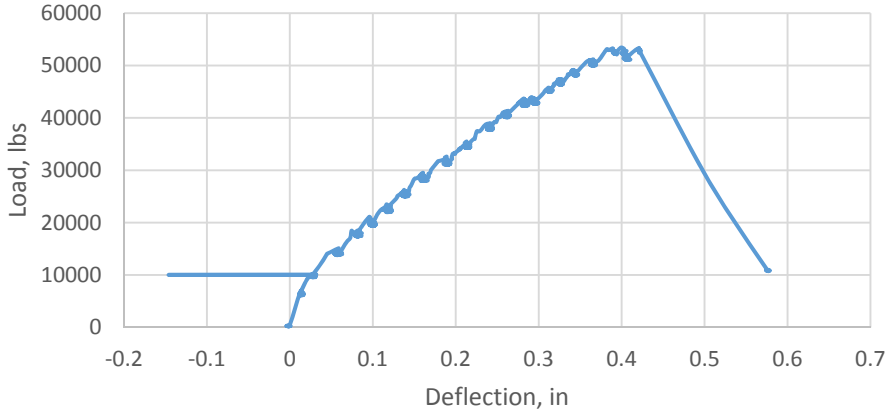

Figure 56: Load-Deflection of Specimen 4 Two Layers C-Grid Zip Tied

shear at 53 kips of load and immediately preceding failure popping noises were heard emanating from the beam. The anticipated shear failure of the beam was at 45 kips of loading. The load-deflection plot for the test is shown in Figure 56, and again during this test the wire potentiometer was hit while marking cracks. The shear failure is shown in Figure 57.

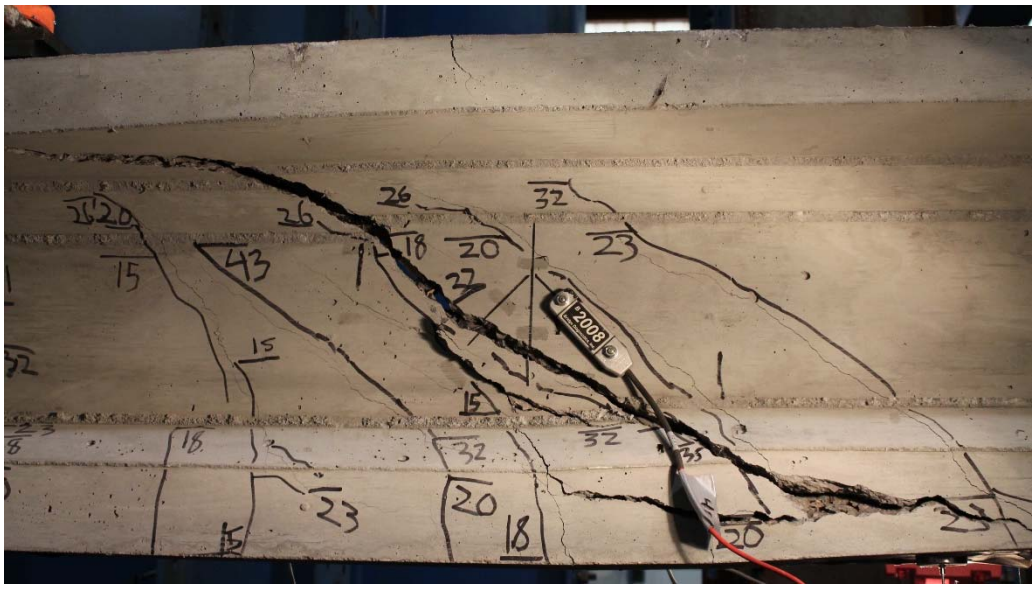

Figure 57: Shear Failure of Specimen 4 Two Layers C-Grid Zip Tied

Cracks width measurements were taken in three locations for this beam. Crack numbers correspond the appearance of the cracks during testing of the specimen. One interesting thing to notice about the cracks on this specimen was that Crack 1 actually started to get smaller after 20

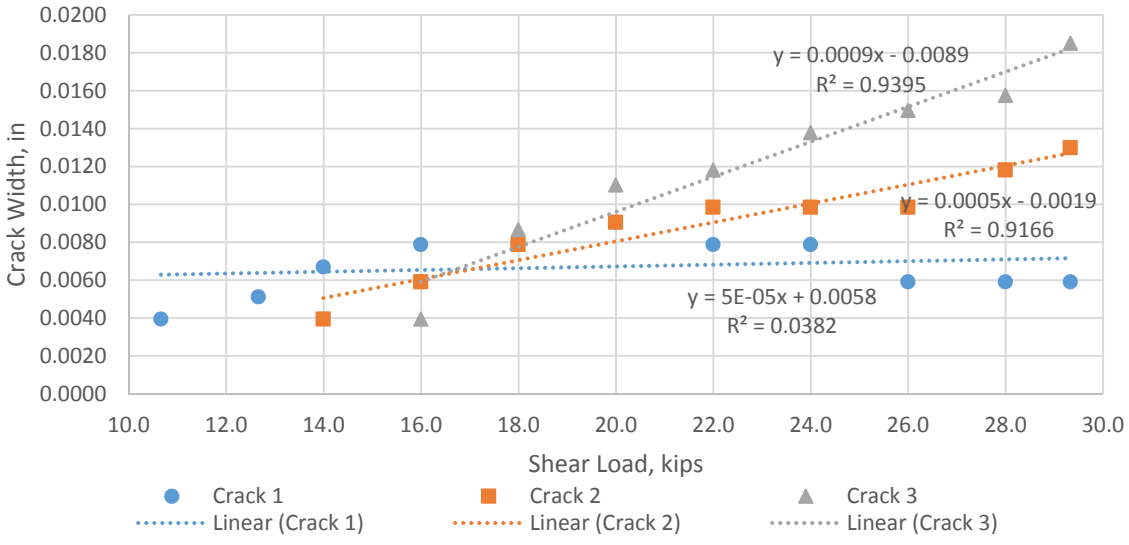

Figure 58: Crack Propagation Specimen 4 Two Layers C-Grid Zip Tied

kips of shear. This happened because another crack opened beside this crack, which caused a reduction in the width of the first crack. Crack widths and best fit lines for propagation are presented in Figure 58. Due to Crack 1 closing back up the linear fit is not useful and is not used in any averages for crack growth.

Measurements of displacement from the vertical LVDTs are presented in Figure 59. From the measurements, shear cracking occurs at 10 kips which is the same cracking load shown in Figure 58. Overall displacement of LVDTs at 25 kips is about 0.02 in., while the crack widths at 25 kips are around 0.012 in. The crack widths are much smaller, again due to the multiple shear cracks throughout the web as shown in Figure 57.

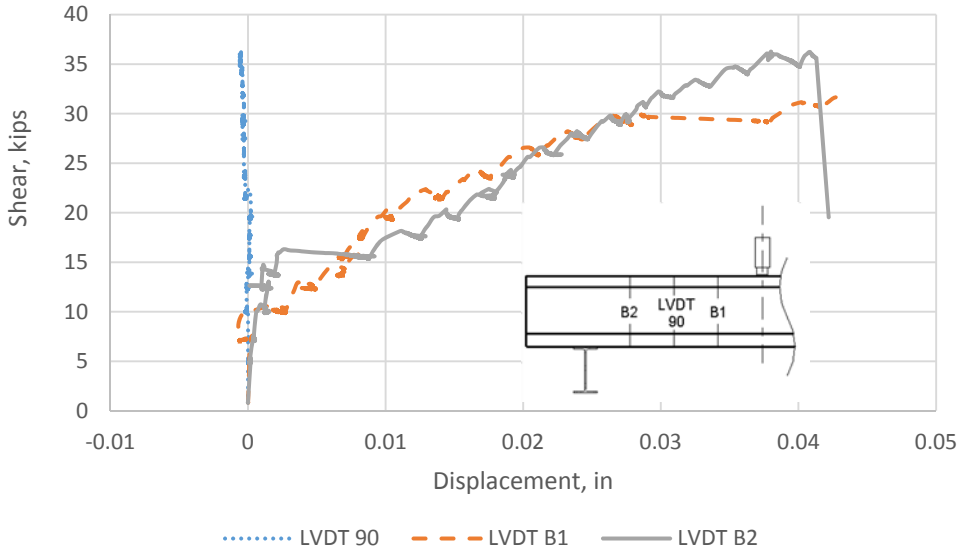

Figure 59: Vertical LVDT Displacements of Specimen 4 Two Layers C-Grid Zip Tied

4.4.8 – Specimen 4 C-Grid Two Layers Spaced

This specimen was used to determine if using multiple layers of C-Grid with a spacing between layers made a difference in the capacity of the beam. A No. 5 bar was used as the top bar to give a larger spacing between grids and help ensure that proper consolidation of the concrete would could be achieved. The cross-section of the specimen is shown in Figure 60.

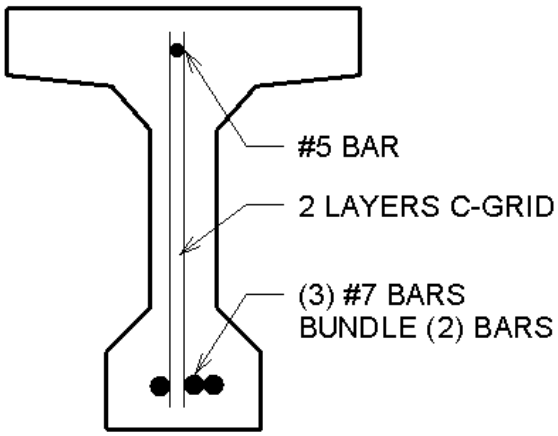

Figure 60: Cross-Section of Specimen 4 Two Layers C-Grid Spaced

Loading was applied in 5-kip increments up to 15 kips and then in 3-kip increments until the end of testing. This side of the specimen also did not yield the longitudinal bars before failure of the shear reinforcing as shown by lack of a yield plateau of the load-deflection plot in Figure 61. Final loading before failure was 56 kips which was higher than the anticipated failure load of 45 kips. Shear failure of the specimen is shown in Figure 62. Upon inspection of the

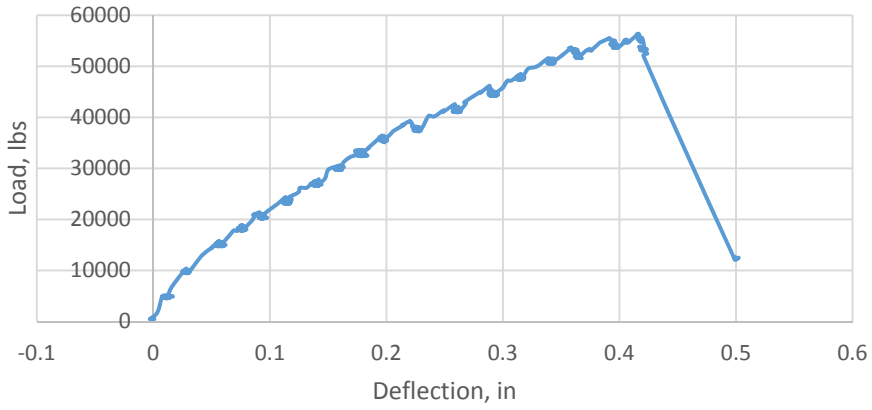

Figure 61: Load-Deflection Specimen 4 Two Layers C-Grid Spaced

failure, nearly all the tows of C-Grid crossing the crack had fractured. The failure was very similar to the specimen with two layers of C-Grid zip tied together.

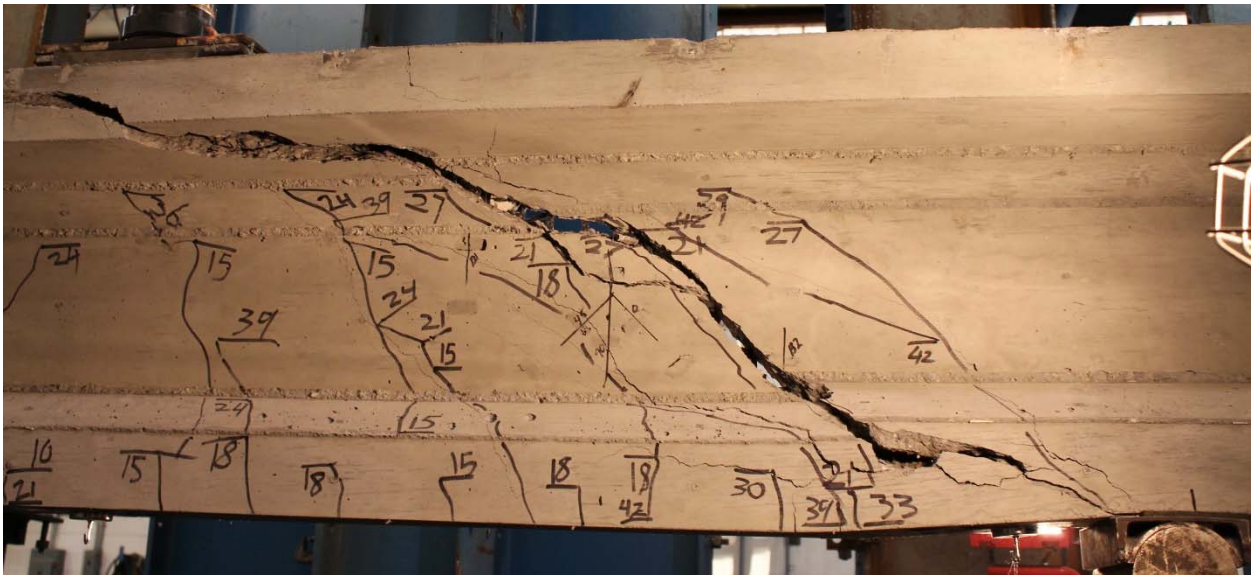

Figure 62: Shear Failure of Specimen 4 Two Layers C-Grid Spaced

Cracking was measured at the first three shear cracks that opened in the web. A reduction in size of crack 3 was noticed at higher loading due to another crack opening beside it and reducing the width on the original crack. These additional cracks create a larger area of higher stress, thus reducing the individual crack widths. A linear best fit was used on the crack propagation. The fit does not work well on crack 3 as it closed back up later in testing and due to

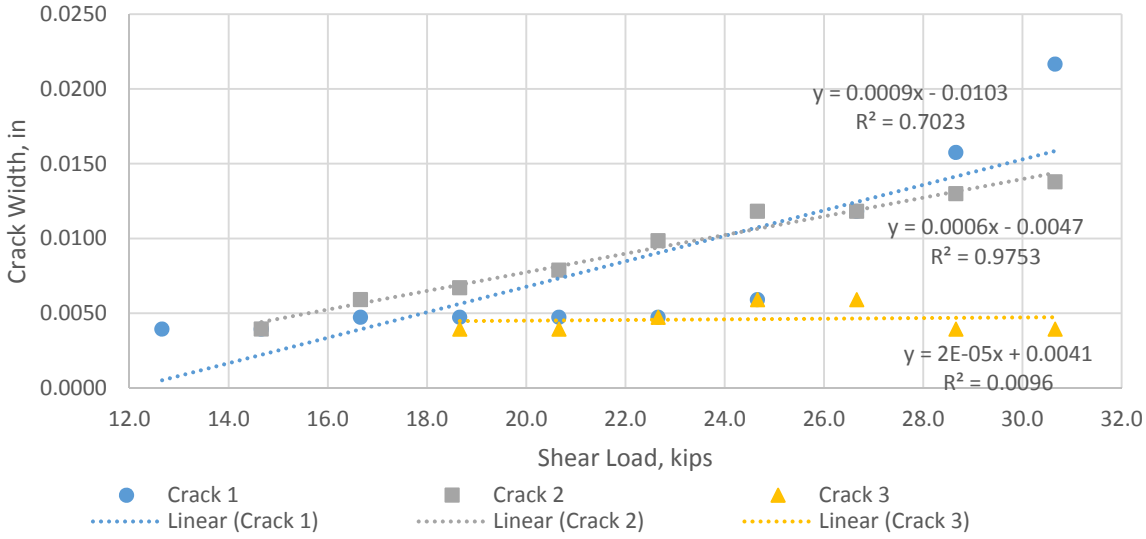

Figure 63: Crack Propagation Specimen 4 Two Layers C-Grid

this it's propagation rate is not used in later averages. Crack 1 shows a large increase in size once higher loads were reached. The cracks widths are presented in Figure 63.

The displacements of the vertical LVDTs are presented in Figure 64. From the movement of LVDTs B1 and B2 the first shear crack opens up at about 11 kips, which correlates well with Figure 63. The crack width at 25 kips is about 0.011 in. which agrees with the LVDT displacement of 0.01 in. at 25 kips. The crack widths and LVDT displacements show a strong agreement in this specimen.

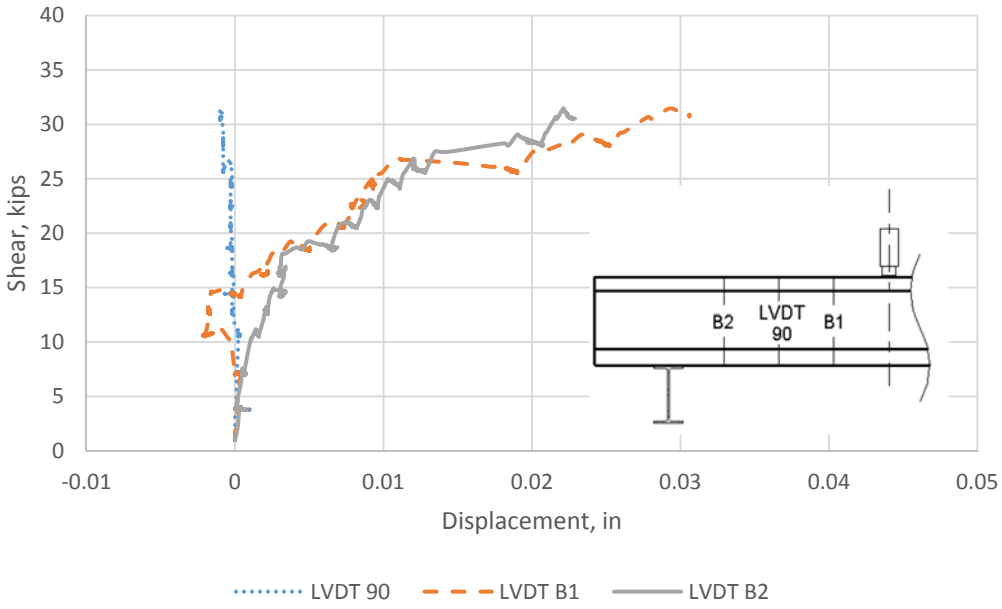

Figure 64: Vertical LVDT Displacements of Specimen 4 Two Layers C-Grid Spaced

4.4.9 – Concrete Material Testing for Beam Tests

The concrete used for the development length tests was specified as a 7,000 psi concrete, using 1/2 in. aggregate, and having a slump of 6 to 8 in. for high workability. The concrete was purchased from the local ready-mix concrete plant, Conrock, and delivered to the lab for each of the two placements. Slump tests for each batch were taken prior to placement to ensure a high workability before placing in the forms. During placement 4 in. by 8 in. cylinders were cast to be used for concrete material testing. Compressive tests were run following ASTM C39 protocol

at approximately 7 and 14 days after placement to determine strength gain of the mix design. Compression testing, splitting tensile following ASTM C496, and elastic modulus following ASTM C469 were also run before and after testing. Beams were allowed to cure approximately 28 days before testing to ensure the concrete reached full strength. Average concrete properties for testing are shown in Table 5, note that Pour 1 was Specimens 1 and 2 and Pour 2 was Specimens 3 and 4. Full concrete test data is available in Appendix B.

Table 5: Beam Test Concrete Properties

Property (ksi)	Pour 1	Pour 2
Compressive Strength	7.99	7.35
Splitting Tensile Strength	0.690	0.605
Modulus of Elasticity	5020	4620

4.4.10 – Steel Longitudinal Reinforcing Material Tests

Steel reinforcing bars used in the construction of the beams were tested to determine material properties. The test procedure follow that outlined in ASTM A370 (2014). Only No. 5 bar was tested even though the beams also used No. 3 and No. 7 bars. All bars were ordered from the same supplier, B&R Rebar in Richmond, Virginia. Since all bars were from the same

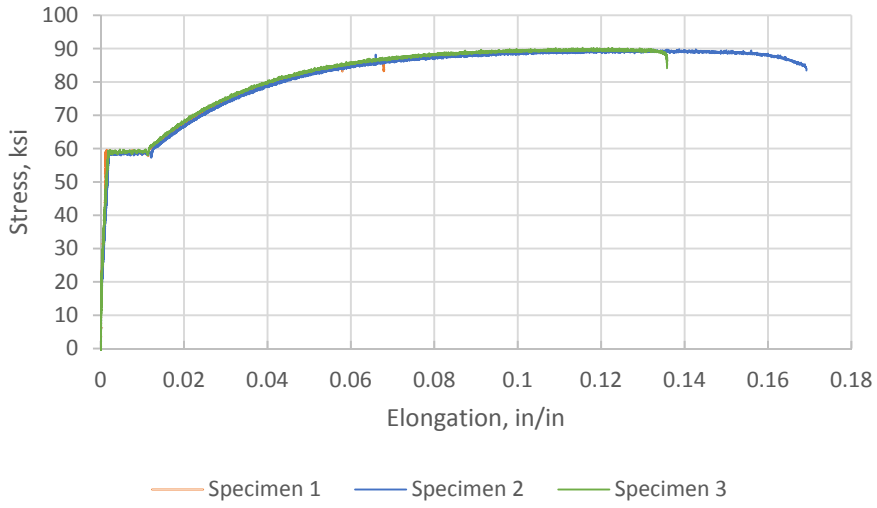

Figure 65: Steel Reinforcing Bar Stress-Strain Curve

yard, the assumption that these bars are similar in material properties is not unreasonable. Three separate 18 in. sections of bar were tested on a floor model Instron SATEC universal testing machine. The average modulus of elasticity was found to be 29,900 ksi for the reinforcing bar. Yield stress was found as 59 ksi and ultimate stress was 90 ksi. The stress-strain curve for the reinforcing bar is shown in Figure 65.

5 – Discussion of Beam Tests

5.1 – Discussion on Rosette Data

Rosettes were used on both sides of the beam to gather strain data that would allow the principal stresses and angles to be calculated. However, after the collection and analysis of the strain data it provided very little useful information due to scatter. The principal angle readings are not consistent, but instead bounce back and forth from positive to negative angles. Angles also show large jumps, which is not consistent with theoretical calculations. Some of the issues are likely due to imprecise set-up of the rosettes and the angles at which the gages are reading.

The BDI rosettes did show principal angles that agree closely with predicted angles from analysis up until shear cracking occurred in the sections. Once the shear cracks opened the BDI gages were very inconsistent with their information. This is thought to occur because maximum displacement of the BDI gages is 0.008 in. Once the concrete cracks the BDI gages are beyond this maximum displacement. After testing it was found that the BDI gages typically had one foot that was no longer attached to the beam, as the bond between the glue and concrete had broken. This meant during testing the BDI gages were extending beyond their range and lost connection to the beam. The data captured by these gages is only valid up until the point of shear cracking, but is still noisy, possibly due to alignment issues.

The LVDT rosettes showed very poor data throughout the loading of the specimens. Before cracking the data was noisy and showed large angle changes with small loading changes up to initial cracking in the web. After cracking some of the noise from the data was gone, but the angles still did not provide good estimates of the principal stresses. Not aligning the rosettes perfectly could lead to some noise in the results. Also, as the cracks opened throughout the beam, inelasticity was concentrated in this area. The cracks caused the local stresses to change quickly in a small area as new cracks opening would relieve the stresses on other cracks. Graphs of principal angles from all beam tests are shown in Appendix C.

5.2 – Shear Design Methods and Discussion

The different shear design methods that were previously discussed in the literature review of this thesis were employed for the design of the beams during testing. The different shear strength calculations are compared to the actual failure load of the specimens to determine which methods provide better results for the different transverse reinforcing materials. The ratio of the ultimate shear to the nominal shear strength is provided for both the design material properties and actual measured material properties. Since every specimen was not pushed until failure, a column indicating failure and failure type was added to the table. This allows any test/nominal ratio to be compared to actual failure, as it may be much higher because the specimen did not fail in shear.

For each shear design method, the design material values are used as well as the actual measured materials values from testing of the materials. The design properties for the CFCC and C-Grid are taken as those specified by the manufacturer, which for the guaranteed strength of the material is the average rupture strength reduced by three standard deviations. The actual properties for the C-Grid are from the material tests discussed in this thesis. The CFCC actual

values are from the quality control testing provided with the stirrup shipment from Tokyo Rope. The material property values are summarized in Table 6.

Table 6: Design and Actual Tested Material Properties

Material and Property	Design	Actual
Concrete f'c Specimens 1&2	7.0 ksi	8.0 ksi
Concrete f'c Specimens 3&4	7.0 ksi	7.4 ksi
Steel Yield Stress	60 ksi	59 ksi
Steel Modulus of Elasticity	29000 ksi	29900 ksi
CFCC Bar Breaking Stress	352 ksi	437 ksi
CFCC Modulus of Elasticity	22500 ksi	21755 ksi
C-Grid Tow Breaking Stress	290 ksi	339 ksi
C-Grid Modulus of Elastiticy	34000 ksi	32600 ksi

Note: CFCC and C-Grid breaking stress reported is the average reduced by three standard deviations

5.2.1 – AASHTO Modified Compression Theory

The calculations presented below followed the method as previously described in section 2.3.1. AASHTO provides a stress limit on reinforcing of 0.0035 times the modulus of elasticity or a maximum of 75 ksi in section 5.8.2.8 of the specifications. For the CFCC stirrups, the maximum stress was limited to 75 ksi due to the large modulus of elasticity. No additional strength reduction was taken for the bend zones as the AASHTO specifications do not cover bend reductions with CFRP products. The C-Grid maximum strength is also limited by a

Table 7: AASHTO Maximum Stirrup Stresses

Design Values (ksi)			
Material	f_y or f_u	0.0035E	f_{max}
Steel	60	102	60
CFCC	352	79	75
C-Grid	290	119	75
Actual Values (ksi)			
Material	f_y or f_u	0.0035E	f_{max}
Steel	59	105	59
CFCC	437	76	75
C-Grid	339	114	75

maximum of 75 ksi, due to its high modulus of elasticity. The beam with two layers of C-Grid has the same capacity, whether spaced or zip-tied because the calculated strength is the same via the AASHTO shear design method. Values for allowable stress are summarized in Table 7.

Table 8 provides results from the calculations using the AASHTO method previously described in this thesis. From these results it is clear than the AASHTO method is conservative for all specimens. The specimens with the best fit are the CFCC stirrups, as they have the ratio closest to 1.0. The AASHTO method also provides a good fit with the steel even though none of the specimens were failed in shear. However, the reduction of strength in the C-Grid due to the high modulus and strength provides a very conservative result. This is an overly conservative predictor of shear strength of C-Grid transverse reinforcing and may result in more heavily reinforced beams than needed.

Table 8: AASHTO MCFT per Code Calculations and Results

Shear Reinforcing	V_n-Design (kips)	V_n-Actual (kips)	Max Shear Load (kips)	Failure	Ratio V_{test}/V_n-Design	Ratio V_{test}/V_n-Actual
Typ Steel	28.52	28.62	43.56	Yes, Compression	1.53	1.52
Min Steel	18.35	18.57	23.02	No	1.25	1.24
Typ C-Grid	-	-	-	-	-	-
Min C-Grid	12.29	12.74	28.90	Yes, Shear	2.35	2.27
Typ CFCC	39.31	39.52	42.62	Yes, Shear	1.08	1.08
Min CFCC	25.01	25.23	33.23	No	1.33	1.32
C-Grid Zip Tied	16.62	16.86	36.26	Yes, Shear	2.18	2.15
C-Grid Spaced	16.62	16.86	38.24	Yes, Shear	2.30	2.27

5.2.2 – AASHTO Modified Compression Theory Using Full Strength

The AASHTO method provided overly conservative nominal shear calculations for the C-Grid due to the reduction of the maximum stress. Therefore it was decided that the method should be used without a reduction in strength for the CFRP materials. This way the full strength of the material would be used as reported by the manufacturer for design. The full strength

means that no specified reductions are taken. Note that the design and actual tested stress values are reduced by three standard deviations. The steel transverse reinforcing sections do not change as they were not originally reduced by the specifications. The full strengths are the allowable breaking stress or yield stress as given in Table 6.

From Table 9, it is apparent that the full strength of the CFCC grid gives a very high value for nominal shear capacity that was not achieved by the specimens. This should not be used for CFCC stirrups as following the code precisely provides good correlation between tested shear capacity and calculated shear capacity. Yet, the value does provide a good fit for results of the C-Grid, especially when two layers are used. This method is still conservative for the C-Grid while only allowing about 20-30% overage in the design. This fit is acceptable and would lead to safe and economical design.

Table 9: AASHTO MCFT Full Strength Calculations and Results

Shear Reinforcing	V_n-Design (kips)	V_n-Actual (kips)	Max Shear Load (kips)	Failure	Ratio V_{test}/V_n-Design	Ratio V_{test}/V_n-Actual
Typ Steel	28.52	28.62	43.56	Yes, Compression	1.53	1.52
Min Steel	18.35	18.57	23.02	No	1.25	1.24
Typ C-Grid	-	-	-	-	-	-
Min C-Grid	18.42	20.10	28.90	Yes, Shear	1.57	1.44
Typ CFCC	95.35	106.20	42.62	Yes, Shear	0.45	0.40
Min CFCC	61.06	69.43	33.23	No	0.54	0.48
C-Grid Zip Tied	29.68	32.61	36.26	Yes, Shear	1.22	1.11
C-Grid Spaced	29.68	32.61	38.24	Yes, Shear	1.29	1.17

5.2.3 – ACI 318 Shear Theory

Since ACI 318 is designed for use with steel reinforcing bars, there is only a maximum stress that is allowed to be placed on the transverse reinforcing in shear. The maximum value allowed is 80 ksi, which is based on the maximum stress that welded wire mesh can take before yielding. Due to this maximum both the CFCC stirrups and the C-Grid are only allowed a maximum stress of 80 ksi, which is much lower than their guaranteed strength from the

manufacturer. The steel follows the typical ACI design method with a maximum stress of 60 ksi. Maximum stresses for the shear design of stirrups are presented in Table 10.

Table 10: ACI 318 Maximum Stirrup Stresses

Design Values (ksi)		
Material	f_y or f_u	f_{max}
Steel	60	60
CFCC	352	80
C-Grid	290	80
Actual Values (ksi)		
Material	f_y or f_u	f_{max}
Steel	59	59
CFCC	437	80
C-Grid	339	80

The results of Table 11 show a good fit with the steel transverse reinforcement which is to be expected for this method. Also, the CFCC stirrups provide a very good fit for the typical reinforcement at only 10% more than design values. The CFCC stirrups ratios compare favorably with the ratios for the steel stirrups. The C-Grid does not show a good correlation of predicted to actual strengths. The ratios are all over 2.5 which means the method is not providing a good estimate of the actual shear strength of the beams. While this method provides a good correlation for the CFCC stirrups as transverse reinforcement, it is overly conservative in calculating the capacity of sections with C-Grid shear reinforcement.

Table 11: ACI per Code Calculations and Results

Shear Reinforcing	V_n-Design (kips)	V_n-Actual (kips)	Max Shear Load (kips)	Failure	Ratio V_{test}/V_n-Design	Ratio V_{test}/V_n-Actual
Typ Steel	27.23	27.51	43.56	Yes, Compression	1.60	1.58
Min Steel	17.88	18.32	23.02	No	1.29	1.26
Typ C-Grid	-	-	-	-	-	-
Min C-Grid	10.97	11.56	28.90	Yes, Shear	2.63	2.50
Typ CFCC	38.70	38.93	42.62	Yes, Shear	1.10	1.09
Min CFCC	21.89	22.12	33.23	No	1.52	1.50
C-Grid Zip Tied	13.25	13.49	36.26	Yes, Shear	2.74	2.69
C-Grid Spaced	13.25	13.49	38.24	Yes, Shear	2.89	2.83

5.2.4 – ACI 318 Shear Theory Using Full Strength

The reduced allowable stress of 80 ksi provides a very conservative estimate of the shear strength of sections reinforced with C-Grid. Therefore, this section compares tests to the ACI 318 method of shear design using the full reported manufacturer and tested strength of the CFRP products. Again, these full strengths are the mean reduced by three standard deviations to ensure a safe design. The steel specimens stay the same as the full yield stress of the reinforcing was already used in the ACI 318 method.

Table 12 presents the results of the ACI 318 calculations using the full CFRP strength. This shows that using the full strength for the CFCC stirrups provides a non-conservative estimate of the shear strength of the section. This result is similar to the findings using the full CFCC strength in the AASHTO method. However, the use of the full strength of the C-Grid provides a better estimate of the shear strength. While the ratio is not as close to 1.0 as the AASHTO method, it stays within a realm that would allow an adequate section that is not grossly overdesigned. This method could be used for design with C-Grid, but following the code precisely should be used for the CFCC stirrups.

Table 12: ACI 318 Full Strength Calculations and Results

Shear Reinforcing	V_n-Design (kips)	V_n-Actual (kips)	Max Shear Load (kips)	Failure	Ratio V_{test}/V_n-Design	Ratio V_{test}/V_n-Actual
Typ Steel	27.23	27.51	43.56	Yes, Compression	1.60	1.58
Min Steel	17.88	18.32	23.02	No	1.29	1.26
Typ C-Grid	-	-	-	-	-	-
Min C-Grid	17.35	19.43	28.90	Yes, Shear	1.67	1.49
Typ CFCC	141.57	173.96	42.62	Yes, Shear	0.30	0.24
Min CFCC	67.61	82.14	33.23	No	0.49	0.40
C-Grid Zip Tied	25.88	29.06	36.26	Yes, Shear	1.40	1.25
C-Grid Spaced	25.88	29.06	38.24	Yes, Shear	1.48	1.32

5.2.5 – ACI 440.4R Shear Theory

The ACI 440.4R method is designed for use with FRP prestressed concrete. Even though prestressed members are not used, the shear design method should work for reinforced members. Also, the main need for CFRP transverse reinforcing is in large prestressed members near coastal areas. Therefore, this method is of importance for the future use of CFRP grids in prestressed concrete.

The ACI 440.4R method limits the maximum stress of the material to 0.002 times the elastic modulus, the guaranteed tensile strength, or the bend radius reduction strength. For steel stirrups and the C-Grid, 0.002 times the elastic modulus of the materials controls the allowable stress. The steel is allowed a maximum stress of 58 ksi, which is close to the typical 60 ksi yield stress. The C-Grid is allowed a maximum stress which translates to 195 lbs per tow instead of the full strength of 830 lbs. The CFCC stirrups are controlled by 0.002 times the modulus as well, which gives them an ultimate strength of 45 ksi. This value is the same strength used in the ACI 318 and AASHTO calculations. The maximum stirrup stresses are shown in Table 13.

Table 13: ACI 440.4 Maximum Stirrup Stresses

Design Values (ksi)				
Material	f_{fu}	f_{fb}	0.002E	f_{max}
Steel	60	-	58	58
CFCC	352	103	45	45
C-Grid	290	-	68	68
Actual Values (ksi)				
Material	f_{fu}	f_{fb}	0.002E	f_{max}
Steel	59	-	60	59
CFCC	437	113	43	43
C-Grid	339	-	65	65

The results of the shear capacity calculations are presented in Table 14. The ACI 440.4 method is very conservative when designing with the C-Grid as the ratios are above 2.7 for

design values. The method is also conservative for the CFCC stirrups. The only material it predicts reasonably well is steel stirrups, as the 0.002 times the modulus is nearly identical to the yield strength of steel. This method was found to be conservative by Grace et al. (2015) as well. The ACI 440.4 method is a very safe method, but will result in significantly more reinforcing than needed in a section.

Table 14: ACI 440.4 Calculations and Results

Shear Reinforcing	V_n-Design (kips)	V_n-Actual (kips)	Max Shear Load (kips)	Failure	Ratio V_{test}/V_n-Design	Ratio V_{test}/V_n-Actual
Typ Steel	26.61	27.51	43.56	Yes, Compression	1.64	1.58
Min Steel	17.57	18.32	23.02	No	1.31	1.26
Typ C-Grid	-	-	-	-	-	-
Min C-Grid	10.6	11.1	28.90	Yes, Shear	2.73	2.60
Typ CFCC	25.46	25.13	42.62	Yes, Shear	1.67	1.70
Min CFCC	16.00	15.99	33.23	No	2.08	2.08
C-Grid Zip Tied	12.53	12.59	36.26	Yes, Shear	2.89	2.88
C-Grid Spaced	12.53	12.59	38.24	Yes, Shear	3.05	3.04

5.2.6 – ACI 440.4R Shear Theory Using Full Strength

The reductions in strength of the CFCC and C-Grid put forth in ACI 440.4R provide very conservative estimates of the shear strength of the section. For this reason, the ACI 440.4 method is used with the full strength of the stirrups. Again, this full strength is the average minus three standard deviations for the CFRP materials and are the values found in Table 6.

Table 15 presents the calculations using the full strength and the ACI 440.4 method. The predicted shear strength of the specimens with steel stirrups barely increase because 0.002 times the modulus of elasticity results in nearly the yield strength of steel reinforcing. The specimens with CFCC stirrups are predicted much higher than the actual capacity. This method should not be used to calculate the capacity of sections with CFCC stirrups. The ratios of the predicted to tested values are much smaller for the C-Grid. However, these ratios are not as close to 1.0 as they are for the full strength ACI 318 and AASHTO methods. Since other methods are better are

predicting the shear strength of the section with C-Grid transverse reinforcement this method is not recommended for design.

Table 15: ACI 440.4 Full Strength Calculations and Results

Shear Reinforcing	V_n-Design (kips)	V_n-Actual (kips)	Max Shear Load (kips)	Failure	Ratio V_{test}/V_n-Design	Ratio V_{test}/V_n-Actual
Typ Steel	27.23	27.51	43.56	Yes, Compression	1.60	1.58
Min Steel	17.88	18.32	23.02	No	1.29	1.26
Typ C-Grid	-	-	-	-	-	-
Min C-Grid	17.35	19.43	28.90	Yes, Shear	1.67	1.49
Typ CFCC	141.57	173.96	42.62	Yes, Shear	0.30	0.24
Min CFCC	67.61	82.14	33.23	No	0.49	0.40
C-Grid Zip Tied	25.88	29.06	36.26	Yes, Shear	1.40	1.25
C-Grid Spaced	25.88	29.06	38.24	Yes, Shear	1.48	1.32

5.2.7 – ACI 440.1R Shear Theory

ACI 440.1R theory provides the basis for FRP reinforced concrete members. The concrete contribution is based upon a cracked section analysis to find the depth to the neutral axis, c. However, since the sections used have large flanges, the neutral axis is not in the web of the beam. As such, the b_w, term is not the proper value for shear capacity of the concrete because the flange is providing a large portion of un-cracked concrete to carry the shear. Therefore, the shear funnel approach was used to determine the concrete's shear resistance. This method is described in a paper from Tureyen, Wolf, and Frosh (2006). The only modification made to the method was that the angle of the taper was used instead of the typical 45° angle suggested. Figure 66 provides a diagram of the shear area used in the calculations. The distance c is the depth to the neutral axis from a cracked section analysis of the beam. The area of the shear funnel replaces the $b_w c$ term in Equation 13 of this thesis.

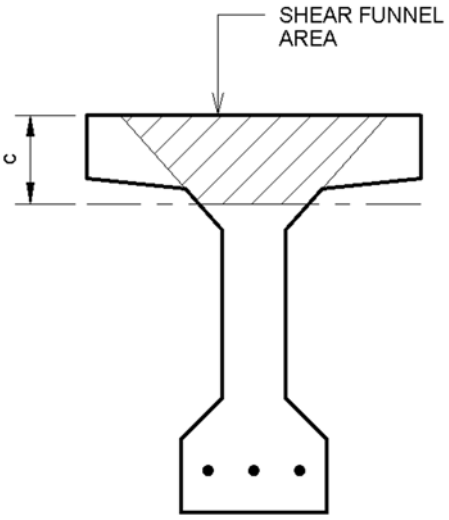

Figure 66: Shear Funnel Diagram for Beam Specimens

The ACI 440.4R method limits the maximum stress of the material to 0.004 times the elastic modulus, the guaranteed tensile strength, or the bend radius reduction strength. For the steel the yield stress of 60 ksi controlled. For the C-Grid the stress resulted in a load of 390 lbs per tow compared to the guaranteed of 830 lbs. The CFCC stirrups were controlled by 0.004 times the modulus of the bar, which resulted in a design value of 90 ksi. The use of 90 ksi is much larger than the value used in the previous calculations. The maximum stirrup stresses are shown in Table 16.

Table 16: ACI 440.1 Maximum Stirrup Stresses

Design Values (ksi)				
Material	f_{fu}	f_{fb}	0.004E	f_{fv}
Steel	60	-	116	60
CFCC	352	170	90	90
C-Grid	290	-	136	136
Actual Values (ksi)				
Material	f_{fu}	f_{fb}	0.004E	f_{fv}
Steel	59	-	120	59
CFCC	437	211	87	87
C-Grid	339	-	130	130

Table 17 presents the ACI 440.1 calculations for the calculated shear capacity and measured shear capacity of the sections. The method is not always conservative as shown by the ratio of less than 1.0 for the Typical CFCC transverse reinforcement. The CFCC values for both the minimum and typical reinforcing are also much higher than the other materials due to the large stress allowed in the stirrups by the design recommendations.

Table 17: ACI 440.1 Calculations and Results

Shear Reinforcing	V_n-Design (kips)	V_n-Actual (kips)	Max Shear Load (kips)	Failure	Ratio V_{test}/V_n-Design	Ratio V_{test}/V_n-Actual
Typ Steel	31.77	32.18	43.56	Yes, Compression	1.37	1.35
Min Steel	22.42	22.99	23.02	No	1.03	1.00
Typ C-Grid	-	-	-	-	-	-
Min C-Grid	17.21	17.76	28.90	Yes, Shear	1.68	1.63
Typ CFCC	49.94	49.28	42.62	Yes, Shear	0.85	0.86
Min CFCC	31.02	31.00	33.23	No	1.07	1.07
C-Grid Zip Tied	24.07	24.21	36.26	Yes, Shear	1.51	1.50
C-Grid Spaced	24.07	24.21	38.24	Yes, Shear	1.59	1.58

The method does a reasonable job of predicting the shear strength of the grid without being overly conservative like ACI 440.4. However, with the additional calculations to find the shear funnel in unusual shapes, the method is more cumbersome than others. This combined with poor estimates of strength for the CFCC stirrups means this method needs some additional study.

5.2.8 – ACI 440.1R Shear Theory Using Full Strength

The reductions in strength of the C-Grid using the ACI 440.1 method provide calculations that have about 50% more shear capacity than calculated. Therefore, the ACI 440.1 method is used with the full strength of the stirrups. Again the CFRP full strength is the average reduced by three standard deviations to ensure a safe design. Also, the sections with steel transverse reinforcement will not increase their predicted shear strength as the steel stirrups had no strength reductions by the design recommendations.

From the calculations presented in Table 18, it is apparent that the steel stirrups have the same design values. The full strength of the CFCC stirrups results in a ratio of less than 1.0, which means this method is not conservative. Due to this, ACI 440.1 with full CFCC strength should not be used for design of transverse reinforcement. However, the values for the C-Grid show a good correlations from calculated to measured values as the ratio is close to 1.0. This method does provide a good fit for the design of Bulb-T beams with C-Grid transverse reinforcing.

Table 18: ACI 440.1 Full Strength Calculations and Results

Shear Reinforcing	V_n-Design (kips)	V_n-Actual (kips)	Max Shear Load (kips)	Failure	Ratio V_{test}/V_n-Design	Ratio V_{test}/V_n-Actual
Typ Steel	31.77	32.18	43.56	Yes, Compression	1.37	1.35
Min Steel	22.42	22.99	23.02	No	1.03	1.00
Typ C-Grid	-	-	-	-	-	-
Min C-Grid	21.89	24.10	28.90	Yes, Shear	1.32	1.20
Typ CFCC	149.03	181.65	42.62	Yes, Shear	0.29	0.23
Min CFCC	75.07	89.83	33.23	No	0.44	0.37
C-Grid Zip Tied	33.34	36.75	36.26	Yes, Shear	1.09	0.99
C-Grid Spaced	33.34	36.75	38.24	Yes, Shear	1.15	1.04

5.2.9 – Summary of Design Methodologies

The four design methodologies presented in this thesis were compared to the actual tested values. Since not every specimen failed in shear it is important to understand that not all the capacity to design ratios are useful. However, comparing the values for the specimens that did fail in shear can provide insight into which methods better predict capacity for which materials.

Since designers will use the given design values of a material and not the actual values, Table 19 presents the design versus tested shear value ratios. This allows a quick comparison of the shear design methods. From the chart, the AASHTO MCFT per the specification has the best fit for the CFCC stirrups while still being conservative. The full strength ACI 440.1 method has the best fit for the C-Grid transverse reinforcement, but it is only 10% closer to the actual shear

failures than the AASTHO method using full strength. The AASHTO method is more straightforward as it is applicable to both prestressed and reinforced concrete. It is not certain how the ACI 440.1 method using the shear funnel would work with prestressed beams.

Table 19: Comparison of All Calculation Methods Using Design Material Values

Shear Reinforcing	Maximum by Code				Full Strength				Failure
	AASHTO MCFT	ACI 318	ACI 440.4	ACI 440.1	AASHTO MCFT	ACI 318	ACI 440.4	ACI 440.1	
Typ Steel	1.53	1.60	1.64	1.37	1.53	1.60	1.60	1.37	Yes, Compression
Min Steel	1.25	1.29	1.31	1.03	1.25	1.29	1.29	1.03	No
Typ C-Grid	-	-	-	-	-	-	-	-	-
Min C-Grid	2.35	2.63	2.73	1.68	1.57	1.67	1.67	1.32	Yes, Shear
Typ CFCC	1.08	1.10	1.67	0.85	0.45	0.30	0.30	0.29	Yes, Shear
Min CFCC	1.33	1.52	2.08	1.07	0.54	0.49	0.49	0.44	No
C-Grid Zip Tied	2.18	2.74	2.89	1.51	1.22	1.40	1.40	1.09	Yes, Shear
C-Grid Spaced	2.30	2.89	3.05	1.59	1.29	1.48	1.48	1.15	Yes, Shear

The table also shows the ACI 440.4 method is very conservative due to the ratios being much higher than all other methods. Due to its 0.002 times the modulus requirement the allowable stress used of CFRP products used for design are often more conservative than needed to ensure a safe and predictable design. This method was noted by Grace et al. (2015) as needing revision due to is conservative nature and the findings of this study support their conclusion. The full strength ACI 318 method provides a good prediction for C-Grid strengths that could be used for an initial calculation or check of the section.

Table 20 presents the same comparison of the shear calculation methods with the use of the actual tested material values. This chart better shows a true prediction of the shear strength when the materials used in section construction are known. From the results, the AASHTO method provides the ratios closets to 1.0 for the CFCC Stirrups, which aligns with the findings using the design values. The C-Grid is best fit by the full strength ACI 440.1 method as the ratios for the two layers are right at 1.0. However, the full strength AASHTO method provides

only a 10% underestimate of the shear strength, which provides a nice prediction with a small amount of room for error.

Table 20: Comparison of All Calculation Methods Using Actual Material Properties

Shear Reinforcing	Maximum by Code				Full Strength				Failure
	AASHTO MCFT	ACI 318	ACI 440.4	ACI 440.1	AASHTO MCFT	ACI 318	ACI 440.4	ACI 440.1	
Typ Steel	1.52	1.58	1.58	1.35	1.52	1.58	1.58	1.35	Yes, Compression
Min Steel	1.24	1.26	1.26	1.00	1.24	1.26	1.26	1.00	No
Typ C-Grid	-	-	-	-	-	-	-	-	-
Min C-Grid	2.27	2.50	2.60	1.63	1.44	1.49	1.49	1.20	Yes, Shear
Typ CFCC	1.08	1.09	1.70	0.86	0.40	0.24	0.24	0.23	Yes, Shear
Min CFCC	1.32	1.50	2.08	1.07	0.48	0.40	0.40	0.37	No
C-Grid Zip Tied	2.15	2.69	2.88	1.50	1.11	1.25	1.25	0.99	Yes, Shear
C-Grid Spaced	2.27	2.83	3.04	1.58	1.17	1.32	1.32	1.04	Yes, Shear

The ACI 440.4 method does not provide a good estimate of any material other than steel. If the full strength of the CFRP products are used, it vastly overestimates the shear capacity from CFCC stirrups, but does provide a closer approximation of shear capacity for C-Grid. The ACI 318 method provides a way to have a quick check of the section capacity. If checking with ACI 318 the method should be followed for CFCC stirrups, but the full strength of C-Grid should be used.

The AASHTO method presents a straightforward method for the calculation of shear capacity of beams using C-Grid transverse reinforcement. However, the shear design ϕ-factor in AASHTO is 0.9. Since the failure of the C-Grid results in a complete loss of load carrying capacity of the section, this value should be reduced to provide more room for errors in calculation. Since a limited amount of testing was completed and no statistical analysis was performed, it is more appropriate to use a smaller ϕ-factor at this time. As such, the recommendation is to use ϕ as 0.75. This is the recommended factor for shear design in all three ACI design methods, including ACI 440.1 and 440.4 which are the design guidelines for CFRP materials.

5.3 – Comparison of Transverse Reinforcement Materials

5.3.1 – Comparison of Performance of Different Materials

The steel stirrups were used as a control in this study to determine crack control, the strength, and predictability of shear failures in concrete beams. Also, since the sponsor of this study, VDOT, has used CFCC stirrups in design they were used again as a second control. These materials were then compared against the C-Grid used as the transverse reinforcing in the webs of the beams.

The steel stirrups performed much as expected in testing, barring the minor hiccup for lack of flexural strength. These beams did exhibit typical shear cracking in the web and helped to prove that most shear design methods underestimate the shear capacity of the section. Also, the beams helped to serve the purpose of instrumentation set up and learning to tie in reinforcing bar. Due to the properties of the steel, if the stirrups did not fit perfectly it was easy to bend them slightly to achieve a better fit. The shorter tail for required development length also meant that steel stirrups were easier to fit in place in the beams.

The CFCC stirrups were very easy to handle and tie in due to their light weight. The tolerances on the CFCC stirrups were very exact on every piece, which was much better than the steel bars. However, the bars cannot be bent once received so if there is a mistake it must be modified in some other way. CFCC stirrups performed with strengths much higher than predicted at both spacings. The ultimate failure was unusual because the shear crack that caused failure occurred between two stirrups in a nearly vertical fashion. The crack control with the CFCC was very good and is discussed in the next section.

The C-Grid material comes on large rolls that are very lightweight. The material is easily rolled out and cut to size with tin snips to fit into the beam. Long single sheets of the grid are

flexible, so lateral support is needed to ensure it stays in place and allows proper consolidation of concrete. Tying multiple layers together was easily accomplished through the use of small zip ties around the intersections of the grid. The C-Grid was easy to put in place due to its light weight, but due to the shipping on a roll it had a residual curl present. The curl was easy to straighten out while tying the material into the beam. Reinforcing bars should be placed between layers to ensure enough room is present for consolidation of the concrete. One note is that the C-Grid is sharp along the edges, so gloves should be worn when handling.

The C-Grid performed well in testing and led to very typical shear failure in all specimens that were tested. The AASHTO modified compression field theory method seemed to predict the shear failure the most closely. The ACI 318 and ACI 440.1 methods are slightly more conservative but are also viable methods for design. The ACI 440.4 method is too conservative to be used for C-Grid. The crack control of the C-Grid was similar to steel and is discussed more thoroughly in the next section.

Based on the findings of this experimental program, the C-Grid is a viable shear design option for concrete beams. It is easy to handle and install due to its light weight and ease of cutting the material. It allows field modifications and can be tied together to increase the stiffness and place more layers in thinner web. Design recommendations for C-Grid are given in the conclusions section.

5.3.2 – Comparison of Crack Control

Any carbon fiber material must be able to provide adequate crack control of the beam so that the chloride laden water cannot make its way into the concrete as easily and cause deterioration. Keeping the cracks smaller also ensures more aggregate interlock in the section. The aggregate interlock provides the majority of the shear resistance on the concrete. To ensure

the cracks stay small, a larger amount of transverse reinforcement can be used to control shear cracks. Steel transverse reinforcement is the baseline for this comparison against the CFCC stirrups and the C-Grid. Crack width graphs for each specimen are shown in the results section of this thesis along with the trend line for the propagation of each crack width.

From the results of testing, the first crack usually grows at a smaller rate than the additional cracks. As the shear load on the beam increases additional cracks open up as the concrete reaches its maximum tensile cracking stress. These additional cracks will cause the previous cracks to close up. Also, the large shear crack from the support to the load point does not typically open until later in testing. As this is the main failure crack, it grows more quickly once it forms in the beam.

Figure 67 shows the point of first cracking and the propagation of the cracks. The propagation slope is based on the average, with poor linear fit results not used in the calculation. The first point is the cracking load of each beam in shear, which is anywhere from about 11 kips

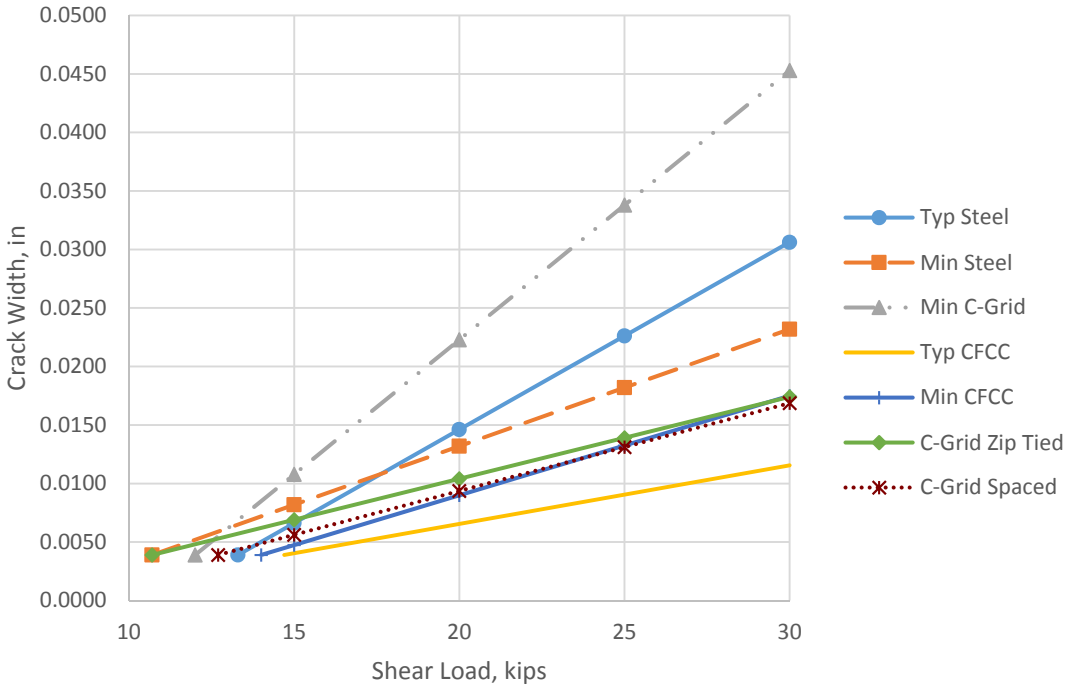

Figure 67: Cracking and Propagation Comparison of Reinforcing Options

to almost 15 kips. Of note is that the minimum C-Grid, two layer of C-Grid Zip tied, and the minimum steel have the lowest initial cracking load. Also, the minimum C-Grid has the highest cracking propagation rate of the materials. The cracks in the steel reinforced beams have higher propagation rates than the rest of the reinforcement options, especially after a 15 kip shear load is achieved on the section. The CFCC options provide the highest shear load to initial cracking and also some of the lowest propagation rates. The two layers of C-Grid seem to help restrain cracks better than steel, but have lower strengths at cracking.

Since cracking is likely to occur in a bridge girder over time, it is important to keep the cracks tightly closed, which the C-Grid and CFCC options seem to do better than steel. The minimum C-Grid ratio shows a higher propagation which is concerning. This can be overcome by prescribing that a minimum of two layers of C-Grid be used as the reinforcement in the beam. The C-Grid does perform nearly as well as steel stirrups in controlling shear crack growth.

Table 21 provides a transverse stiffness of the reinforcing options in the specimens. This is found by calculation the transverse reinforcing ratio and then multiplying by the modulus of elasticity of the material. The steel and CFCC provide a similar transverse stiffness for the typical and minimum values. However, the C-Grid has a much lower shear stiffness and still provides adequate crack control. This is probably due to the grid having tows in both directions

Table 21: Transverse Stiffness of the Specimens

Shear Reinforcing	E (ksi)	A_v ($in^{2)}$	b_w (in)	s (in)	ρ_v	$E\rho_v$
Typ Steel	29000	0.11	3	6	0.0061	177.2
Min Steel	29000	0.11	3	12	0.0031	88.6
Typ C-Grid	-	-	-	-	-	-
Min C-Grid	34000	0.00286	3	1.6	0.0006	20.3
Typ CFCC	22500	0.09	3	4	0.0075	168.8
Min CFCC	22500	0.09	3	9	0.0033	75.0
C-Grid Zip Tied	34000	0.00572	3	1.6	0.0012	40.5
C-Grid Spaced	34000	0.00572	3	1.6	0.0012	40.5

and the high modulus of elasticity. The C-Grid provides better crack control than the other materials when factoring in the transverse stiffness.

5.3.3 – Comparison of Vertical LVDT Displacements

The vertical LVDTs during testing helped to provide some additional confirmation on first shear crack forming and also on crack width measurements. The results did provide good correlation between the crack data of each individual specimen. Comparing the vertical LVDT displacements for the specimens against one another should provide a more thorough picture of crack control and overall web movement of the beams.

Table 22 provides an average displacement reading of the vertical LVDTs at 20 and 25 kips of shear load. These averages were determined from the graphs presented in section 4.4 of this thesis. Since the minimum steel and C-Grid specimen did not reach 25 kips of shear with the instrumentation attached, those displacements are not applicable. When determining the averages any individual LVDT that registered very different results was discounted. For example, on Specimen 1 Typical Steel Reinforcement the readings of LVDT B2 and LVDT 90 were not used in the average at 20 kips.

Table 22: Average Vertical LVDT Displacements

Shear Reinforcing	Average Displacement (in)	
	20 k	25 k
Typ Steel	0.012	0.013
Min Steel	0.006	-
Typ C-Grid	-	-
Min C-Grid	0.028	-
Typ CFCC	0.007	0.012
Min CFCC	0.011	0.018
C-Grid Zip Tied	0.011	0.020
C-Grid Spaced	0.007	0.010

Based on the results of the vertical LVDT displacements, the CFCC, two layers of C-Grid, and steel stirrups all result in similar amounts of movement. One layer of C-Grid allows

larger web movement, which corresponds to the higher crack propagation found previously. Using two layers of C-Grid helps reduce this movement, and according to the readings spacing the layers helps minimize this movement as well. The spaced C-Grid did provide slightly smaller cracks at equivalent loads and the first shear crack did appear later. The CFCC stirrups remain the best option to control cracks and limit the shear displacement in the web. However, using two layers of C-Grid provides adequate control of shear stresses and cracks while doing so with a much lower transverse stiffness.

6 – Conclusions and Design Recommendations

6.1 – Proposed Design Methods

Based on the findings of the thesis the following proposed design and handling methods are given below:

- Use manufacturer's reported strength and modulus of elasticity for C-Grid
- Use the AASHTO Modified Compression Field Theory equation based format for shear calculations using manufacturer's data
- Use a minimum of two layers of C-Grid C50 1.6x1.8 in design to help minimize crack propagation
- Use a minimum of 4 in. of development length with C-Grid C50 1.6x1.8
- Cut C-Grid using tin snips and wear gloves when handling
- C-Grid layers can be tied together with zip ties at approximately 12 in. on center
- Provide lateral support for C-Grid in vertical direction at a minimum of 18 in. on center

- Use minimum of 5/8 in. or No. 5 reinforcing bar between layers of C-Grid for consolidation of concrete
- Recommended use of maximum 1/2 in. aggregate and 6-1/2 in. slump for concrete to allow proper consolidation of concrete
- Recommended ϕ-factor for shear as 0.75 due to limited testing and failure of C-Grid as shear reinforcing results in a complete loss of section's load carrying capacity

6.2 – C-Grid Design Example

The design example comes from the PCI Bridge Design Manual Chapter 9, Section 9.4 (PCI Bridge Design Manual Steering Committee, 2003). The example is the Bulb-Tee (BT-72) Single Span, Composite Deck, LRFD Specifications example. This example provides guidance for the use of C-Grid transverse reinforcement to ensure adequate shear capacity of the BT-72 beam.

The bridge is a 120 ft span with no skew made up of BT-72 prestressed girders. The girders are spaced at 9 ft on center with an 8 in. uniform thickness composite deck above, which includes the 1/2 in. wearing surface. This provides a composite structural deck of 7-1/2 in. The design live load is specified as AASHTO HL-93. The design for flexure resulted in the use of 48 1/2 in. prestressing strands distributed in ten layers. The top 12 strands were harped in the section, with the harping occurring over the final 48 ft 6 in. of the beam.

Section 9.4.11 of the example provides the necessary information to perform the shear design. The critical shear depth, d_v, is 73.14 in. as shown in 9.4.11.1.3. Continuing through the calculations of the section shows an ultimate shear load, V_u, as 316.2 kips at the critical section as previously found in section 9.14.11.2.1. Calculation of the strain in the tensile steel led to the

values of θ=22.8°, and β=2.94 as shown in 9.4.11.2.2. The shear resistance of the concrete, V_c, is 103.9 kips and the prestressing shear resistance, V_p, is 23.4 kips. Using the design equations and ϕ factor of 0.90 for normal weight concrete sections in shear, the shear resistance of the reinforcing, V_s, must be at least 188.9 kips. The 0.9 is based on a multitude of testing and great confidence in the method when using steel stirrups. Due to the limited testing the ϕ-factor for shear is recommended to be used as 0.75. Therefore, the V_s required becomes 294.3 kips.

To provide this reinforcing the C50 1.6x1.8 grid is used as it the largest and tightest spacing of the C-Grid available from Chomarat. From the AASHTO method, the shear formula is given in this thesis as Equation 3. However, when using the equation it is easy to modify to find the number of grids required as shown below. Where n is the number of layers of grid needed and F_{frp} is the strength of the grid given by the manufacturer. Ensure F_{frp} is reduced by three standard deviations from the mean of testing. The other terms are the same as indicated in the AASTHO method.

$$n = \frac{V_s s}{F_{frp} d_v \cot\theta} \qquad \text{(Eq 17)}$$

The C50 grid has 1.6 in. spacing in this design and F_{frp} is 0.83 kips/tow. From the example all other relevant variables to solve Equation 17 are given. Plugging in and solving provides a value for n as shown below in Equation 18.

$$n = \frac{294.3\ k * 1.6\ in}{0.83\ k * 73.14\ in * \cot 22.8°} = 3.26 \qquad \text{(Eq 18)}$$

This would round up to four layers of C50 1.6x1.8 grid for the beam. Also, the grid meets all applicable spacing requirements of the beam and minimum reinforcement areas of the beam. The next important step is to ensure the grid has enough embedment in the flange and bulb of the beam to develop full strength. The top flange of the beam provides 7-1/2 in. for

development and the bulb provides 10-1/2 in. as shown Figure 68. Since the C-Grid can develop in 4 in., the beam provides adequate embedment for full development with room for clear cover. The three layers of C-Grid will also fit easily into the 6 in. thick web with clear cover.

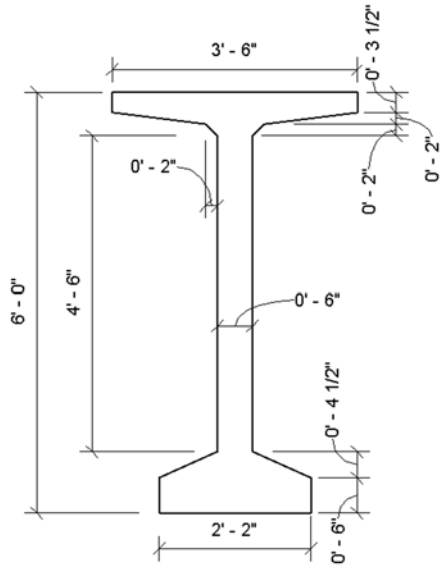

Figure 68: BT-72 Beam from PCI Bridge Design Manual

To summarize the design:

- Use four layers of C-Grid C50 1.6x1.8 with the 1.6 in. direction acting as the stirrups
- Provide 1 in. minimum spacing between layers in web
- Use one layer of C-Grid on each side of prestressing strands to allow for ease of placement and spacing of grid
- Laterally support grid vertically every 18 in. to ensure grid does not buckle during concrete placement
- Provide 1-1/2 in. clear cover at bottom
- Top will be covered with deck so cover not mandatory

6.3 – Conclusions

The observed experimental results and comparison of the data to current codes, specifications, and design recommendations has led to the following conclusions for C-Grid reinforcing:

- C-Grid is a viable shear reinforcement option for concrete bridge girders
- C-Grid provides crack control nearly identical to steel when a minimum of two layers of grid are used
- C-Grid C50 1.6x1.8 has a development length of 4 in.
- AASHTO modified compression field theory equations provide the best prediction of shear strength for C-Grid when using the manufacturer's reported strength
- Do not reduce C-Grid stress to code prescribed maximum or results will be overly conservative
- Use a shear design ϕ-factor of 0.75 due to limited amount of testing
- The manufacturer's reported strength can be used as long as it is reduced by three standard deviations
- Failure of beam with C-Grid results in complete loss of load carrying capacity of section, as there is no additional yielding with CFRP materials
- The AASHTO modified field theory with equations most accurately predicts the shear capacity of a section with CFCC stirrups

7 –Recommendations for Future Research

While this thesis provided some baseline recommendations on the use of CFRP transverse reinforcement, several areas could use further research. The initial results of the C-

Grid are promising, but require more work. Also there are additional CFRP grids that could be better suited for use as transverse reinforcement. The following are suggestions for additional study:

- Testing to determine C-Grid buckling loads and the need for lateral support in formwork to ensure grid does not buckle during concrete placement.
- Full-scale reinforced and prestressed beam tests with C-Grid transverse reinforcement to ensure designs scale up properly and to ensure safe design recommendations.
- Bond tests of multiple layers of C-Grid that are tied together with zip ties to ensure that the development length does not change with multiple layers of grid.
- Testing C-Grid with the tows at 45 degree angles to the length of the beam to determine if aligning tows with the shear stresses increases shear capacity and reduces cracking.
- Testing to determine the required clear cover to fully develop C-Grid to ensure a splitting failure of the concrete face does not occur.
- Testing to determine the viability of C-Grid as horizontal shear reinforcement to provide adequate composite interaction between bridge deck and girders.
- The testing of other CFRP grid materials to determine their mechanical properties, development lengths, and design recommendations.
- Additional study and new recommendations for shear design using ACI 440.4 methods due to the conservative shear capacity calculations present in the current recommendations.
- Additional study and revisions to the ACI 440.1 method to provide different recommendations for different transverse reinforcing materials.

- Additional testing with C-Grid as shear reinforcement to help determine the reliability, properly calibrate the ϕ-factor, and to determine if a maximum allowable strain of C-Grid is needed for a safe shear design.
- Research to find CFRP alternatives in the anchorage zone of prestressed concrete sections.
- Research to find CFRP materials for the use of confinement reinforcing in prestressed concrete beams.

References

AASHTO. (2012). AASHTO LRFD bridge design specifications, 6th Ed., Washington, DC.

American Concrete Institute (ACI). (2004). "Prestressing concrete structures with FRP tendons." ACI 440.4R-04, Farmington Hills, MI.

American Concrete Institute (ACI). (2006). "Guide for the design and construction of structural concrete reinforced with FRP bars." ACI 440.1R-06, Farmington Hills, MI.

American Concrete Institute (ACI). (2014). "Building code requirements for structural concrete." ACI 318-14, Farmington Hills, MI.

ASTM A370-14. (2014). Standard Test Methods and Definitions for Mechanical Testing of Steel Products. ASTM International, West Conshohocken, PA.

ASTM C39/C39M-14a. (2014). Standard Test Method for Compressive Strength of Cylindrical Concrete Specimens. ASTM International, West Conshohocken, PA.

ASTM C469/C469M-14. (2014). Standard Test Method for Static Modulus of Elasticity and Poisson's Ratio of Concrete in Compression. ASTM International, West Conshohocken, PA.

ASTM C496/C496M-11. (2011). Standard Test Method for Splitting Tensile Strength of Cylindrical Concrete Specimens. ASTM International, West Conshohocken, PA.

Chomarat North America. (2010). Technical Data Sheet C50 1.8 x 1.6. Chomarat North America, Anderson, SC.

Chomarat North America. (2011). Test Method for Individual Strand Tensile Strength of C-Grid Products. Chomarat North America, Anderson, SC.

Cousins, T., Roberts-Wollmann, C., & Brown, M. (2013). NCHRP 733: High-Performance/High-Strength Lightweight Concrete for Bridge Girders and Decks. Transportation Research Board, Washington, DC.

Ding, L., Rizkalla, S., Wu, G., & Wu, Z.S. (2011). Bond Mechanism of Carbon Fiber Reinforced Polymer Grid to Concrete (pp. 589-592). Berlin, Heidelberg: Springer Berlin Heidelberg.

Fam, A. Z. Y. H. (1996). Carbon fibre-reinforced plastic prestressing and shear reinforcements for concrete highway bridges. (Dissertation/Thesis), ProQuest, UMI Dissertations Publishing. Retrieved from http://vt.summon.serialssolutions.com/2.0.0/link/0/eLvHCXMwY2BQMLdMNTMyAR3snWqYkmhsapFsnmhokWiQlmKSmmoJvmgCseMdqTR3E2JgSs0TZZB1cw1x9tCFFY3xKTk58eYmoBlHUHdFjIE3EbT4O68EvEksRYJBwcLSIi3ZLCnNONU82SQlNTXJJDXF1DDNMMXU0iA1MdUEACoQJfw

Grace, N. F. (2000). Response of continuous CFRP prestressed concrete bridges under static and repeated loadings. PCI Journal, 45(6), 84-102.

Grace, N. F., Enomoto, T., Sachidanandan, S., & Puravankara, S. (2006). Use of CFRP/CFCC reinforcement in prestressed concrete box-beam bridges. ACI STRUCTURAL JOURNAL, 103(1), 123-132.

Grace, N. F., Jensen, E. A., Eamon, C. D., & Shi, X. W. (2012). Life-Cycle Cost Analysis of Carbon Fiber-Reinforced Polymer Reinforced Concrete Bridges. ACI STRUCTURAL JOURNAL, 109(5), 697-704.

Grace, N. F., Rout, S. K., Ushijima, K., & Bebawy, M. (2015). Performance of Carbon-Fiber-Reinforced Polymer Stirrups in Prestressed-Decked Bulb T-Beams. *JOURNAL OF COMPOSITES FOR CONSTRUCTION, 19*(3), 4014061. doi: 10.1061/(ASCE)CC.1943-5614.0000524

Grace, N. F., & Singh, S. B. (2003). Design approach for carbon fiber-reinforced polymer prestressed concrete bridge beams. ACI STRUCTURAL JOURNAL, 100(3), 365-376.

Grace, N., Ushijima, K., Baah, P., & Bebawy, M. (2013). Flexural Behavior of a Carbon Fiber–Reinforced Polymer Prestressed Decked Bulb T-Beam Bridge System. JOURNAL OF COMPOSITES FOR CONSTRUCTION, 17(4), 497-506. doi: 10.1061/(asce)cc.1943-5614.0000345

Jeong, S. K., Lee, S., Kim, C. H., Ok, D. M., & Yoon, S. J. (2006). Flexural behavior of GFRP reinforced concrete members with CFRP grid shear reinforcements. 306-308, 1361-1366.

Lee, C., Jeong, S. M., & Park, J. W. (2009). Use of fibre sheet strip stirrups for internal shear reinforcement of concrete beams. MAGAZINE OF CONCRETE RESEARCH, 61(9), 731-743. doi: 10.1680/macr.2008.61.9.731

Morphy, R., Shehata, E., & Rizkalla, S. (1997). Bent effect on strength of CFRP stirrups. Paper presented at the Proceedings of the Third International Symposium on Non-Metallic (FRP) Reinforcement for Concrete Structures.

Nabipaylashgari, M. (2012). Shear Strength of Concrete Beams Prestressed with CFRP Cables. (Dissertation/Thesis), ProQuest, UMI Dissertations Publishing. Retrieved from http://vt.summon.serialssolutions.com/2.0.0/link/0/eLvHCXMwY2BQSDQG9hLMk8yTk5JNU5KB7flE42TQoTBmFmlGlibgu1MQO96RSnM3IQam1DxRBjk31xBnD11Y0RifkpMTbwy6FdvQ0AzYXxFj4E0Erf7OKwHvEkuRYFAwtUwzN05OSzE1SUw0STI3TDIDNiRMUlOTkhKNLIFcADjJJW8

Nislon, Arthur H. (1987). *Design of Prestressed Concrete*: *Second Edition.* Hoboken, NJ. Wiley.

PCI Bridge Design Manual Steering Committee. (2003). Precast Prestressed Concrete Bridge Design Manual.

Shehata, E., Morphy, R., & Rizkalla, S. (1998, January). USE OF FRP AS SHEAR REINFORCEMENT FOR CONCRETE STRUCTURES. In Second International Conference on Composites in Infrastructure (Vol. 1).

Steffen, R., Scott, D., Goodspeed, C., Bowman, M. D., & Trunfio, J. (2003). DESIGN ISSUES AND CONSTRUCTIBILITY OF A CFRD GRID REINFORCED BRIDGE DECK. In High Performance Materials in Bridges. Proceedings of the International Conference.

Tokyo Rope Mfg Co. Ltd. (n.d.) Characteristics of CFCC: Carbon Fiber Composite Cable. Retrieved from: http://www.tokyorope.co.jp/english/products/cfcc/feature/index.html

Tureyen, A. K., & Frosch, R. J. (2003). Concrete shear strength: another perspective. ACI Structural Journal, 100(5).

Tureyen, A. K., Wolf, T. S., & Frosch, R. J. (2006). Shear strength of reinforced concrete T-beams without transverse reinforcement. ACI structural journal, 103(5).

Vecchio, F. J., & Collins, M. P. (1986). The modified compression-field theory for reinforced concrete elements subjected to shear. In ACI Journal Proceedings (Vol. 83, No. 2). ACI.

Appendix A: Development Length Graphs

All load-displacement plots from the development length testing are shown below.

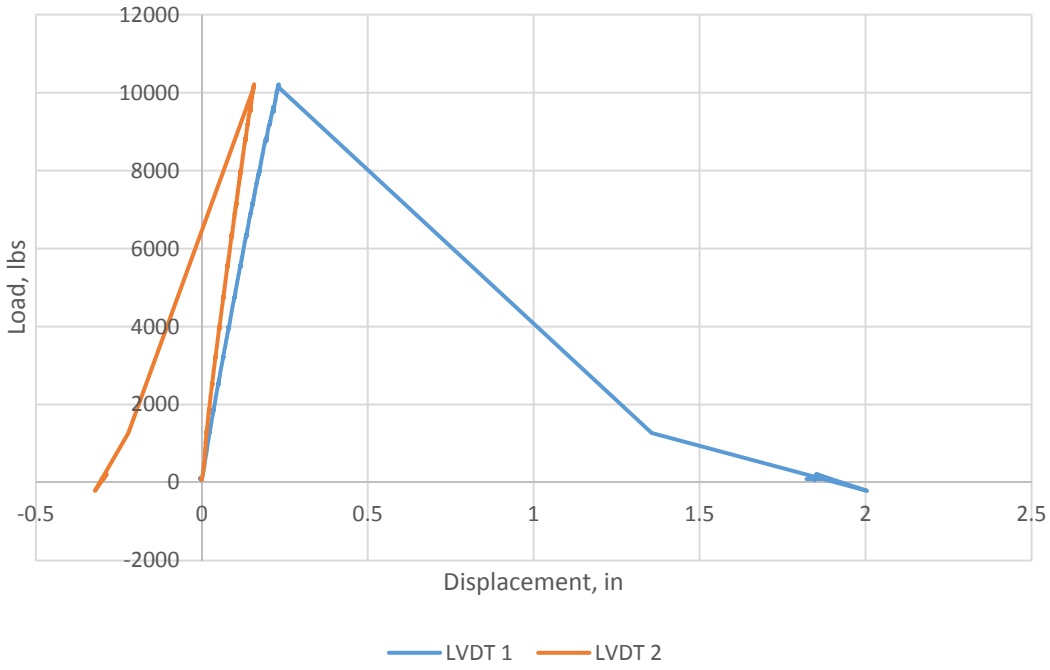

Figure 69: Development Length Load-Displacement Specimen 8-2

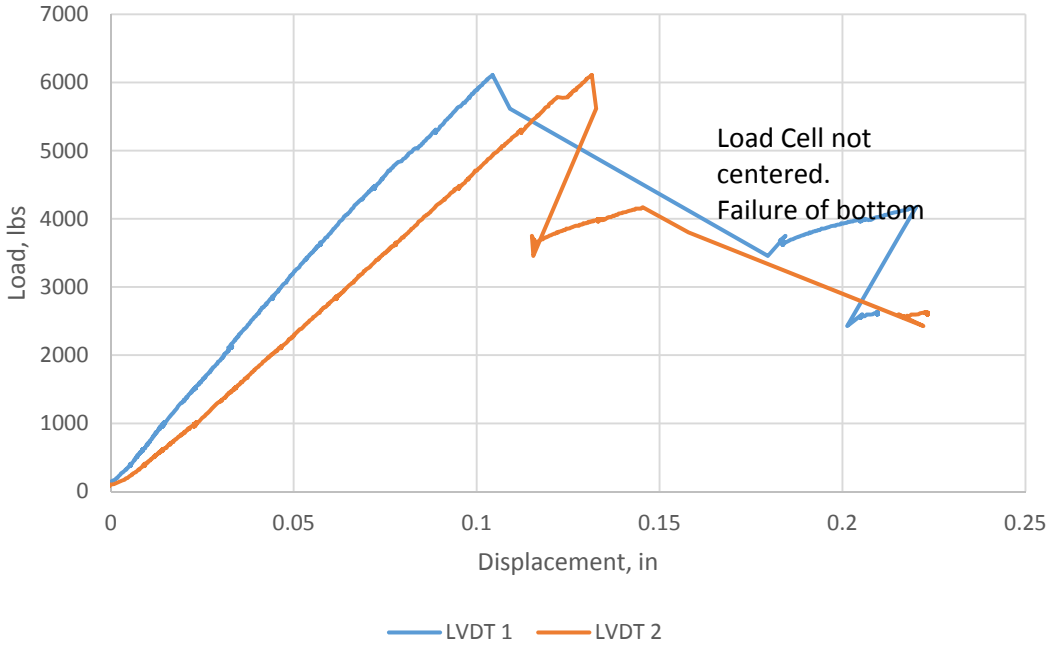

Figure 70: Development Length Load-Displacement Specimen 8-1

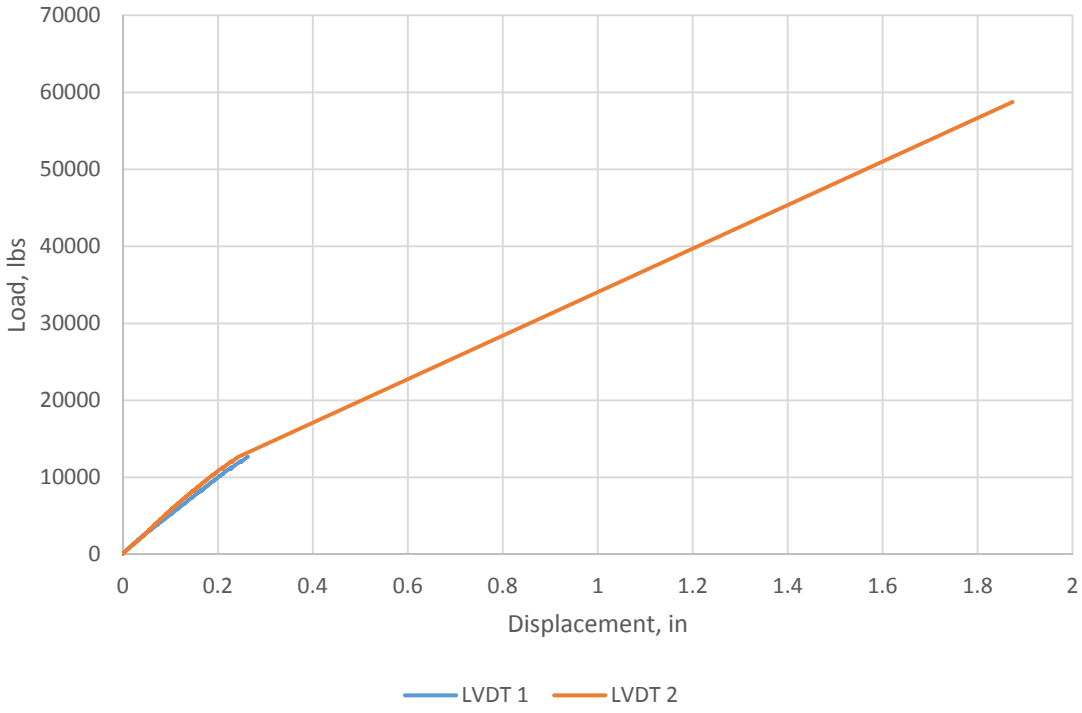

Figure 71: Development Length Load-Displacement Specimen 7-2

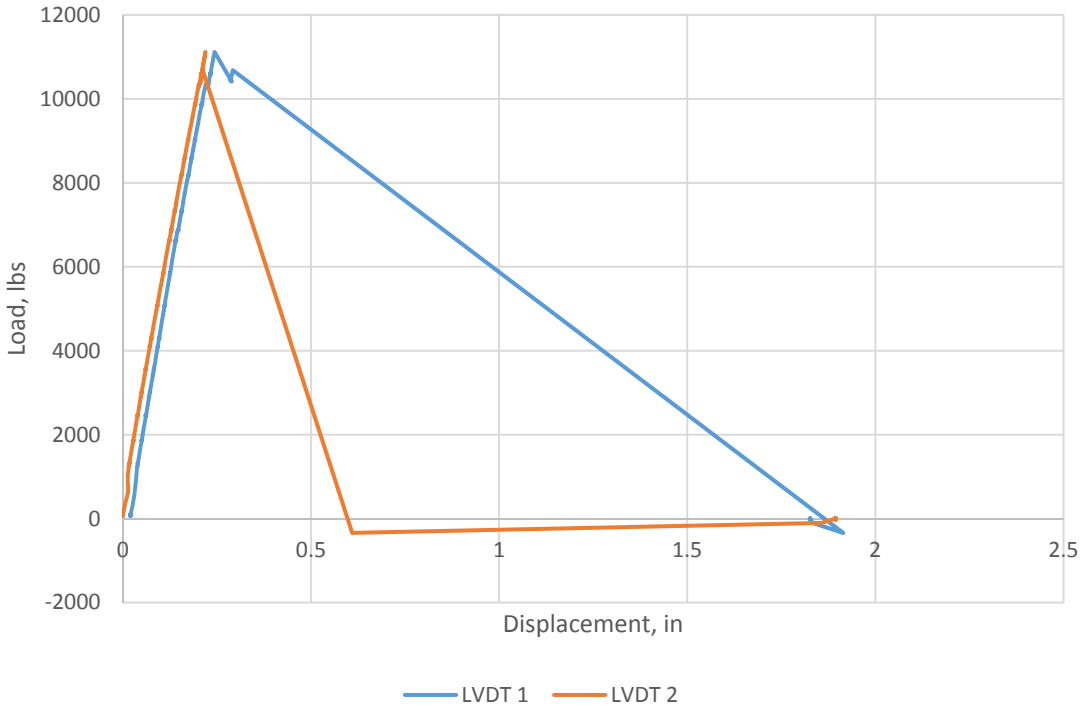

Figure 72: Development Length Load-Displacement Specimen 7-1

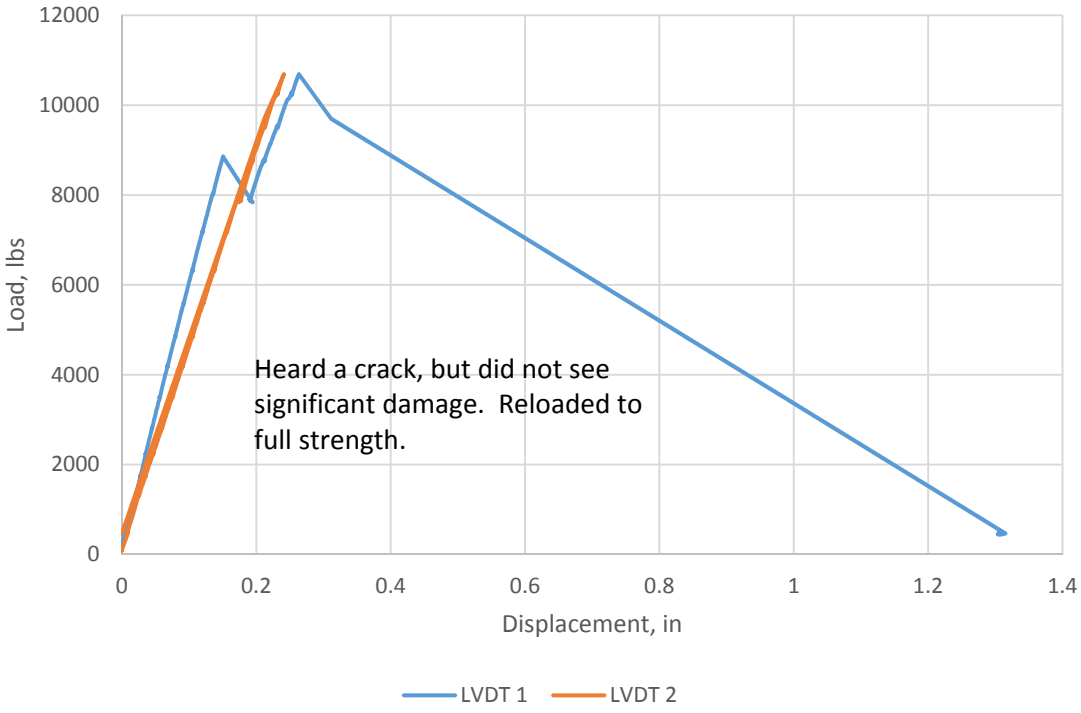

Figure 73: Development Length Load-Displacement Specimen 6-2

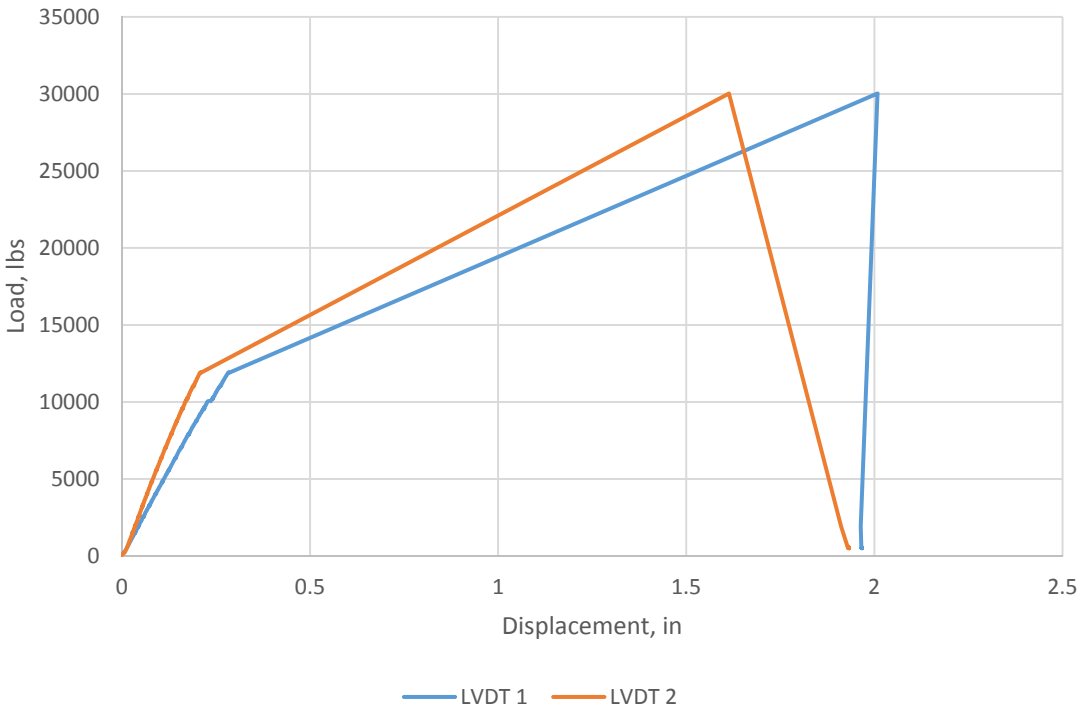

Figure 74: Development Length Load-Displacement Specimen 6-1

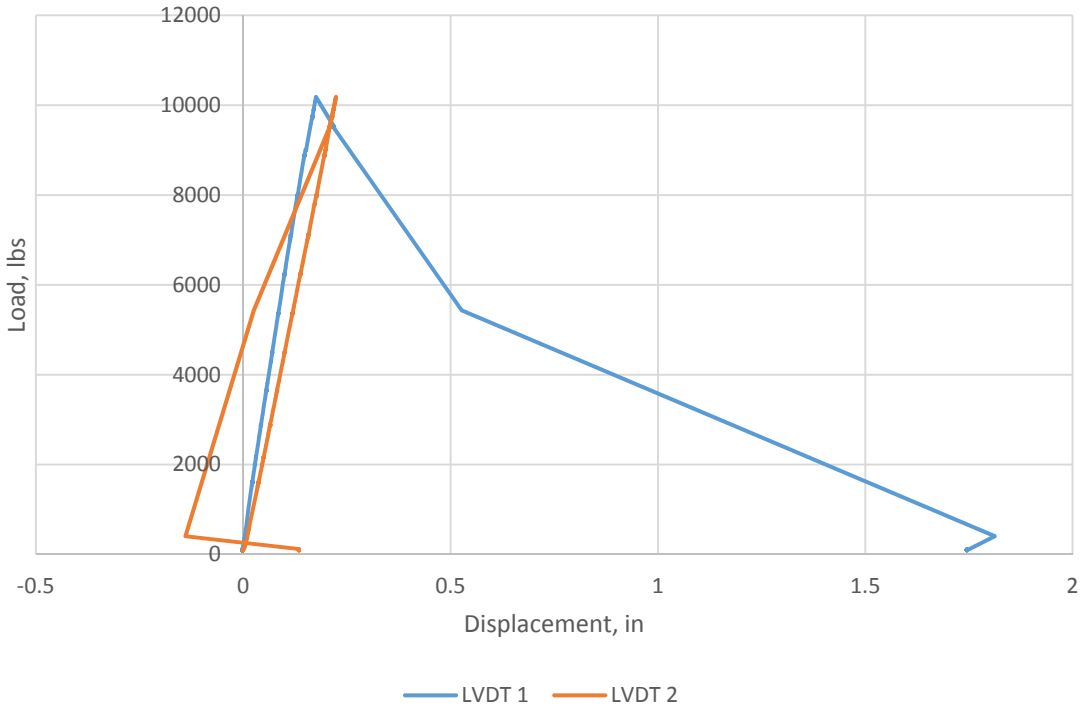

Figure 75: Development Length Load-Displacement Specimen 5-2

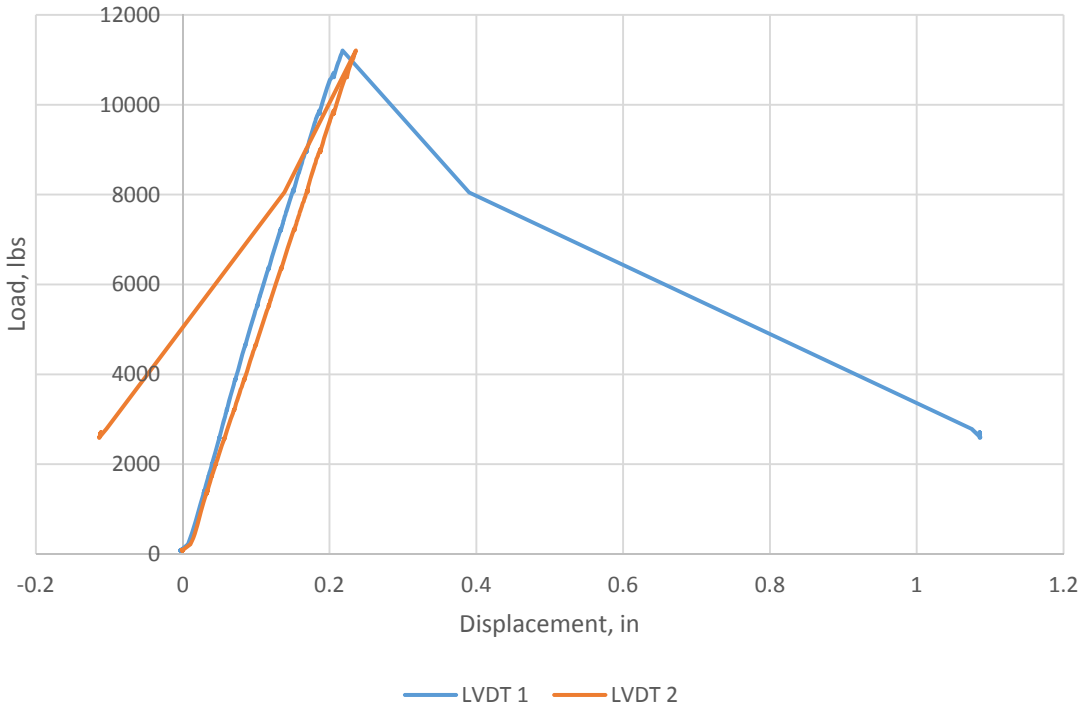

Figure 76: Development Length Load-Displacement Specimen 5-1

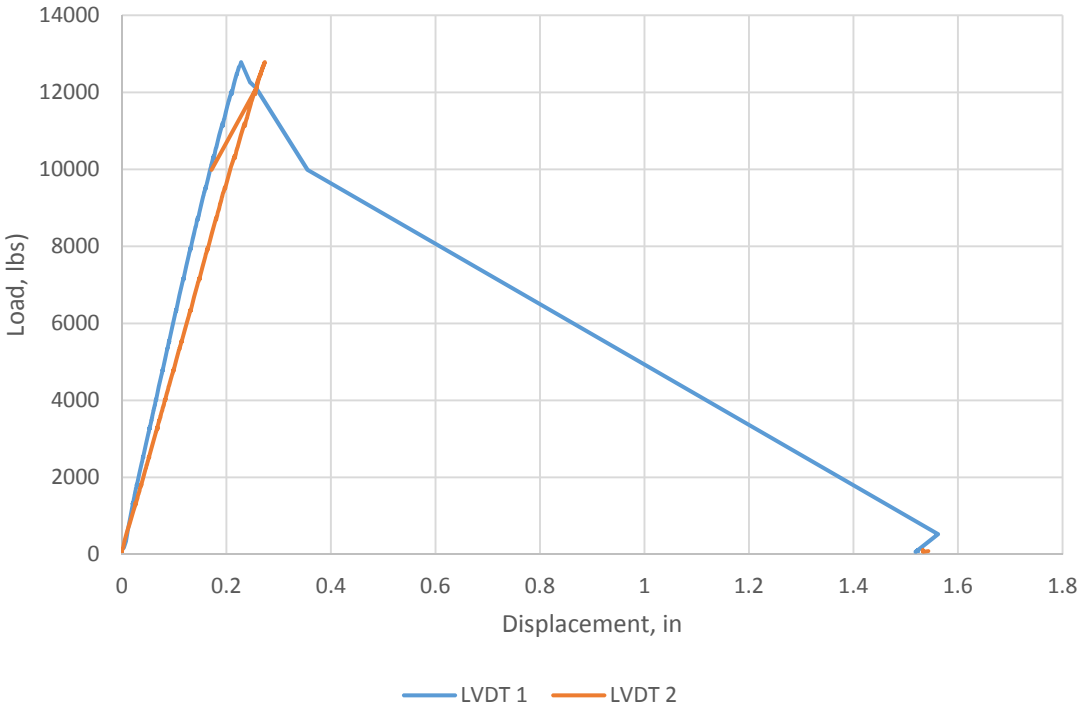

Figure 77: Development Length Load-Displacement Specimen 4-2

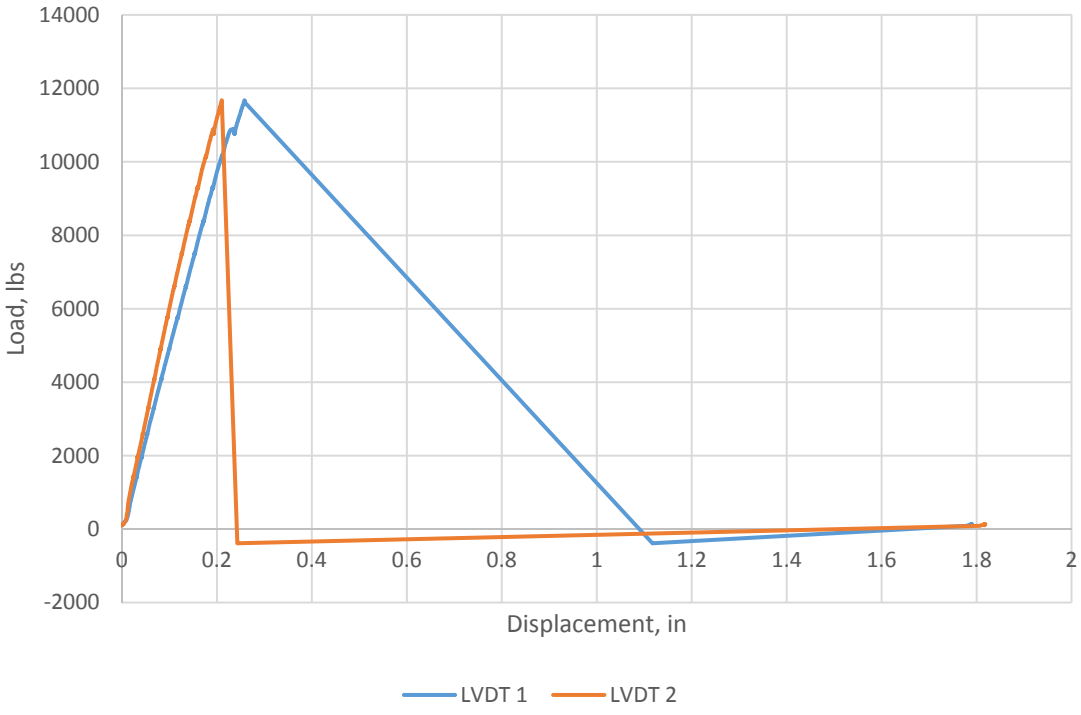

Figure 78: Development Length Load-Displacement Specimen 4-1

Appendix B: Concrete Data

Data from cylinder testing of concrete used in beams is presented below. Each entry is an individual cylinder that was tested.

Table 23: Complete Concrete Data for Beam Tests

Placement #1			**Placement #2**		
7 Day Tests			***9 Day Tests***		
Compression			*Compression*		
	5690	psi		6130	psi
	5450	psi		6570	psi
	5730	psi		5810	psi
14 Day Tests			***14 Day Tests***		
Compression			*Compression*		
	6840	psi		6450	psi
	6450	psi		6170	psi
	6880	psi		6600	psi
25 Day Tests			***27 Day Tests***		
Compression			*Compression*		
	7400	psi		7080	psi
	7360	psi		7240	psi
	7840	psi		7560	psi
Splitting Tensile			*Splitting Tensile*		
	765	psi		695	psi
	665	psi		695	psi
	585	psi		495	psi
Modulus of Elasticity			*Modulus of Elasticity*		
	5030	ksi		4380	ksi
	4750	ksi		4540	ksi
	4820	ksi		4660	ksi
55 Day Tests			***37 Day Tests***		
Compression			*Compression*		
	8400	psi		7680	psi
	8630	psi		6760	psi
	8320	psi		7800	psi
Splitting Tensile			*Splitting Tensile*		
	635	psi		555	psi
	755	psi		595	psi
	725	psi		595	psi
Modulus of Elasticity			*Modulus of Elasticity*		
	5220	ksi		4840	ksi
	5140	ksi		4550	ksi
	5160	ksi		4740	ksi

Appendix C: Complete Rosette Principal Angle Results

The complete principal angle calculation graphs are presented below. The scatter in the data made the results impossible to draw any significant conclusions from the data.

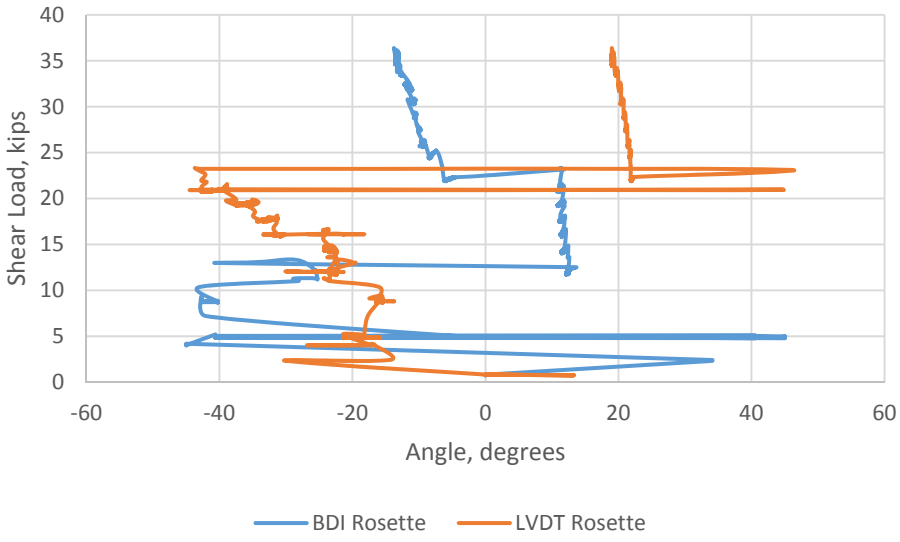

Figure 79: Shear Load v. Principal Angle Specimen 1 Typical Steel

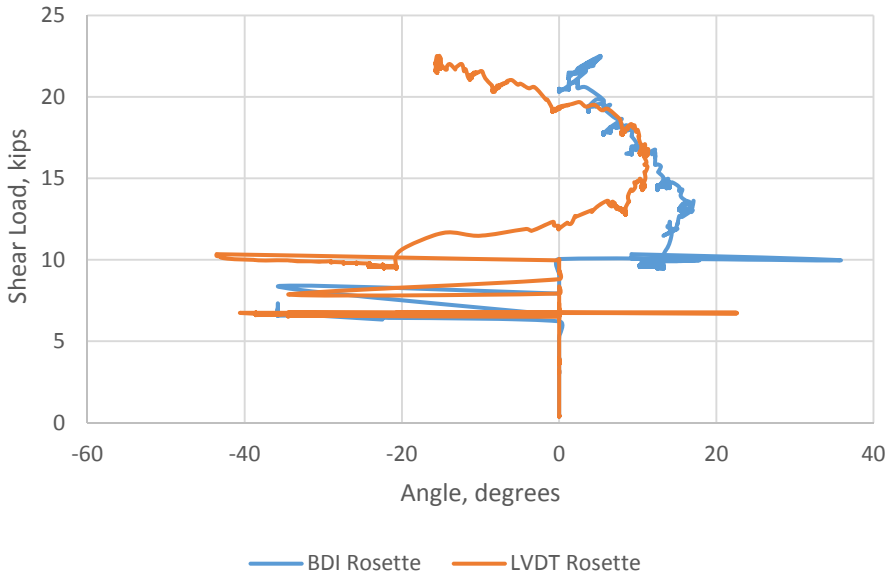

Figure 80: Shear Load v. Principal Angle Specimen 1 Minimum Steel

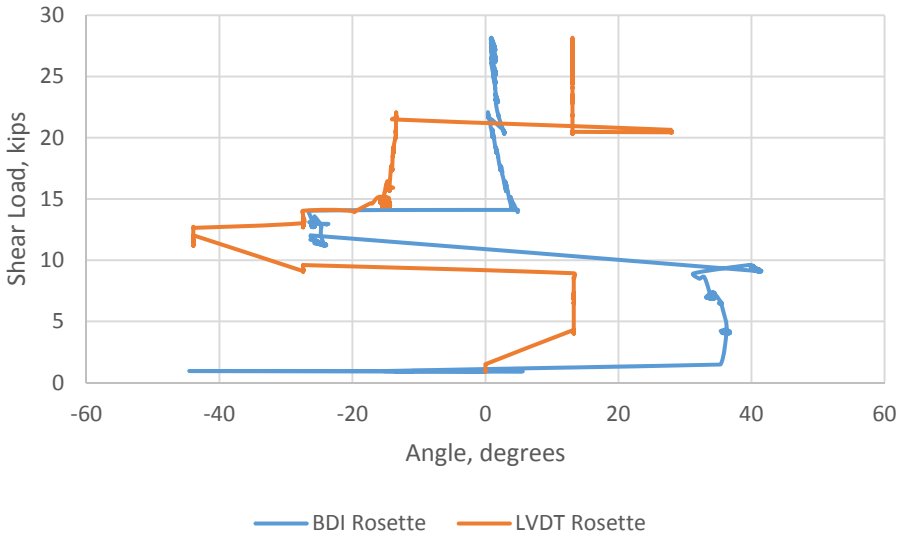

Figure 81: Shear Load v. Principal Angle Specimen 2 Minimum C-Grid

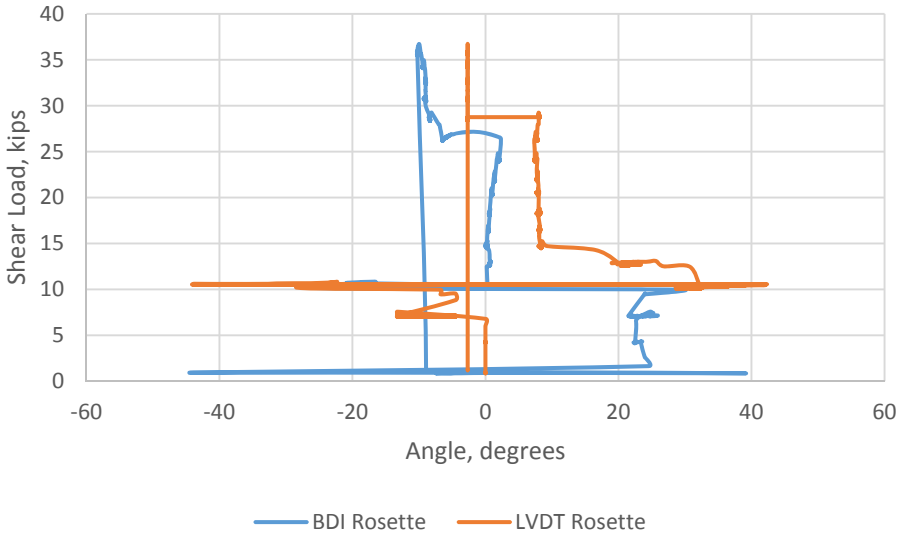

Figure 82: Shear Load v. Principal Angle Specimen 3 Typical CFCC

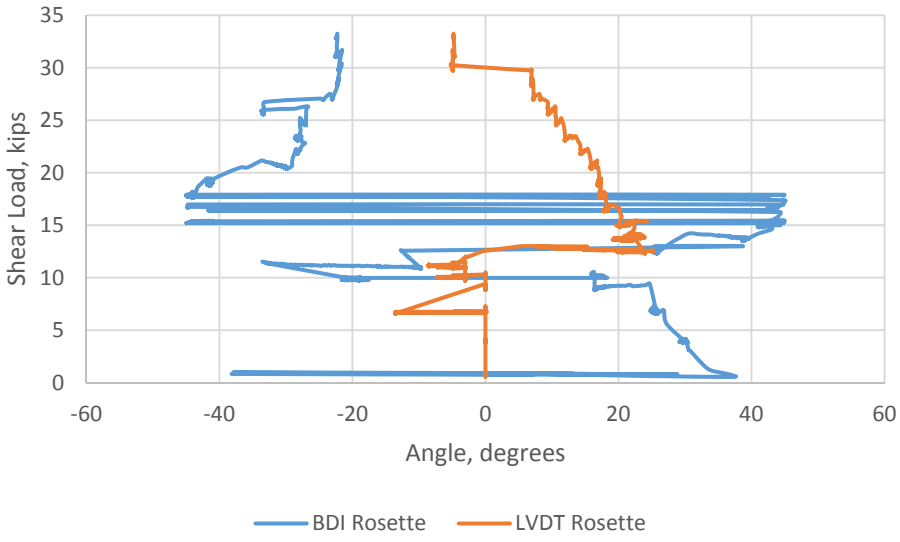

Figure 83: Shear Load v. Principal Angle Specimen 3 Minimum CFCC

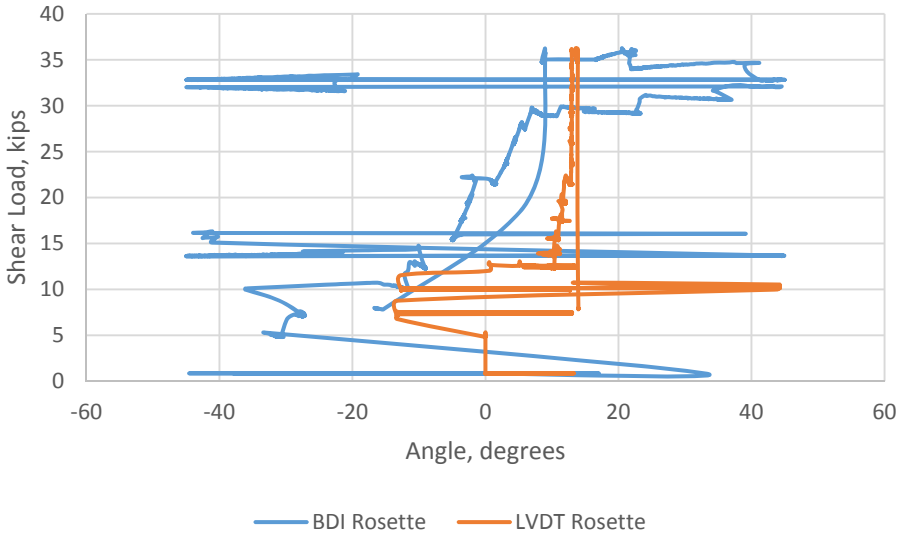

Figure 84: Shear Load v. Principal Angle Specimen 4 Two Layers C-Grid Zip Tied

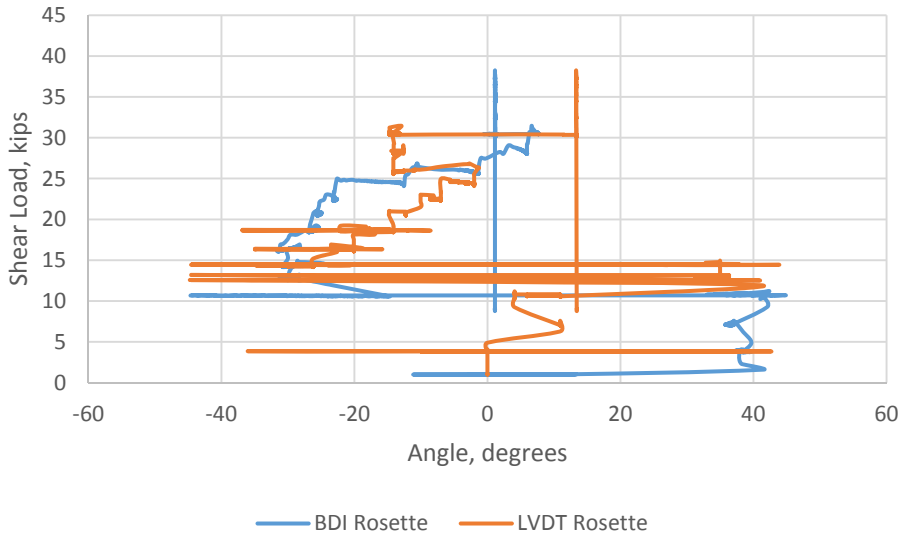

Figure 85: Shear Load v. Principal Angle Specimen 4 Two Layers C-Grid Spaced

Appendix D: Diagrams of C-Grid Embedment for Development Length Specimens

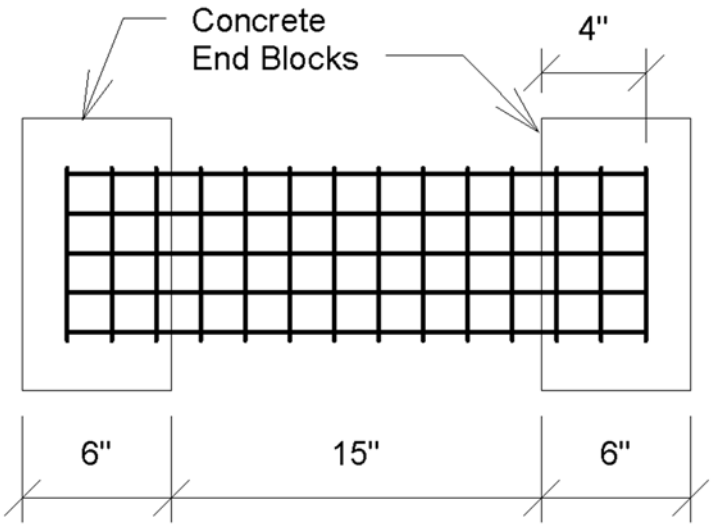

Figure 86: 4 in. Embedment Length Specimen

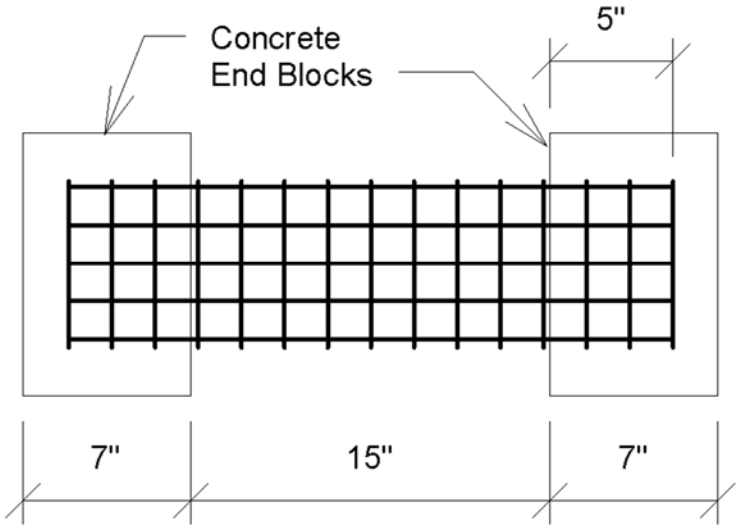

Figure 87: 5 in. Embedment Length Specimen

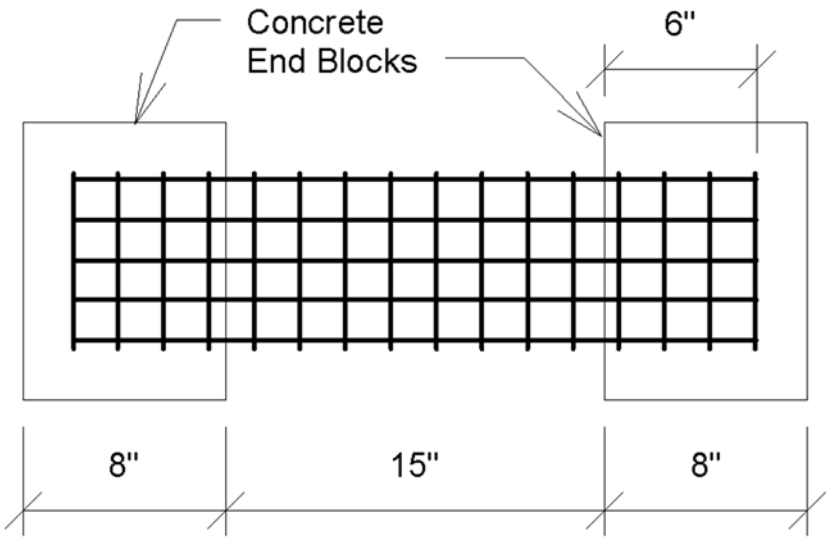

Figure 88: 6 in. Embedment Length Specimen

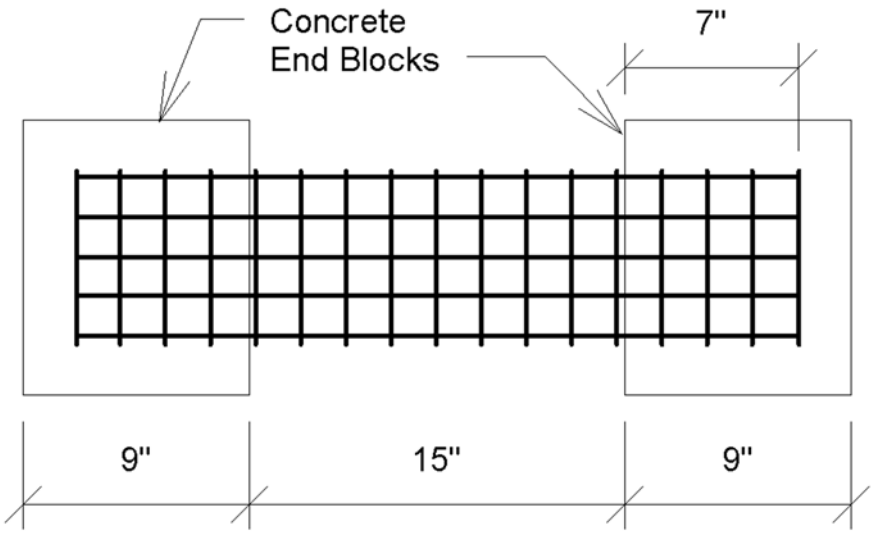

Figure 89: 7 in. Embedment Length Specimen

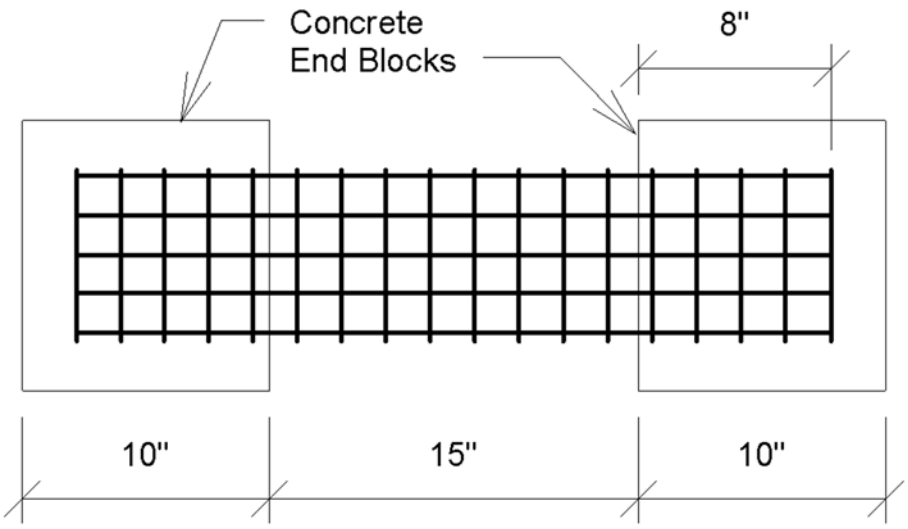

Figure 90: 8 in. Embedment Length Specimen